Kinetic Studies on Different DNA Polymerases Using 4'-Alkylated 2'-Deoxynucleotide Probes

Dissertation

zur Erlangung des akademischen Grades
des Doktors der Naturwissenschaften
(Dr. rer. nat.)
an der Universität Konstanz
Naturwissenschaftliche Sektion
Fachbereich Chemie

vorgelegt von

Dipl.-Chem. Frank Streckenbach

Konstanz, August 2010

Prüfungsvorsitz: Prof. Dr. Ulrich Groth
1. Referent: Prof. Dr. Andreas Marx
2. Referent: Prof. Dr. Jörg Hartig

Datum der mündlichen Prüfung: 24.08.2010

Diese Arbeit entstand in der Zeit zwischen November 2006 und Juli 2010 im Fachbereich Chemie der Universität Konstanz am Lehrstuhl für Organische Chemie / Zelluläre Chemie von Prof. Dr. Andreas Marx.

Teile dieser Arbeit sind veröffentlicht in:

Angew. Chem. Int. Ed. **2010**, *in press*.	Betz K.[+], **Streckenbach, F.[+],** Schnur, A., Exner, T., Welte, W., Diederichs, K. and Marx, A. 2010. "Structures of DNA polymerase caught processing size-augmented nucleotide probes" ([+]equal contribution).
ChemBioChem **2009**, *10*, 1630-1633.	**Streckenbach, F.**, Rangam, G., Möller, H. M., Marx, A. "Steric constraints dependent on nucleobase pair orientation vary in different DNA polymerase active sites".

1 Introduction

Polynucleotide polymerases might be one of the first nanites that appeared in evolution. Their fascinating enzymatic activity, to catalyze selectively nucleic acid synthesis according to Watson-Crick rule in a template-directed manner, is a prerequisite for an accurate replication, recombination, repair, lesion bypass as well as transcription. One form of nucleic acids is the 2'-deoxyribonucleic acid (DNA), a polymeric macromolecule that stores the genetic information in every cell. In 1953, *Watson and Crick* proposed a structure model of DNA, which is now generally accepted [*Watson and Crick,* 1953a, 1953b]. DNA consists of two anti-parallel strands that wind up to a double-helical structure (**Figure 1-1**). Under physiological conditions, the double helix forms a so-called B-type structure, which consists of two unequally sized grooves, a major and a minor groove.

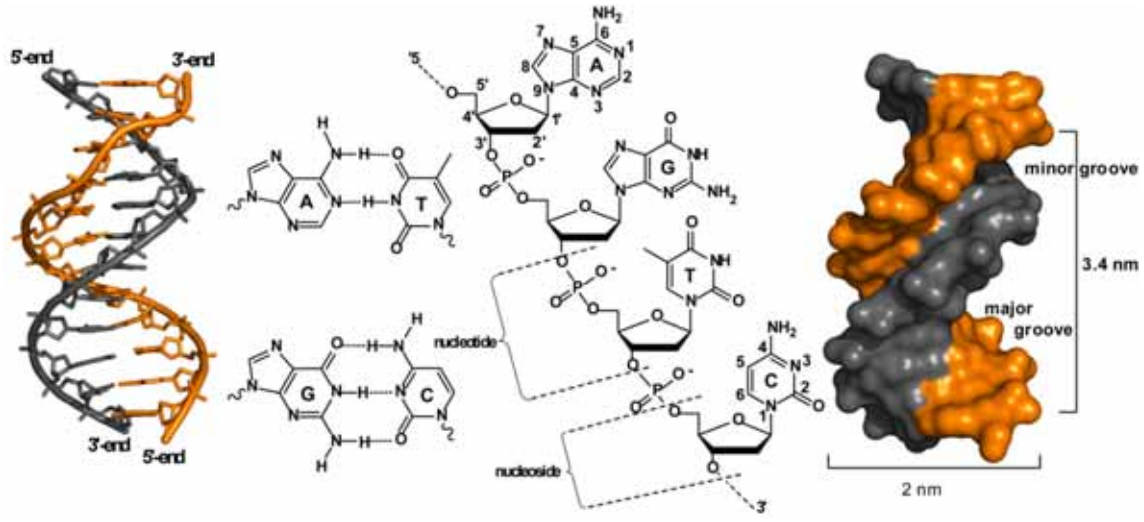

Figure 1-1 *Double-helical structure of DNA. Stick- (left) and surface model (right). Watson-Crick base pairing of A with T and G with C (middle). PDB-code: 1BNA.*

In DNA 2'-deoxyribose units are linked over phosphodiester bridges between the third (C3') and the fifth (C5') carbon atom of adjacent sugars. The sugar-phosphate backbones entwine around an axis, orthogonal to which the nucleobases of the two

strands pair each other. Watson-Crick rule states that always the purine base adenine is bridged over two hydrogen bonds with the pyrimidine thymine, whereas purine guanine selectively forms three hydrogen bonds to the pyrimidine cytosine [*Chargaff*, 1950, *Watson and Crick,* 1953b]. This complementary base pairing guarantees information storage, where three adjacent nucleotides form a codon triplet that codes for a particular amino acid. Replicating an organism's genomic material is a complex process. It involves the coordinated efforts of a protein ensemble, to accurately initiate, propagate, and terminate each biochemical event [*Stillman*, 2005, *Johnson and O'Donnell*, 2005, *Bartek and Lukas*, 2007].

1.1 DNA Polymerases

1.1.1 General Function and Classification

The core pieces to ensure the integrity of the genome are the DNA polymerases [*Lehman* et al., 1958, *Kornberg*, 1956, 1979, 1988,]. DNA polymerases are highly evolved enzymes that selectively catalyze the addition of 2'-deoxynucleoside monophosphates to a growing DNA strand (primer) in a template-directed manner to build up DNA. They maintain an impressive degree of specificity despite the fact that their substrates change during each cycle of nucleotide incorporation due to the heteropolymeric nature of the genomic message. Remarkably only one of four potential 2'-deoxynucleoside triphosphates (dNTPs) is selectively incorporated opposite a template base. Nevertheless, the enzyme still features the flexibility to recognize four distinct pairing partners (template-dNTP: adenine-thymine, guanine-cytosine, thymine-adenine and cytosine-guanine). After unwinding of the two DNA strands, each strand of the helix serves as a template for the synthesis of a new complementary strand. This semiconservative replication makes sure that the genomic information is precisely transferred [*Echols and Goodman*, 1991, *Kunkel and Bebenek,* 2000].

Besides replicative DNA polymerases copying the genome, other DNA polymerases participate in repair mechanisms of certain DNA damages (abasic site, single or double strand break and other damages induced by radiation, reactive metabolism or exogenous chemicals) [*Loeb and Preston*, 1986, *Lindahl*, 1993, *Sancar*, 1996, *Lindahl and Wood*, 1999, *Goodman*, 2002, *Scharer*, 2003]. If DNA lesions cannot be repaired, translesion synthesis (TLS) of these bulky substrates is performed by lesion bypass DNA

polymerases [*Friedberg* et al., 2002, *Prakash* et al., 2005, *Lehmann* et al., 2007, *Yang and Woodgate*, 2007]. Sequence alignment of the different DNA polymerases in organisms allowed a classification into certain families (A, B, C, D, X, Y and RT) [*Filee* et al., 2002]. Polymerases of one family often accomplish similar functions, e.g. family A polymerases are mainly replicative and repair enzymes, whereas family Y includes translesion synthesis polymerases.

1.1.2 DNA Polymerases Selectivity

Remarkably, the information transfer into daughter nucleic acids is achieved by some DNA polymerases with intrinsic error rates as low as one mistake within one million synthesized nucleotides [*Goodman*, 1997, *Kunkel and Bebenek,* 1988, 2000]. In the very beginning of understanding this astonishing DNA replication fidelity, hydrogen bonding patterns were suspected of directing correct base pairing [*Watson and Crick,* 1953a, 1953b]. However, the error rates were far below the value that would be expected, when merely the energetic differences between canonical (e.g. according to Watson-Crick) and non-canonical nucleobase pairing would be considered [*Bruskov and Poltev*, 1979, *Petruska* et al., 1988, *Johnson*, 1993]. Thus, geometric factors became generally accepted to govern DNA polymerase selectivity [*Echols and Goodman*, 1991, *Goodman*, 1997, *Kool*, 2002, *Kool* et al., 2000, *Kool and Sintim, 2006*].

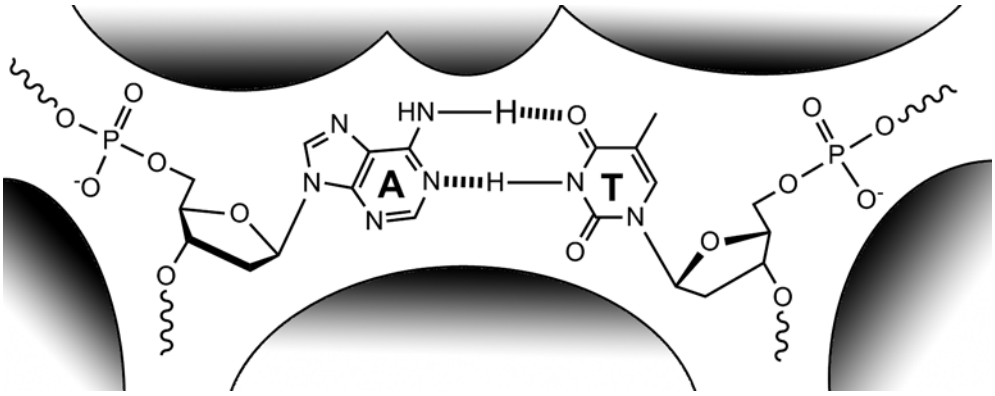

Figure 1.1-1 *Schematic depiction illustrating the space-filling shapes of a deoxyadenosine-thymidine nucleobase pair in DNA polymerase active sites.*

High-fidelity DNA polymerases are believed to mostly select the canonical nucleotide based on close steric complementarities of the nascent base pair to the geometry of the active site in the enzyme (**Figure 1.1-1**). Besides the geometrical aspects, selectivity of complementary base pairs varies among different orientations (e.g. template A : nucleotide T versus template T : nucleotide A) [*Kunkel and Bebenek,*

1988, *Kunkel and Bebenek,* 2000, *Minnick* et al., 2002]. This orientation effect might be related to the ability of DNA polymerase to correctly recognize one out of four structurally similar 2'-deoxynucleoside triphosphates. Moreover, rates for a mismatch composed of the same two bases can vary depending on orientation (e.g., dT-dGTP versus dG-dTTP) [*Minnick* et al., 2002]. Since then, DNA selectivity and fidelity has been a matter of continuing interest and many further discussion and efforts led to a plurality of detailed information [*Kunkel and Bebenek,* 2000, *Goodman*, 2002, *Kunkel*, 2004, *Rothwell and Waksman*, 2005, *McCulloch and Kunkel*, 2008].

The first experiments to understand mechanisms of DNA polymerases were based on functional studies of natural enzymes [*Bryant* et al., 1983, *Boosalis* et al., 1987, *Dahlberg and Benkovic*, 1991, *Creighton* et al., 1995]. X-ray crystallography has come along with functional studies [*Brick* et al., 1983, *Ollis* et al., 1985, *Freemont* et al., 1988, *Beese* et al., 1993a, 1993b, *Jacobo-Molina* et al., 1993, *Korolev* et al., 1995, *Kim* et al., 1995]. Proceedings therein resulted in lots of detailed insights [*Brautigam and Steitz*, 1998, *Li* et al., 1998, 1999, *Li and Waksman*, 2001, *Ling* et al., 2001, 2004, *Boudsoq* et al., 2002, *Johnson and Beese*, 2004, *Rothwell and Waksman*, 2005, *Irimia* et al., 2007, *Durniak* et al., 2008]. The crystal structures helped to identify specific enzyme contacts of certain amino acid to their substrates as well as to reveal conformational changes that take place upon binding to the substrates [*Steitz*, 1998].

1.1.3 DNA Polymerase Structure

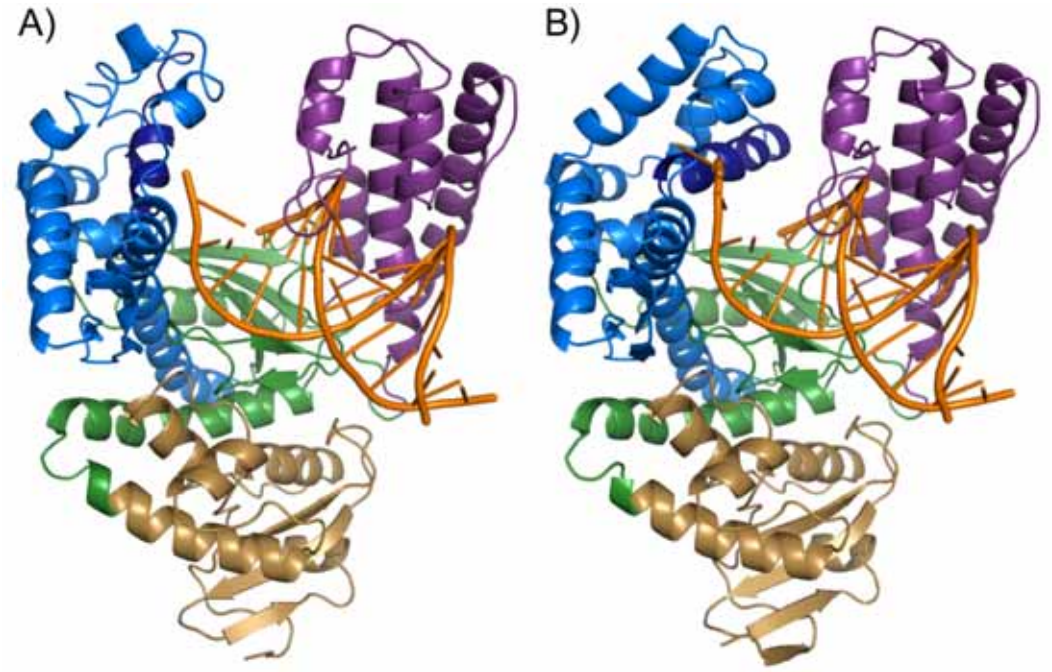

Figure 1.1-2 *Crystal structure of thermostable Klenow fragment of DNA polymerase I from Thermus aquaticus (KlenTaq) in the open form (A) and in the closed form (B). The structures are very similar to a right hand consisting of a finger (blue), a thumb (magenta) and a palm (green) domain. PDB-code: 2KTQ and 3KTQ.*

DNA polymerase structure is generally compared to a right hand. Derived from this shape, palm, thumb and finger domains are described composed of different protein motifs (**Figure 1.1-2**) which are responsible for the tight DNA binding. The palm domain accommodates the catalytically active amino acids in two motifs A and C, which are highly conservative among different species. Together with the finger domain it forms the active site of the polymerase. The finger domain, which is less conservative among the different polymerases, interacts with the incoming dNTP after its binding, whereas the thumb domain contacts the minor groove of the DNA and supports translocation. Some polymerases, like e.g. DNA polymerase I of *Escherichia coli*, additionally possess exonuclease domains, which accomplish further different functions, like e.g proof-reading.

All reported structures resemble this kind of shape, like the first reported structures of e.g. the N-terminal shortened, 5'-3' exonuclease deficient, Klenow Fragment (KF) of DNA polymerase I from *Escherichia coli* [*Ollis* et al., 1982, *Beese* et al., 1993a, 1993b], its analogues from *Bacillus stearothermophilus* [*Kiefer* et al., 1997] or *Thermus aquaticus* [*Korolev* et al., 1995, *Kim* et al., 1995; *Li* et al., 1998]. Two different conformations have been found upon crystallization of these polymerases with DNA in

a binary complex and polymerase with DNA and nucleotide in a ternary complex [*Li* et al., 1998].

The structure of a polymerase bound to DNA resembles a "semi-closed hand", the so-called open form. After binding of the incoming nucleotide, the finger domain undergoes a transition of "closing the hand" into a closed form. Interactions with the finger domain orientate the nucleotide and the primer into a reactive conformation to catalyze the subsequent reaction. After the incorporation and the release of a pyrophosphate, the transition back to the open form takes place to allow translocation for further nucleotide binding or dissociation from the DNA. Based on the structural and functional studies a simplified mechanism for all polymerases is now generally accepted [*Steitz*, 1998]

1.1.4 Mechanistic Reaction Pathway

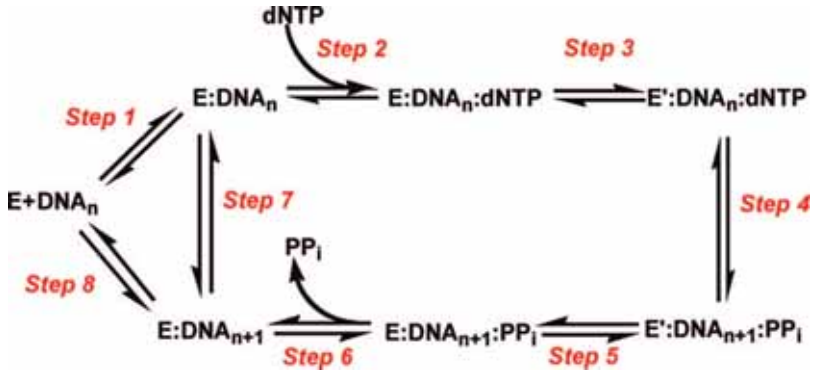

Figure 1.1-3 *Schematic representation of DNA polymerase catalyzed DNA synthesis. The reaction pathway is separated into eight different kinetic steps.*

The reaction pathway of nucleotide incorporation is similar for all polymerases. After binding of the DNA primer-template pair, the polymerase remains in the open form to allow nucleotide binding [step 1] (**Figure 1.1-3**). The association of the dNTP leads to the ternary complex E:DNA$_n$:dNTP [step 2]. This incident triggers a conformational change to form the binding pocket by closing of the finger domain [step 3]. The conformational change is proposed as "induced-fit" mechanism to discriminate against dNTP misincorporation [*Wong* et al., 1991]. Since misaligned substrates are believed to not fit to the geometry of the polymerase's active site, the following chemical step would be hindered. Geometrically matching nucleotides as well as the primer end are considered to be now correctly orientated for the nucleotidyl transfer reaction [step 4, see also **Chapter 1.1.5**]. The finger domain moves back to the polymerase's open form releasing a pyrophosphate [step 5 and 6]. The polymerase may

now translocate the DNA primer-template to continue primer elongation [step 7] or dissociate from its substrate [step 8].

Another impressing feature of DNA polymerases is the speed of incorporation. Despite the fact that the whole reaction circle involves six distinct steps, some polymerase are able to insert up to 1000 bp/s [*Skarstad and Wold*, 1995]. Both the conformational change [step 3] and the chemical transfer reaction [step 4] have been discussed to be rate-limiting for enzyme catalysis [*Rothwell* et al., 2005]. Studies applying α-thio modified dNTP compared to natural substrates on the KF and DNA polymerase from bacteriophage T4 revealed a small elemental effect [*Kuchta* et al., 1988]. If the chemical reaction would be rate-limiting, the less electronegative, non-bridging sulfur atom should destabilize the required electron density for the transition state, thus decreasing the reaction rate constant. Kinetic experiments on these enzymes using 2-aminopurine templates associated the rate-limiting step preceding the chemical reaction [*Frey* et al., 1995]. It should be noted, that the magnitude of the thio-elemental effect is under a strong debate [*Herschlag* et al., 1991, *Showalter and Tsai*, 2002]. Moreover, results from spectroscopic stopped flow kinetic measurements on human polymerase β report that the induced-fit occurs too fast, assigning the rate-limiting step to the nucleotidyl transfer [*Sucato* et al., 2007]. These experiments indicate that replicative polymerases opposed to repair or translesion synthesis polymerases may achieve rate limitations differently.

1.1.5 Chemical Reaction in Detail

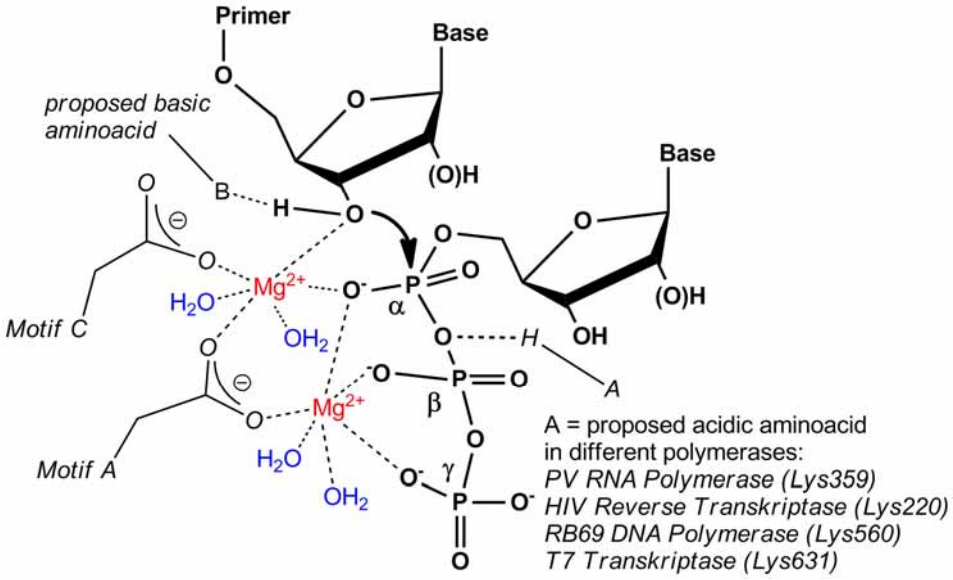

Figure 1.1-4 *Extended two-metal-ion mechanism of a general acid catalysis (figure according to [Castro et al., 2009]). Depicted is the transition state of the nucleotidyl transfer reaction. Primer end nucleotide and incoming nucleoside triphosphate are depicted in bold, protein residues are depicted in regular. One divalent metal cations (Mg^{2+}, red) is coordinated by the three phosphates of the nucleoside triphosphate and an aspartate residue located in motif A of all polymerases. The other metal ion is coordinated by the C3'-OH of the primer terminus, the α-phosphate of the nucleoside triphosphate and widely conserved aspartate residues of structural motifs A and C. Additional water molecules complete the coordination sphere (blue). A proposed acidic amino acid (A) was reported to protonate the pyrophosphate leaving group. Moreover, a not identified basic amino acid should provoke deprotonation of the C3'-OH.*

The chemical reaction that is catalyzed by DNA polymerases is generally described as a nucleophilic attack of the C3'-OH of the primer end on the α-phosphorous atom of the nucleotide (see **Figure 1.1-4**). This attack involves two divalent ions (typically Mg^{2+}), which are complexed through two widely conserved aspartates. The two Mg^{2+} are proposed to stabilize the trigonal-bipyramidal transition state and lower the pK_a of the C3'-OH. Recently, this mechanism was extended by observations that a proposed acidic amino acid side chain provokes protonation of the pyrophosphate [*Castro* et al., 2009]. It is believed that a basic amino acid residue additionally helps deprotonating the C3'-OH. However, this residue remains unclear and further studies need to be performed to reveal its contribution.

1.1.6 Enzyme Kinetics on DNA Polymerases

Two main kinetic techniques to study DNA polymerase reaction mechanism exist [*Berdis*, 2009]. The classical Michaelis-Menten kinetic gives information about the reaction in steady-state (additional details in **Chapter 6.3.12**). A simplified enzyme mechanism is given in (**1**):

(1) $$\text{Substrate} + \text{Enzyme} \underset{k_{-1}}{\overset{k_1}{\rightleftharpoons}} [\text{ES}] \xrightarrow{k_2} \text{Enzyme} + \text{Product}$$

After a short interval of the formation of the enzyme-substrate complex [ES], the steady-state of an enzyme reaction is reached. In this phase the concentration of [ES] is almost constant and the reaction velocity is at its maximum. To guarantee steady-state for DNA polymerase catalyzed reactions, a primer-template complex should be hit by only one polymerase, so that the measured data derives from the conversion by no more than one enzyme (*single completed hit conditions*) [*Boosalis* et al., 1987, *Creighton* et al., 1995]. Practically, enzyme concentration has to be below 5% of the primer-template and only 20% of the primer should be extended. Steady-state kinetics allow the measurement of $K_M = (k_{-1}+k_2)/ k_1$ (Michaelis-Menten constant, an apparent first-rate order constant) and V_{max} (reaction velocity) or k_{cat} ($k_{cat} = V_{max} / [E]_0$; enzyme concentration at t_0). The reaction over all six distinct steps can be measured by this technique. Steady-state kinetics can easily be performed and do not require complex machines. However, a comparison of the measured data is difficult. Most discussion relies on the ratio of k_{cat} / K_M, which is generally referred to as the incorporation efficiency or specificity. The reaction velocity k_{cat} correlates to the overall reaction velocity. The Michaelis-Menten constant K_M only gives a hint on the affinity of the substrate to the enzyme, as $K_D = k_{-1}/k_1$. Only if the k_2 can be neglected, it resembles the substrate affinity.

Transient- or presteady-state enzyme kinetics under *single turnover conditions* enable measurements uncoupled from association and dissociation processes (additional details in **Chapter 6.3.13**). By using enzyme concentration in excess over the DNA substrate concentration, such that the entire DNA is bound to a polymerase at the beginning of the experiment, the reaction is limited to a single turnover. The observed rate represents the rate of steps up to and including the nucleotidyl transfer that results in primer elongation (see **Chapter 1.1.4**). As the substrate binding steps [step 1 and 2]

are rapid, the reaction rate is limited either by the conformational change [step 3] or by the following chemical transfer step [step 4] (see ***Figure 1.1-3***) [*Dahlberg and Benkovic*, 1991]. Through measuring the rate at a series of dNTP concentrations, the dissociation constant K_D, reflecting the binding of the nucleotide to form the ternary complex, as well as the maximal reaction rate k_{pol} can be determined. The ratio k_{pol} / K_D describes the efficiency of incorporation of a nucleotide substrate. The ratio of the efficiencies of incorporation of a dNTP and a corresponding e.g. modified dNTP is a measure of the discrimination between the two substrates. However, presteady-state kinetic experiments require complex instruments to control reaction times within millisecond range (a scheme of such an apparatus and details on the calculations can be found in **Chapter 6.3.13**).

Further details on both techniques have been reviewed recently [*Johnson*, 1998, *Barman* et al., 2006].

1.1.7 Protein Mutagenesis to Probe Selectivity

Besides kinetic studies on natural enzymes, random mutations as well as rational mutations are valuable tools for probing DNA polymerase selectivity and function. These mutations have been brought into DNA polymerases through different well described techniques [*Lawrence*, 2002, *Braman*, 2002]. Studies using random mutations, like error-prone PCR, sequence saturated mutagenesis or gene shuffling, intended to create libraries for directed evolution to find polymerase mutants with new functions, like higher selectivity or acceptance of specific substrates. *Marx* and coworkers used directed evolution through error-prone PCR to increase polymerase selectivity. They could prove that through an exchange of three amino acids QVH (Gln, Val, His) of motif C by nonpolar amino acids the selectivity of *KlenTaq*, *KF* and *Pfu* are increased [*Summerer* et al., 2005, *Strerath* et al., 2007b, *Rudinger* et al., 2007].

Besides the hunting for new properties, rational mutations are aimed for studying polymerase function and selectivity. First studies targeted the exchange of specific amino acids that were suspected to be involved in catalyses. The objective of some mutations was to prevent certain interactions at different positions of the substrates, like interfering hydrogen bonding or excluding water [*Jung* et al., 1990, *Pandey* et al., 1993, 1994, *Copeland* et al., 1995, *Kim* et al., 1997, *Liu and Tsai*, 2001].

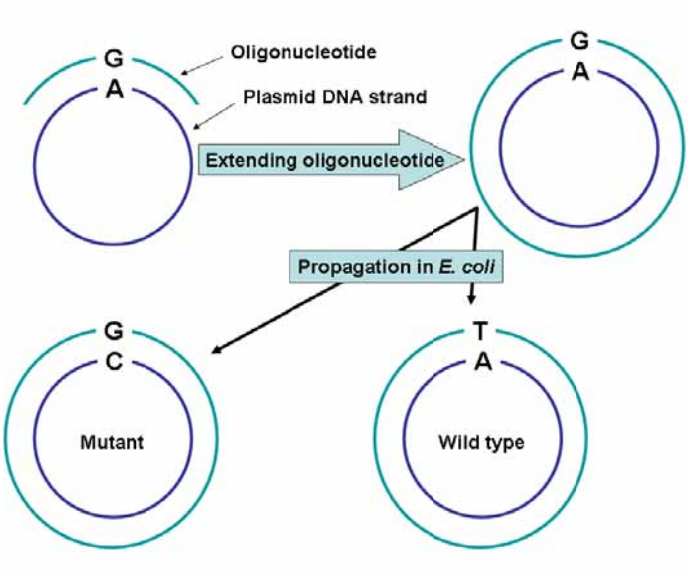

Figure 1.1-5 *Schematic illustration on site-directed mutagenesis. A designed primer pair is used in a plasmid PCR to produce rationally designed enzyme mutants.*

Site-directed mutagenesis is a commonly applied rational mutation technique that uses a designed, complementary primer pair for a plasmid PCR on the polymerase gene [*Gillam and Smith*, 1979]. The primers carry a codon coding for the desired amino acids that should be introduced into the enzyme. The primers bind to a plasmid carrying the polymerase gene around the mutation site (see **Figure 1.1-5**). The PCR products are closed to the desired plasmids after transformation into *Escherichia coli* by the bacterial repair machinery. After overexpression and purification the rationally designed polymerase mutant can be applied in functional studies. This mutagenesis technique has been applied in this work.

1.2 Nucleoside Analogues to Probe DNA Polymerases Selectivity

1.2.1 Nucleobase Modifications

Chemical synthesis of special substrate analogues have brought up new tools for understanding molecular details on polymerase functions. Several synthetically nucleotides have been developed and applied in enzyme kinetic studies to further probe enzyme-substrate interactions on selectivity [*Strazewski and Tamm*, 1990, *Goodman*, 1997, *Verma and Eckstein*, 1998, *Morales and Kool*, 1998, 2000a, 2000b, *Kool*, 2002, *Summerer and Marx*, 2004, *Marx* et al., 2004].

Such nucleoside analogues possess well-defined properties. Some of them are isosteric or isoelectronic to their natural counterpart. Others exhibit desired modifications, such as steric enlargements, lacking hydrogen bonding capacities, electronic deviations or even functionalities [*Jung and Marx*, 2005]. Besides their possible use as inhibitors in different applications (e.g. as drugs directed against viral polymerases) or as tools in analytics (e.g. sequencing, SNP detection etc.), these probes helped to understand specific mechanisms in DNA polymerases. They allowed explaining the involvement of the different hydrogen bonding on selectivity as well as the participation of different amino acid through contacts to their substrates on the recognition process.

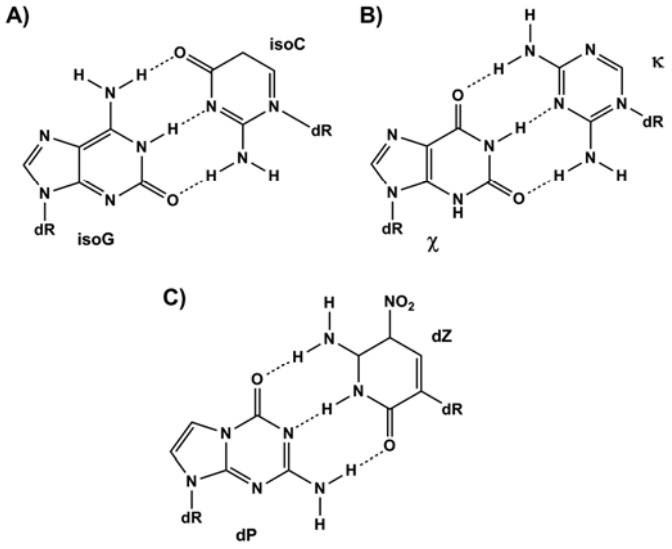

Figure 1.2-1 *Schematic drawing of artificial base pairs* ***isoC·isoG*** *[Switzer et al., 1989] as well as* ***κ*** *(2,6-diaminopyrimidine) and* ***χ*** *(xanthosine) [Piccirilli et al., 1990]. 6-Amino-5-nitropyridin-2(1H)-one (****dZ****) is complementary to 2-aminoimidazo[1,2-a][1,3,5]triazin-4(8H)-one (****dP****) [Yang et al., 2006].*

First efforts have been made by *Benner* et al. concentrating on changing the hydrogen bonding pattern of the nucleobases (**Figure 1.2-1**) [*Switzer* et al., 1989, *Piccirilli* et al., 1990]. Newer analogues have even been accepted by certain polymerases in applications like PCR (*Yang* et al., 2006, 2007, 2010). Inspired by these results, *Kool* et al. developed base analogues that lack the ability for hydrogen bonds, but still have similar size and shape compared to the natural bases (**Figure 1.2-2**) [*Schweitzer and Kool*, 1994, *Morales and Kool*, 1998, *Sintim and Kool*, 2006]. 2,4-Difluorotoluene (**F**), a isosteric mimetic of thymine, was accepted by DNA polymerases as substrates in a selective manner. The base analogue was selectively incorporated opposite of the respective correct template base. Furthermore, it was used as a template base selectively addressing for the correct triphosphate [*Moran* et al., 1997a, 1997b]. Further studies evolved a selective artificial base pair **F** and **Z** (adenine analogue) [*Morales and Kool*, 1998], which was accepted by Klenow Fragment with almost comparable efficiencies than the natural base pair **A**:**T (Figure 1.2-2**).

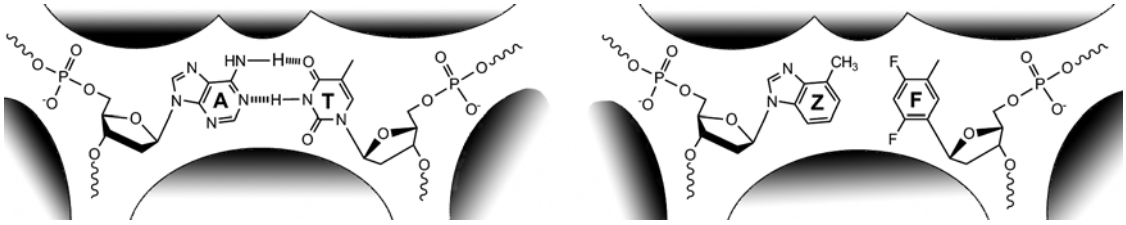

Figure 1.2-2 *Schematic depiction illustrating a comparison of the space-filling shapes of a **A**:**T** nucleobase pair with **Z**:**F** isosters in DNA polymerase active sites.*

Their results lead to the postulation of the "*steric exclusion model*", in which nucleobase pairs have to fit to a certain geometry in the rigid binding pocket to be recognized as substrates (*active site tightness*) [*Kool* et al., 2000, *Kool*, 2002, *Kool and Sintim*, 2006, *Krueger and Kool*, 2007].

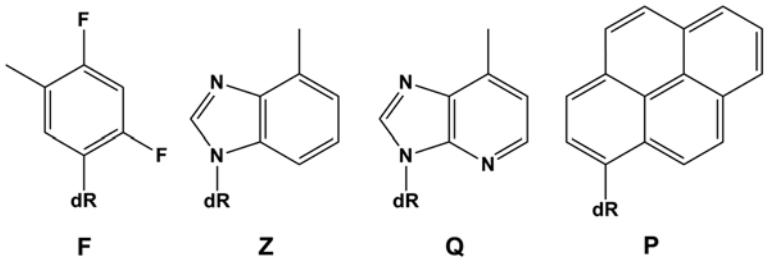

Figure 1.2-3 *Hydrophobic nucleobase analogues. Non-polar isostere of thymine (2,4-difluorotoluene,* ***F****) [Schweitzer and Kool, 1994] and adenine (4-methylbenzimidazole,* ***Z****) [Morales and Kool, 1998]; 9-methylbenzimidazole (****Q****) [Morales and Kool, 1999] as polar isoster for adenine. The pyrene fragment (****P****) as base pair mimetic opposite abasic sites [Matray and Kool, 1999].*

Further evidence for the steric model was derived from the pyrene nucleotide (**P**) as base pair mimetic opposite abasic sites in DNA templates [*Matray and Kool*, 1999, *Smirnov* et al., 2002] and the **Q** nucleoside analogue [*Morales and Kool*, 1999, 2000a, 2000b] with an additional hydrogen acceptor pointing towards the minor groove (**Figure 1.2-3**).

However, different investigated DNA polymerases varied within their acceptance for the non-polar surrogates [*Morales and Kool*, 2000b, *Mizukami* et al., 2006]. Most polymerases of family A, B and RT achieve selective incorporation, if the base pair geometry shows little deviation. Deviations in the acceptance of the shape complementary substrates by certain polymerases (e.g. Y family polymerases) might be explained by increased flexibility of their active site that increases the importance of hydrogen bonding [*Kool and Mizukami*, 2006].

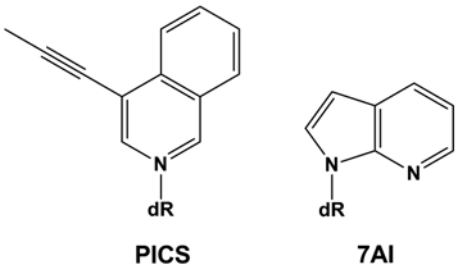

Figure 1.2-4 *Hydrophobic isocarbostyryl derivatives: 7-propinylisocarbostyril (****PICS****) and* 7-azaindole (**7AI**) *[McMinn et al., 1999, Tae et al., 2001].*

The idea of new nucleotide base pairs has been further pursued by development of non-natural hydrophobic base pairs. These base pair analogues head towards an extension of the genetic code. The concepts of X- and Y-DNA by *Kool* and coworkers [*Lynch* et al., 2006] showed first results that also back up the hypothesis of steric exclusion, despite from how the genetic information is extended. Another promising example, which picks up this pattern, is the base pair analogue 7-azaindole (**7AI**) and

7-propinylisocarbostyril (**PICS**) from *Romesberg* and *Schultz* (**Figure 1.2-4**) [*McMinn* et al., 1999, *Tae* et al., 2001]. Astonishing, the exonuclease deficient Klenow fragment (KF exo-) processed this base pair in high efficiencies [*Ogawa* et al., 2000, *Wu* et al., 2000]. However, further incorporation of natural nucleotides following this base pair was inhibited. This probably results from lacking hydrogen interaction to the minor groove and restricted flexibility at the primer terminus [*Matsuda* et al., 2006]. Through introduction of further functionalities as hydrogen donor or acceptors, hydrogen bridges inside the minor groove of the nascent primer strand enabled orientations for further elongation catalysis [*Yu* et al., 2002; *Matsuda* et al., 2003, 2007] (**Figure 1.2-5**).

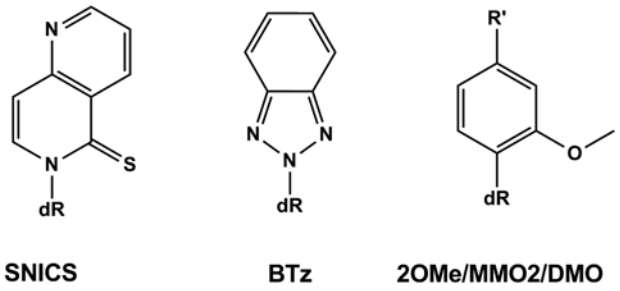

Figure 1.2-5 *Artificial nucleobase analogues: 10-thio-6-N-isocarbostyryl (SNICS) [Yu et al., 2002], benzotriazole (BTz) [Matsuda et al., 2003] and methoxy-substitated phenyl analogues [Matsuda et al., 2007]: R': H (2OMe), Me (MMO2), OMe (DMO).*

Summarizing, these results corroborate the assumption that DNA polymerases catalyze DNA synthesis efficiently and selectively by steric exclusion within the active site. Thereby, hydrogen bonding seems to play only minor roles within correct base pairing. Nevertheless, it participates in minor groove contacts in the course of further primer extension. The new nucleotide base pair has to accommodate a certain geometry whose shape only fits into the binding pocket, if both nucleotides are paired corresponding Watson-Crick rule. Nucleotides of the same geometrical shape like natural substrate can be recognized instead of these. These results tremendously expanded the understanding of how DNA polymerases gain selectivity.

1.2.2 4'-*C*-Modified Nucleotide Probes

The fact that the active site constraints differ among DNA polymerases from rigid to more flexible encouraged approaches beside base pair modifications. Apparently, the 2'-deoxyribose fulfills another starting point for the synthesis of additional active site probes. Structural and functional data on DNA polymerases show that the sugar residues of the nucleotides are part of the substrate recognition process and provide the

enzyme with additional paths for achieving selectivity besides inspection of nucleobase conformation [*Johnson and Beese*, 2004, *Rothwell and Waksman*, 2005].

Polar 4'-*C*-size-augmented thymidine probes by *Giese* and coworkers have shown to decrease oligonucleotide synthesis of different polymerases I and reverse transcriptase variants [*Hess* et al., 1997, *Marx* et al., 1997, 1998, 1999]. Since then, *Matsuda* [*Nomura* et al., 1999] and *Ohrui* [*Kodama* et al., 2001, *Hayakawa* et al., 2004, *Kohgo* et al., 2004] have tested 4'-modified probes further on their potency against cancer or viruses.

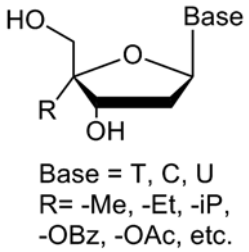

Figure 1.2-6 *Examples of different 4'-modified nucleosides developed by Marx and coworkers.*

Summerer and *Marx* employed 4'-*C*-alkylated thymidine-5'-*O*-triphosphates with gradually expanding residues to probe interactions between DNA 2'-deoxyribose backbone and protein motifs within DNA polymerases active site [*Summerer and Marx*, 2001] (**Figure 1.2-6**). These residues point towards the DNA minor grove, and thus do not interfere with the hydrogen bonding of the nucleobases or base stacking [*Detmer* et al., 2002, 2003]. These modified probes are substrates for incorporation and thus give information on steric interactions during the dynamic catalysis of the DNA polymerase.

Kinetic analyses using 4'-alkylated nucleoside triphosphates and 4'-alkylated nucleotides in templates by *Summerer* and *Strerath* indicated that the selectivity of the nucleotide incorporation increased [*Summerer and Marx*, 2001, 2002; *Strerath* et al., 2002a, *Cramer* et al., 2002]. Incorporation of the 4'-alkylated nucleoside triphosphates opposite non-canonical nucleobases as well as misincorporation of non-canonical nucleotides opposite these probes as templates is significantly diminished. The size expansion is believed lead to specific interactions of the probes with amino acid residues in the polymerase active site to cause less conformational flexibility. Thus, the small geometric deviations within the DNA polymerase-substrate complex reduced the tolerance of non-canonical base pairs.

These results allowed an application for the detections of single nucleotide polymorphism (SNP, single base variations within a population with an occurrence >1%) in allele specific PCR [*Strerath* et al., 2004, *Gaster and Marx*, 2005, *Strerath* et al., 2007a]. Besides 4'-alkylated thymidine analogs, polar 4'-modified thymidine and cytosine analogues as well as 4'-alkylated uridine analogs have been developed and applied in different applications [*Gaster and Marx*, 2005, *Rangam* et al., 2005].

Recent kinetic studies applied transient kinetics on 4'-alkylated thymidine triphosphates and 4'-alkylated primer probes comparing polymerases of different families [*Cramer* et al., 2008, *Di Pasquale* et al., 2008]. Polymerases of family A and Y accepted 4'-alkylated thymidine triphosphates, whereas human pol β did not incorporate these probes. Interestingly, pol β is able to extend 4'-alkylated primer ends, which is not the case for polymerases of family A and Y. These results further highlighted the importance of tight fitting of the nucleotide substrate within the DNA polymerase active site. However, nucleotide incorporation selectivity often varies significantly depending on the DNA polymerase.

2 Aim of this Work

Although numerous studies have already been done over the past decades, on how DNA polymerases in particular work and how they achieve their fascinating high performance in DNA replication shaped by nature's power of evolution, the detailed mechanistic steps are still not entirely clear and are a matter of intense debate. Thus, scientist invented a plethora of new chemical probes to further explore the active site of DNA polymerase.

Previous studies in our group by *Summerer*, *Strerath* and *Di Pasquale* used thymidine analogues to probe selectivity (*Summerer and Marx*, 2001, 2002; *Strerath* et al., 2002, *Di Pasquale* et al., 2008). They could show that the 4'-*C*-alkylated thymidines were substrates for DNA polymerases and the formation of non-canonical base pairing opposed to these probes is significantly diminished.

This work aimed for more detailed functional studies of DNA polymerases by different kinetic techniques using synthetically made 4'-*C*-modified nucleotide probes.

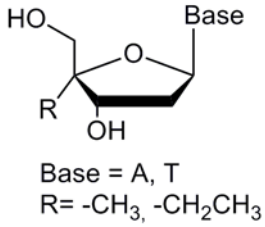

Scheme 2-1 *Schematic drawing of the aimed nucleoside probes.*

Here the advantages of a new synthesis strategy should enable the synthesis of a modified complementary base pair (**Scheme 2-1**). Using these substrates, the described orientation effect (**Chapter 1.1.2**) within DNA polymerase active site should be subjected to steric constraints by the 4'-*C*-alkyl modification. Probing binding pockets at different locations in the active site was supposed to lead to additional information on active site tightness without interference of hydrogen bonding patterns. The strategy for

synthesizing 4'-alkylated nucleosides from a 4'-functionalized ribose compound, which Dr. Gopinath Rangam, AG Marx, had recently established [*Rangam* et al., 2005], was intended to be used in order to obtain 4'-alkylated deoxyadenosine and thymidine nucleosides. These nucleosides are versatile for several further steps. First, the 4'-alkylated nucleosides should be converted into phosphoramidite building blocks, which can be used for the automated DNA synthesis of modified oligonucleotides. These oligonucleotides can serve as templates in incorporation studies with several DNA polymerases. Furthermore, the coupling of the 4'-modified nucleoside to solid supports was to be performed to make them applicable as starting points for automated DNA synthesis. These solid supports allow the synthesis of 3'-end modified primer strands. Finally and most importantly, the 4'-alkylated nucleosides should be converted into the corresponding nucleoside triphosphates following reported synthesis strategies. Nucleoside triphosphates are the substrates of DNA polymerases. Thus, great attention is focused on their binding and reactivity behavior within the active site. The obtained modified 2'-deoxyadenosine and thymidine triphosphates are intended to be used in complementary incorporation assays. Base pairing orientation in two DNA polymerases of different families should be compared by steady-state kinetic methods. The editing of the incoming dNTP sugar residue might provide DNA polymerases with an additional option to achieve canonical base pair formation through indirect readout of the sugar conformations. Furthermore, the binding pockets are supposed to be subjected to additional steric hindrance through the incorporation of the 4'-alkylated probes opposite 4'-alkylated template nucleotides. Here, the flexibility of the active site should reach its limit.

Next experiments should focus on detailed functional and structural studies of *KlenTaq* DNA polymerase. As functional data on processing 4'-alkylated dTTPs by *KlenTaq* DNA polymerase lack, presteady-state kinetic techniques should be applied. Obtained binding constants and polymerization rates should help to understand the mechanism of processing sterically enlarged probes. These experiments should be accompanied by structural studies. Karin Betz, in a cooperation of AG Marx and AG Welte, Universität Konstanz, used 4'-alkylated nucleoside triphosphates for the first time in crystallization trials to gain structural information.

3 Results and Discussion

3.1 Steric Constraints Dependent on Nucleobase Pair Orientation Vary in Different DNA Polymerase Active Sites

3.1.1 Introduction

Many tailor-made probes have been synthesized to investigate steric constraints like "tightness" in DNA polymerases since the proposal of this concept (see **Chapter 1.1.2**).

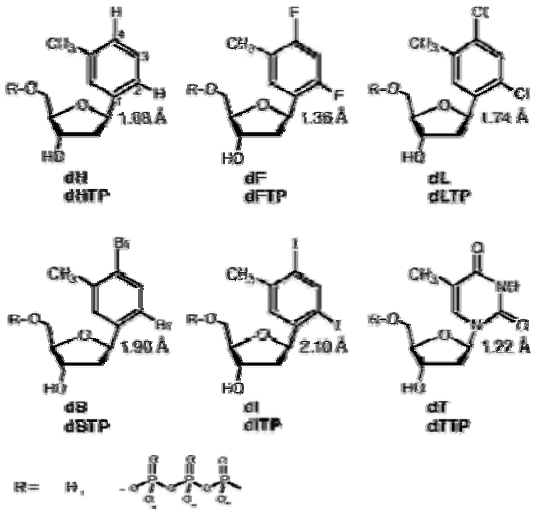

Figure 3.1-1 *Incrementally enlarged steric nucleotide probes by Kool et al. [Mizukami et al., 2006].*

Recently, *Kool* et al. have employed gradually expanding thymidine analogues to probe tightness and polar effects within the active site of DNA polymerase IV of *Sulfolobus solfataricus* (Dpo4) acting on the nucleobase [*Mizukami* et al., 2006]. They used non-polar nucleobase surrogates with only limited ability to form hydrogen bonds. Moreover, they increased the size of these compounds incrementally by use of halogen atoms substituting the oxygen atoms of the base (**Figure 3.1-1**). When incorporating these, Dpo4 showed less distinct deviations between the different substrates than the

exonuclease deficient Klenow fragment (KF exo-) of DNA polymerase I of *Escherichia coli.* This behavior was explained by more flexibility inside the active site of Dpo4. Interestingly, similar results were obtained for *Escherichia coli* DNA polymerase IV [*Silverman* et al., 2007]. These results expanded the proposal of the concept of active site tightness for Y family DNA polymerases and revealed variations within selectivity between different DNA polymerases.

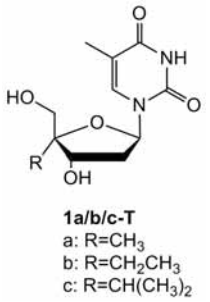

Figure 3.1-2 *Nucleoside probes developed by Marx et al. [Summerer and Marx, 2001].*

Marx and coworkers focused on the sugar part of nucleosides. They targeted the 4'-position of the 2'-deoxyribose ring for introducing functional groups [*Summerer and Marx*, 2001; *Strerath* et al., 2002, *Gaster and Marx*, 2005]. Therefore, they have developed and utilized 4′-alkyl-modified nucleotides, which continually increase in steric bulk for probing steric effects in DNA polymerase function acting on the 2'-deoxyribose (**Figure 3.1-2**). Alkyl groups were employed, because electronic effects of the functionality as well as potential effects on hydrogen bonding patterns and conformations of the nucleotides on DNA polymerase function are minimized. Their results revealed an important contribution of steric effects on DNA polymerase selectivity and variations thereof to be involved in varied selectivity among different enzymes (for details see **Chapter 1.2.2**) [*Summerer and Marx*, 2001; *Strerath* et al. 2002; *Di Pasquale* et al., 2008].

However, until now the work was limited on 4'-alkylated thymidine derivatives. With the help of a complementary modified nucleobase pair, additional information on the influence of steric constraints on the orientation effect (**Chapter 1.1.2**) as well as steric effects on both ends of the binding pocket should become observable.

3.1.2 Chemical Synthesis of 4'-Alkylated 2'-Deoxynucleosides

In this work, 4'-alkylated 2'-deoxynucleoside-5'-triphosphates and 2'-deoxynucleoside-3'-phosphoramidites have been synthesized as probes for DNA polymerases. For the 4'-alkylated thymidine probes **1a/b/c-T** established procedures already existed (**Figure 3.1-2**) [*Summerer and Marx*, 2001, *Waga* et al., 1993]. However, these strategies have been shown to be unsuitable for other nucleosides because of low yields and undesired side products.

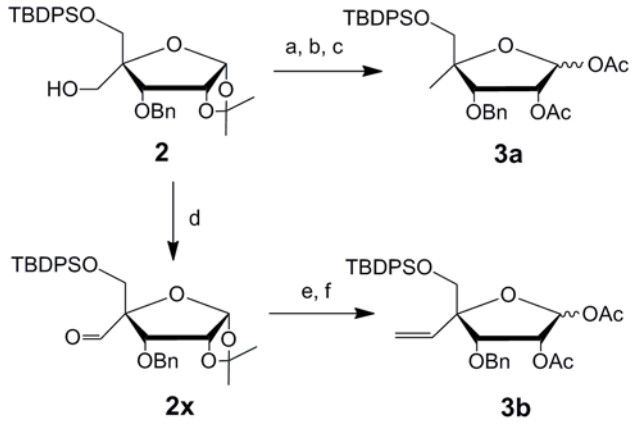

Scheme 3.1-1 *Reagents and conditions: a) Ph_3P, imidazole, I_2, toluene, reflux, 5 h, 89%; b) n-Bu_3SnH, AIBN, toluene, reflux, 12 h, 96%; c) AcOH, Ac_2O, H_2SO_4, 16 h, 79%; d) Dess-Martin periodinane, CH_2Cl_2, 0.5 h, 92%; e) $MePPh_3Br$, n-BuLi, THF, 3 h, 97%; f) AcOH, Ac_2O, H_2SO_4, 16 h, 90%.*

Dr. Gopinath Rangam, AG Marx, first developed a strategy for 4'-alkylated uridine compounds starting from literature known alcohol **2** [*Obika* et al., 2002, *Imanishi and Obika*, 2002] (**Scheme 3.1-1**) to yield the glycosyl donors **3a** and **3b** [*Rangam* et al., 2005]. Later on, this synthesis strategy was adapted to 4'-alkylated 2'-deoxyadenosines and thymidines [*Streckenbach* et al., 2009]. This allowed access to the nucleosides and their corresponding phosphoramidites and nucleoside triphosphates.

In this work the alcohol **2** was synthesized from 1,2:5,6-di-*O*-isopropylidene-α-D-glucofuranose similar to a published route [*Beaucage*, 2001]. Alcohol **2** was converted into the respective iodide through treatment with Ph_3P, I_2 and imidazole in toluene (**Scheme *3.1-1***). Reduction using *n*-Bu_3SnH and AIBN in refluxing toluene afforded the desired alkyl derivative in high yields. Following protection group manipulations involved cleavage of the acetal group and conversion to the bis-acetate **3a**.

In order to synthesize the 4'-*C*-ethylated nucleoside the alcohol **2** was oxidized to yield the corresponding aldehyde **2x** using the Dess-Martin reagent (**Scheme 3.1-1**) [*Dess and Martin*, 1991]. Wittig type reaction allowed the introduction of a C1-unit to

yield the 4-*C*-vinylated ribose derivative. By protection group manipulations, the bis-acetate **3b** was obtained.

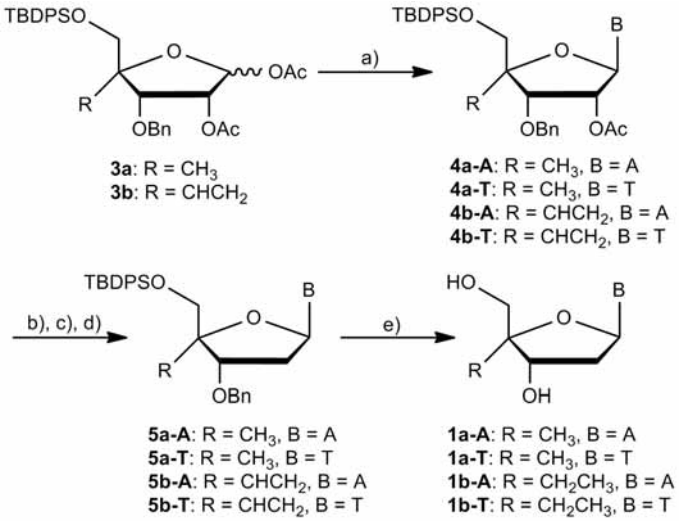

Scheme 3.1-2 *a) Thymine, N,O-bis(trimethylsilyl)acetamide, TMSOTf, CH_3CN, reflux, 2 h, 62% (Me) / 61% (Et); N^6-Benzoyladenine, TMSOTf, CH_3CN, 0°C, 1h, 55% (Me) / 48% (Et); b) NaOMe, MeOH, r.t. 1-12 h; c) PhOCSCl, DMAP, CH_3CN, r.t., 1 h; d) n-Bu_3SnH, AIBN, toluene, reflux, 1 h, 72% (T^{Me}) / 56% (T^{Et}) / 73% (A^{Me}) / 78% (A^{Et}) over 3 steps; e) 10% Pd/C, H_2, THF-EtOH, reflux, 24 h followed by TBAF, THF, r.t., 7 h, 61% (dT^{Me}) / 63% (dT^{Et}); 10% Pd/C, H_2, THF-EtOH, 1N NaOH, reflux, 5-10 days, 94% (dA^{Me}) / 98% (dA^{Et}).*

The respective nucleobases were introduced by Vorbrüggen glycosylation to yield **4a/b-A/T** (62% T^{Me}, 61% T^{Et}, 55% A^{Me}, and 48% A^{Et})**.** Next, saponification and subsequent deoxygenation of the 2'-hydroxyl group by tributyltin hydride via a thiocarbonate in a Barton-like reaction afforded the protected 2'-deoxynucleosides **5a/b-A/T.** A following cleavage of the protection groups gave **1a/b-A/T** in 9-41% overall yield (**Scheme 3.1-2**, further details in [*Streckenbach* et al., 2009]). For the successful hydrogenolysis of the benzyl ethers in **4a/b-A**, basic conditions were required in order to suppress side reactions that occurred to a significant extent in the absence of NaOH. The hydrogenolysis also reduced the vinyl residue to the corresponding ethyl group.

3.1.3 Conformational Analysis of the Nucleosides

In order to gain insight into potential effects of the modifications on the sugar conformations NMR conformational analysis has been performed in cooperation with Prof. Dr. Heiko Möller, Universität Konstanz. This analysis is based on $^{3}J_{HH}$-coupling constants deduced from 1D-^{1}H-NMR spectra recorded in D_2O as described by *Altona* and coworkers (**Table 3.1-1**) [*De Leeuw and Altona*, 1983, *Rinkel and Altona*, 1987].

Nucleoside	Fraction of (S)-type and (N)-type conformation	
	% (S)	% (N)
dA	70	30
1a-A	55	45
1b-A	57	43
dT	58	42
1a-T	42	58
1b-T	47	53

Table 3.1-1 *2'-Deoxyribose conformation of* ***1a/b-A/T*** *as determined from ^{1}H-NMR spectroscopic data (in D_2O, 600 MHz).*

Unmodified nucleosides were found to adopt about 60-70% southern conformation [(S)-type], while for **1a/b-A/T** approximately 50% (S)-type conformations were observed, indicating that 4´-alkylation had only moderate impact on sugar puckering in solution in general. Noteworthy, the observed effects on the conformational equilibria are independent of the nature of the nucleobase as indicated by comparable fractions of (S)-type conformations for all nucleotides (**1a/b-A/T**).

3.1.4 Synthesis of 5'-Triphosphates

The corresponding triphosphates were synthesized employing standard conditions [*Kovacs and Ötvös*, 1988]. FPLC purification over an ion-exchange resin and further RP-MPLC purification yielded the highly pure dNTP analogues (**Scheme 3.1-3**, further details in [*Streckenbach* et al., 2009]).

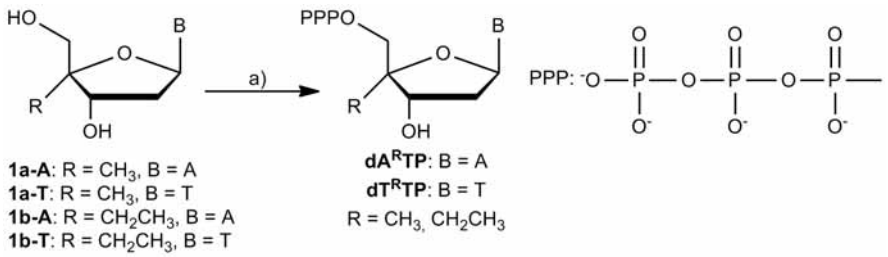

Scheme 3.1-3 *a) 1. $POCl_3$ in $PO(OMe)_3$, (proton sponge for T) 0°C -> r.t., 2 - 4h, 2. Bu_3N, $(Bu_3NH)_2H_2P_2O_7$ in DMF, 0°C, 15 min, 3. TEAB buffer, 40 min, 25% ($dT^{Me}TP$) / 41% ($dT^{Et}TP$) / 9% ($dA^{Me}TP$) / 11% ($dA^{Et}TP$)*

3.1.5 Synthesis of 3'-Phosphoramidite Building Blocks

Introduction of the modified nucleosides into oligonucleotides for the use as templates was accomplished by means of standard phosphoramidite chemistry (**Scheme 3.1-4**). The exocyclic amino function of 4'-alkylated 2'-deoxyadenosine was protected as a formamidine protecting group. Without further purification, the protected adenosine building blocks as well as their thymidine analogues were transformed into the 5'-dimethoxytrityl protected compounds. After column purification phosphitylation of the nucleosides with 2-cyanoethyl-*N*,*N*-(diisopropylamino)-chlorophosphoramidite using Huenig base afforded the desired building blocks in good overall yields (60-90%).

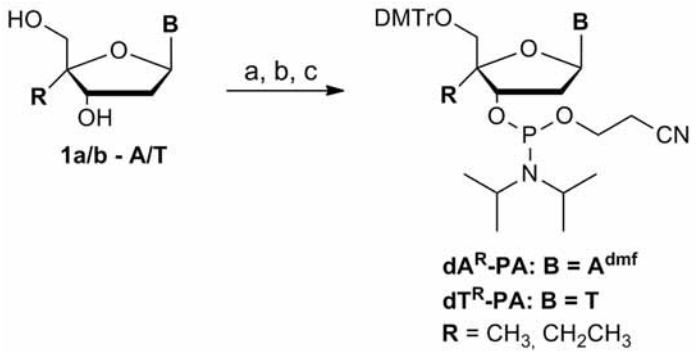

Scheme 3.1-4 *a) For A: DMF-Acetal, DMF, 4h, r.t., quantitativ; b) DMTr-Cl, Pyr, 4-16h, r.t., 97% (dT^{Me}) / 99% (dT^{Et}) / 83% (dA^{Me}) / 94% (dA^{Et}); c) 2.2 eq 2-cyanoethyl-N,N-(diisopropylamino)-chlorophosphoramidite, 5 eq Huenig base, 4-12h, r.t., 72% (dT^{Me}) / 94% (dT^{Et}) / 96% (dA^{Me}) / 91% (dA^{Et}).*

Phosphoramidites **dA^R-PA** and **dT^R-PA** were used in an automated solid support synthesis to obtain modified oligonucleotides. Coupling times of the modified phosphoramidites as well as of the subsequent coupling have been increased to 10 min. The 36 nt long oligomers, still containing the 5'-*O*-DMTr group, were purified by RP-HPLC and additionally after cleavage of the protection group by preparative polyacrylamide gel electrophoresis (PAGE).

3.1.6 Synthesis of 4'-Modified Primer and Template Strands

25 nt Primer sequences bearing 4'-alkylated nucleotides at the primer 3'-end have been synthesized on modified solid supports. Treatment of the 5'-*O*-DMTr-protected nucleosides with EDC, Et_3N and DMAP in pyridine with an succinylated LCAA CPG resin over night yielded the desired solid supports (**Scheme 3.1-5**) [standard protocol: *Beaucage,* 2001].

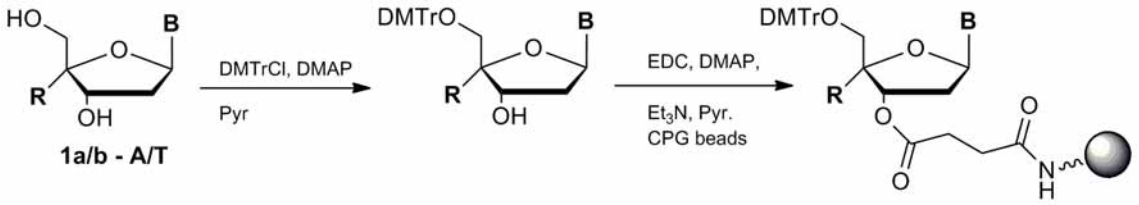

Scheme 3.1-5 *Schematic drawing of the attachment of nucleosides to LCAA CPG resin.*

All synthesized primer and template sequences (modified and unmodified) are shown in **Table 3.1-2**. Primers bearing the **dA^R** modification have been used in melting temperature experiments to see whether the modifications have any influence on the stability of DNA helices.

Primer-Template Complex	T_M [°C]
5´-GTG GTG CGA AAT TTC TGA CAG ACA **T*** 3´-CAC CAC GCT TTA AAG ACT GTC TGT ACT GTC TGC GTG	T* = H: 56.9 T* = Me: 56.9 T* = Et: 56.9
5´-GTG GTG CGA AAT TTC TGA CAG ACA 3´-CAC CAC GCT TTA AAG ACT GTC TGT **T*** CT GTC TGC GTG	n.a.
5´-GTG GTG CGA AAT TTC TGA CAG ACA **A*** 3´-CAC CAC GCT TTA AAG ACT GTC TGT TCT GTC TGC GTG	A* = H: 60.9 A* = Me: 60.9 A* = Et: 60.9
5´-GTG GTG CGA AAT TTC TGA CAG ACA 3´-CAC CAC GCT TTA AAG ACT GTC TGT **A*** CT GTC TGC GTG	n.a.

Table 3.1-2 *Primer and template sequences synthesized in this work. Melting temperature experiments using 4'-modified primers (A*) have been performed. Values for T* are taken from [Summerer, 2004].*

Summerer had already observed no effect in melting temperature experiments for **dT^R** in corresponding primers [*Summerer*, 2004]. In the same manner, the melting temperatures at the primer end were not decreased for **dA^R**. In other studies, *Detmer* investigated the influence of a single 4'-alkylated thymidine in *Dickerson-Drew-Dodecamers* [*Detmer* et al., 2003]. This sequence is often used for studying intrinsic properties of B-form DNA [*Wing* et al., 1980]. The influence there proved to be small, most prominent for **dT^{iP}**-modified oligonucleotides (1.0 °C lower melting point). Thus, 4'-alkylation seems to have little impact on the duplex stability.

3.1.7 Functional Studies on 4'-Alkylated 2'-Deoxynucleoside Triphosphates

The complementary 4'-alkylated 2'-deoxyadenosine triphosphate probes allowed functional comparison studies on DNA polymerases. Different kinetic behavior for the incorporation of dTTP opposite a template base dA on the one hand and dATP opposite template base dT on the other hand has already been reported [*Kunkel and Bebenek*, 1988]. Using the 4'-modified nucleotides, the rigidity of the binding pocket could be investigated and give additional information to affirm the model of steric complementarity [*Kool* et al., 2000].

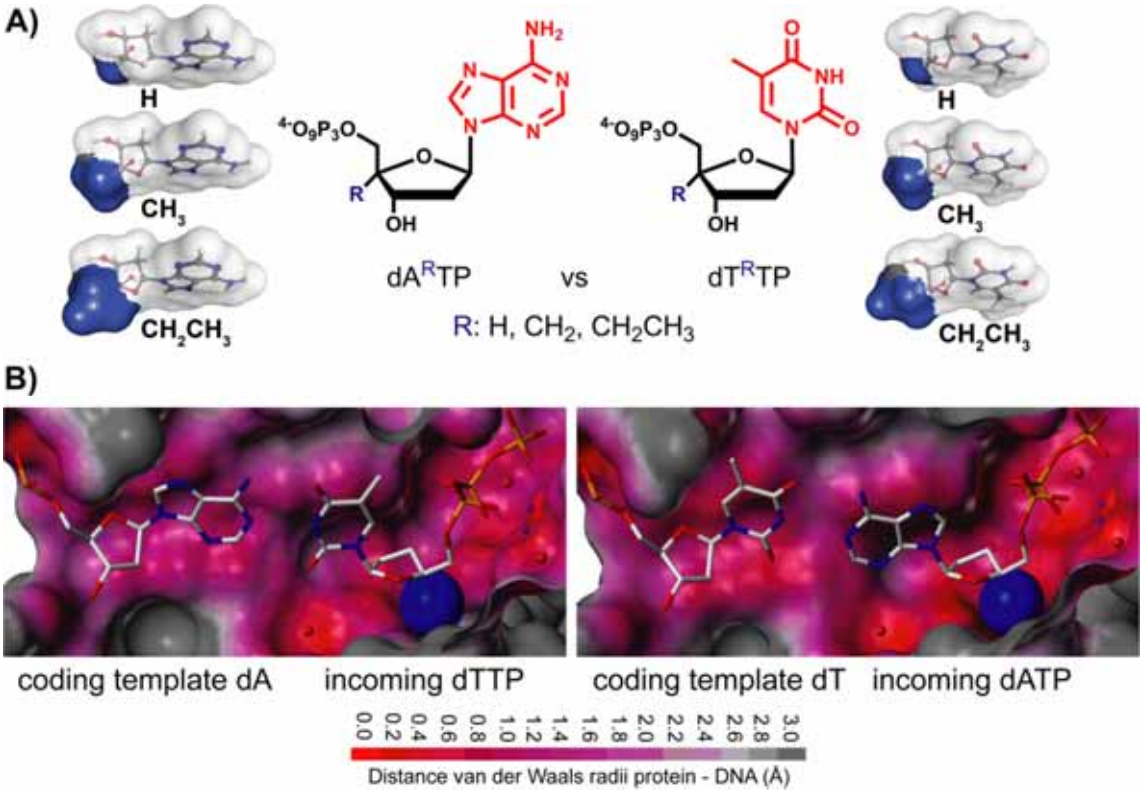

Figure 3.1-3 *A) Size-augmented 2'-deoxynucleoside-5'-triphosphates as steric probes. Models showing the increasing steric demand of the 4'-residues (blue) for the six Nucleoside derivatives (**dA^{R}TP** left, **dT^{R}TP** right) visualized by a Connolly surface using* Sybyl 7.2 MolCad module. *B) Graphic representation of the distances of the van der Waals radii between DNA and protein for KlenTaq DNA polymerase. The separated surfaces were calculated from PDB-files (1QSY for dATP, 1QTM for dTTP) using* Sybyl 7.2 (Tripos). *View of the nascent base pair (incoming and templating nucleotides). The blue sphere illustrates the modification position. Color range is given in the figure [Streckenbach et al., 2009].*

Therefore, the effects of probes **dA^{R}TP** and **dT^{R}TP** were tested on the exonuclease-deficient variant of the Klenow fragment of *Escherichia coli* DNA polymerase I (KF exo-), a relatively high-fidelity enzyme extensively used as a model in investigations of the intrinsic DNA polymerase mechanism and function. In addition, DNA polymerase IV of *Sulfolobus solfataricus P2* (Dpo4), a member of the

error-prone, Y-family, TLS polymerases, was investigated. The depicted graphical representation illustrates the shape of the employed probes as well as the orientation of their 4'-residue inside a binding pocket. For this illustration, the reported crystal structures (1QSY for dATP and 1QTM for dTTP) have been chosen, as no adequate structures for both nucleotides complexed with the Klenow fragment or Dpo4 exist (**Figure 3.1-3**). A blue sphere illustrates the position of the 4'-alkyl moiety.

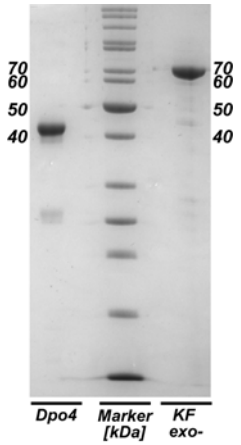

Figure 3.1-4 SDS-PAGE of purified Dpo4 polymerase (left) and KF exo- (right).

Plasmids of both DNA polymerases have been transformed in *Escherichia coli*. According to established protocols in our group, overexpression and subsequent purification by Ni-NTA affinity chromatography afforded both polymerases in sufficient amounts and purity (KF exo- 68 kDa, Dpo4 42 kDa) (**Figure 3.1-4**).

```
5'-GTG GTG CGA AAT TTC TGA CAG ACA
3'-CAC CAC GCT TTA AAG ACT GTC TGT A^RCT GTC TGC GTG-5'
                                   T^R
```

Figure 3.1-5 *Primer and template sequence with the modified position highlighted.*

To monitor polymerase function, a gel-based single nucleotide insertion assay was used, in which a 24 nt primer was designed to hybridize with a corresponding 36 nt template strand that codes for the insertion of the respective canonical dNTP adjacent at the primer 3'-end (**Figure 3.1-5**).

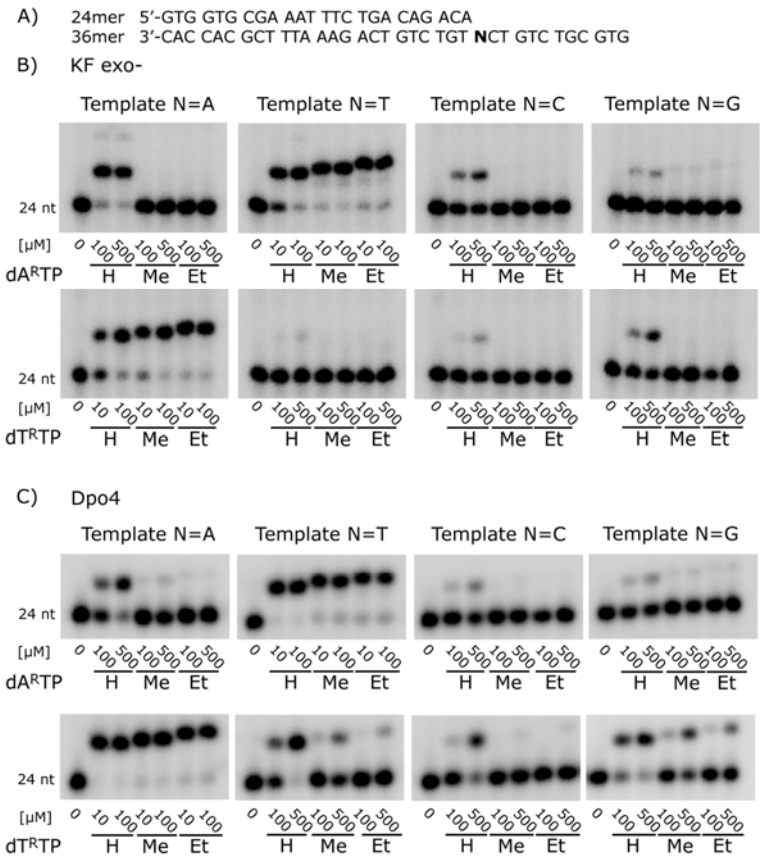

Figure 3.1-6 *Nucleotide insertion catalyzed by KF exo- and Dpo4: A) Primer/template sequence. B) Reactions catalyzed by KF exo-. C) Reactions catalyzed by Dpo4. Conditions: Primer/template complex (150nM), KF exo-/Dpo4 (10nM), 37°C, 15 min matched / 45 min mismatched. In each case, the nucleotide concentrations [μM] are given in the figure [Streckenbach et al., 2009].*

First, a preliminary qualitative incorporation assay using different dNTP concentrations already disclose the different mechanistic behavior of the two polymerases (**Figure 3.1-6**). In accordance with earlier studies, we found that **dT^{R}TPs** were substrates for KF exo- and were incorporated opposite the canonical dA. The same was found for the corresponding **dA^{R}TPs**. KF exo- was able to incorporate the natural dATP opposite dA in higher concentrations. For both, **dT^{R}TPs** and **dA^{R}TPs**, incorporation opposite non-canonical templates was significantly diminished as expected. Other natural mismatches were formed with low yields even using high nucleoside triphosphates concentrations. Consistently, Dpo4 showed comparable results. However, Dpo4 was able to process modified **dT^{R}TPs** opposite dT and dG template sites.

DNA polymerase	Template Base N*	Nucleotide	K_M (μM)	k_{cat} (min^{-1})	k_{cat} / K_M ($mM^{-1}min^{-1}$)	rel. efficiency (Alkyl/H)
KF exo-	A	dTTP	0.05 ± 0.01	6.04 ± 0.15	121000	**1**
		$dT^{Me}TP$	3.50 ± 0.44	10.9 ± 0.6	3110	**0.03**
		$dT^{Et}TP$	2.45 ± 0.19	14.8 ± 0.6	6080	**0.05**
	T	dATP	0.02	8.28 ± 0.34	414000	**1**
		$dA^{Me}TP$	1.29 ± 0.09	11.0 ± 0.2	8530	**0.02**
		$dA^{Et}TP$	1.90 ± 0.31	10.1 ± 0.5	5320	**0.01**
Dpo4	A	dTTP	5.36 ± 0.66	18.5 ± 0.8	3450	**1**
		$dT^{Me}TP$	4.79 ± 0.28	10.1 ± 0.2	2110	**0.61**
		$dT^{Et}TP$	12.5 ± 0.59	6.72 ± 0.14	538	**0.16**
	T	dATP	3.96 ± 0.48	22.6 ± 0.8	5710	**1**
		$dA^{Me}TP$	11.8 ± 2.2	9.17 ± 0.78	777	**0.14**
		$dA^{Et}TP$	11.4 ± 1.4	5.21 ± 0.26	457	**0.08**
	G	dTTP	807 ± 123	8.32 ± 0.47	10.3	**1**
		$dT^{Me}TP$	274 ± 33	0.81 ± 0.05	2.96	**0.29**
		$dT^{Et}TP$	233 ± 36	0.29 ± 0.01	1.24	**0.12**
	T	dTTP	877 ± 122	5.80 ± 0.27	6.61	**1**
		$dT^{Me}TP$	372 ± 68	0.71 ± 0.06	1.91	**0.29**
		$dT^{Et}TP$	160 ± 24	0.19 ± 0.01	1.19	**0.18**

Table 3.1-3 *Steady-state kinetic analyses of nucleotide insertion by KF exo- and Dpo4. Data shown represent averages derived from 3-times repeated experiments.*

**Primer-template substrates used:*
5'-GTG GTG CGA AAT TTC TGA CAG ACA *primer (24nt)*
*3'-CAC CAC GCT TTA AAG ACT GTC TGT **N**CT GTC TGC GTG* *template (36nt)*

Michaelis-Menten steady-state kinetics under single completed hit conditions have been performed in order to compare and quantify the different behavior of the two polymerases on the modified substrates [*Creighton* et al., 1995]. The matched cases for KF exo- showed that dATP was more efficiently processed than dTTP in absolute values. Interestingly, the opposite turned out for the size-augmented nucleotides. To some extent size-augmentation was better tolerated in the thymidines **$dT^{R}TPs$** (relative efficiencies 4'-alkyl/4'-H) in respect to the **$dA^{R}TP$** counterparts (see **Table 3.1-3**). This effect was most significant for the bulkiest 4'-ethylated analogues. However, within the respective nucleotide the differences between 4'-methyl and 4'-ethyl were only small.

A partly different picture was observed for Dpo4. Again, alkylated **$dT^{R}TPs$** were processed more efficiently compared to their unmodified analogues than the corresponding **$dA^{R}TP$** analogues, while unmodified dATP yielded likewise higher

absolute values. When comparing the relative incorporation efficiencies (4'-alkyl/4'-H) of **dN^{Me}TPs** by both enzymes it was evident that the error-prone Dpo4 processed the bulkier nucleotides more efficiently in respect to the unmodified nucleotides than KF exo-.

Interestingly, Dpo4 was able to incorporate the **dT^{R}**-residues opposite non-canonical template dG and dT in efficiencies measurable under single completed hit conditions. The corresponding **dA^{R}TP** analogues were processed significantly more selective and only minor amounts of incorporation products were observed opposite non-canonical templates.

3.1.8 Additional Size-Augmentation in the Coding Template Strand

The results gained from 4'-alkylated 2'-deoxynucleoside triphosphates encouraged further studies employing additional steric augmentation in the coding template strand (**Figure 3.1-7**). With this additional steric constraint, the binding pocket's flexibility should reach its limits.

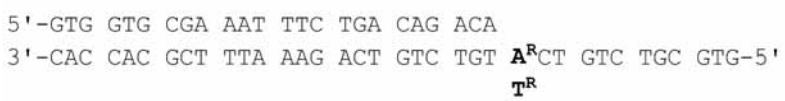

Figure 3.1-7 *Primer and template sequence with the modified position highlighted.*

Modified thymidines in the coding template strand have already been investigated by *Strerath* [*Strerath* et al., 2002]. Albeit the fact that the incorporation of canonical nucleotides opposed to it was influenced less than in the reversed case (size-augmentation in the nucleotides opposite dA), the modification decreased the incorporation of non-canonical nucleotides corresponding to higher selectivity. This observation was explained by additional constraints that can be overcome in the matched case and not in the mismatched case.

However, with complementary nucleotides in hand access to a comparison of nucleobase orientation paired with steric clashes on both ends of the binding pocket became possible. Again, the effects on both KF exo- and Dpo4 have been investigated. Resulting Michaelis-Menten constants are shown in **Table 3.1-4** (for KF exo-) and **Table 3.1-5** (for Dpo4).

DNA polymerase	Template Base N*	Nucleotide	K_M (μM)	k_{cat} (min^{-1})	k_{cat} / K_M ($mM^{-1}min^{-1}$)	rel. efficiency (Alkyl/H)
KF exo-	A^{Me}	dTTP	0.03 ± 0.01	0.46 ± 0.02	15300	**1**
		$dT^{Me}TP$	5.09 ± 0.41	11.4 ± 0.3	2240	**0.15**
		$dT^{Et}TP$	3.02 ± 0.38	9.47 ± 0.40	3140	**0.21**
	A^{Et}	dTTP	0.06 ± 0.01	1.03 ± 0.03	17200	**1**
		$dT^{Me}TP$	29.0 ± 4.7	14.2 ± 0.8	490	**0.03**
		$dT^{Et}TP$	24.6 ± 4.0	12.1 ± 0.6	492	**0.03**
	T^{Me}	dATP	0.08 ± 0.02	3.28 ± 0.15	41000	**1**
		$dA^{Me}TP$	2.12 ± 0.35	10.2 ± 0.5	4810	**0.12**
		$dA^{Et}TP$	3.48 ± 0.49	11.7 ± 0.5	3360	**0.08**
	T^{Et}	dATP	0.09 ± 0.01	4.36 ± 0.15	48400	**1**
		$dA^{Me}TP$	6.09 ± 1.21	7.63 ± 0.54	1250	**0.03**
		$dA^{Et}TP$	5.02 ± 0.69	7.59 ± 0.42	1510	**0.03**

Table 3.1-4 *Steady-state kinetic analyses of nucleotide insertion by KF exo- and Dpo4. Data shown represent averages derived from triplet experiments.*

**Primer-template substrates used:*
5'-GTG GTG CGA AAT TTC TGA CAG ACA *primer (24nt)*
*3'-CAC CAC GCT TTA AAG ACT GTC TGT **N**CT GTC TGC GTG* *template (36nt)*

The results confirmed aforementioned findings that dATP was more efficiently incorporated than dTTP. The previously described triphosphate effect (**dT^RTP** > **dA^RTP** relative efficiencies 4'-alkyl/4'-H) was only observable for 4'-methyl modified templates. The bulky substrates **dT^RTPs** were relatively better incorporated compared to their **dA^RTP** counterparts. For the 4'-ethyl modified templates this discrepancy vanished. Nevertheless, again dATP was incorporated more efficiently opposite dT than dTTP opposite dA.

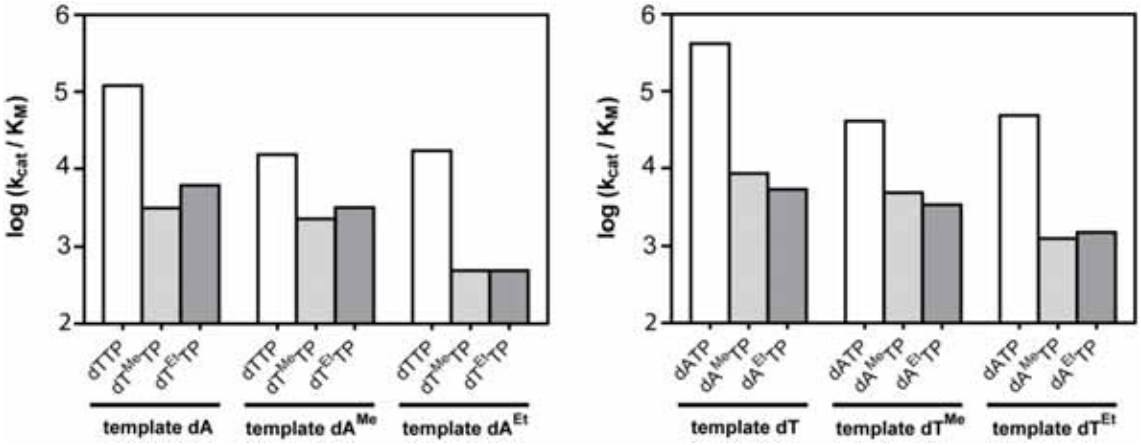

Figure 3.1-8 *Bar chart comparing the incorporation efficiencies (K_M / k_{cat}) of KF exo- (template* ***dA^R*** *left,* ***dT^R*** *right).*

Comparing effects of modifications inside the template with the respective modified nucleoside triphosphates, the template effect is slightly lower than the triphosphate effect (**Figure 3.1-8**). It was even less pronounced for 4'-alkylated triphosphates. Interestingly, the effects of templating **dA^R** and **dT^R** did not differ significantly.

Besides incorporation efficiencies, two effects attracted attention within the different templates. First, for unmodified dNTP the first order kinetic constant k_{cat} decreased remarkably upon size-augmentation in the template strand, whereas for modified **dN^{R}TP** k_{cat} remained almost unaffected. The second effect is less distinct. K_M to some extent remained almost constant in most cases for the natural dNTP, while for modified **dN^{R}TP** it increased between the different templates. This was most significant opposite the 4'-ethylated coding nucleotide. It should be noted that the discussion of K_M and k_{cat} should be treated cautiously, as Michaelis-Menten kinetics give only results on the overall reaction process in steady-state. The enzyme catalysis of DNA polymerases consists of several steps that cannot be resolved by this technique (detailed discussion see **Chapter 1.1.6**).

DNA polymerase	Template Base N*	Nucleotide	K_M (μM)	k_{cat} (min^{-1})	k_{cat} / K_M ($mM^{-1}min^{-1}$)	rel. efficiency (Alkyl/H)
Dpo4	A^{Me}	dTTP	40.7 ± 2.9	12.5 ± 0.3	307	**1**
		$dT^{Me}TP$	39.4 ± 5.5	8.74 ± 0.36	222	**0.72**
		$dT^{Et}TP$	176 ± 12	8.16 ± 0.21	46.4	**0.15**
	A^{Et}	dTTP	196 ± 31	11.6 ± 0.7	59.2	**1**
		$dT^{Me}TP$	150 ± 23	2.85 ± 0.17	19.0	**0.32**
		$dT^{Et}TP$	359 ± 47	2.32 ± 0.11	6.46	**0.11**
	T^{Me}	dATP	13.8 ± 2.0	7.35 ± 0.24	533	**1**
		$dA^{Me}TP$	91.5 ± 6.4	13.9 ± 0.4	152	**0.29**
		$dA^{Et}TP$	117 ± 10	14.0 ± 0.6	120	**0.23**
	T^{Et}	dATP	82.1 ± 6.1	13.5 ± 0.3	164	**1**
		$dA^{Me}TP$	176 ± 16	3.26 ± 0.11	18.5	**0.11**
		$dA^{Et}TP$	167 ± 27	1.64 ± 0.12	9.82	**0.06**

Table 3.1-5 *Steady-state kinetic analyses of nucleotide insertion by KF exo- and Dpo4. Data shown represent averages derived from 3-times repeated experiments.*

**Primer-template substrates used:*
5'-GTG GTG CGA AAT TTC TGA CAG ACA *primer (24nt)*
*3'-CAC CAC GCT TTA AAG ACT GTC TGT **N**CT GTC TGC GTG* *template (36nt)*

The results for Dpo4 upon increased steric constraints in the template strand affirmed the observed triphosphate effects already reported before. Like in case of KF exo-, dATP showed higher absolute incorporation efficiencies than dTTP. Once more, **$dT^{R}TPs$** were relatively more efficiently incorporated than **$dA^{R}TPs$**. As observed for unmodified template, the relative efficiencies were significantly higher than for KF exo-. However, this difference became marginal in the bulkiest case, **$dN^{Et}TPs$** opposite **dN^{Et}** (4'-alkyl/4'-H: 0.11 and 0.06 versus 0.03 and 0.03, respectively).

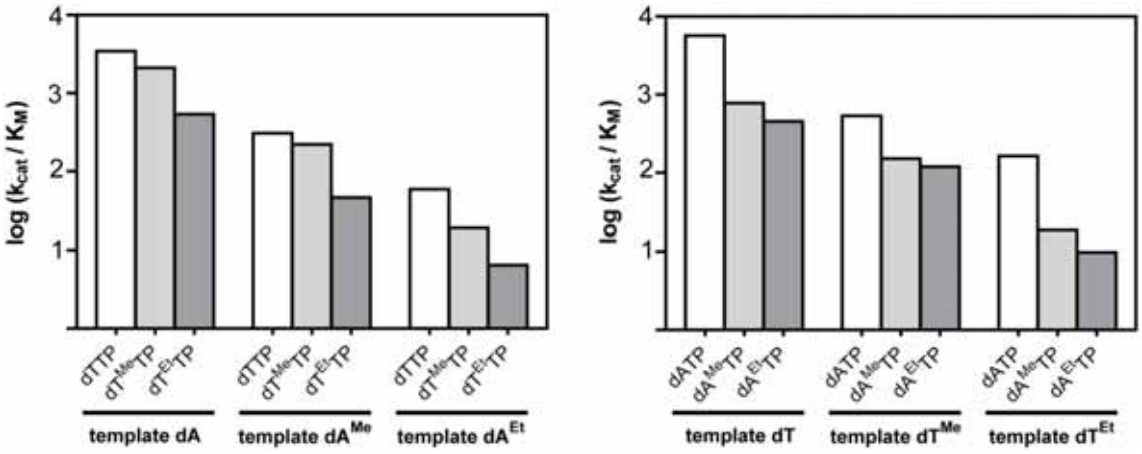

Figure 3.1-9 *Bar chart comparing the incorporation efficiencies (K_M /k_{cat}) of Dpo4 (template* ***dA^R*** *left,* ***dT^R*** *right).*

Curiously, the modified template had the same impact on incorporation efficiency by Dpo4 for all triphosphates (see bar charts in **Figure 3.1-9**). This decrease resulting from modified templates was even stronger than the effect caused by introduction of alkyl residues in the triphosphates.

The observations on K_M and k_{cat} made for KF exo- were not observed for Dpo4. K_M increased in all cases upon size-augmentation, whereas at the same time k_{cat} did not behave consistently.

3.1.9 Discussion Triphosphate Effect

The qualitative gel-based single nucleotide insertion assay already revealed to some degree the polymerases diversity. While in matched case both enzyme processed the natural and the size-augmented substrates, in mismatched case the size-augmented probes **dT^{R}TPs** were incorporated opposite the two non-canonical template bases dG and dT only by Dpo4. Other non-canonical base pairing was discriminated efficiently by the sterically increased probes, whereas natural dATP and dTTP showed extension to some degree in some cases for both enzymes. This behavior already indicated the reported flexibility in the active site of the TLS polymerase Dpo4. Noteworthy, under the applied conditions (concentrations in the range of K_M) the gel analysis showed higher incorporation for the modified substrates probably reflecting the higher k_{cat} values.

The kinetic results further corroborate these findings in many respects. First, the error-prone TLS DNA polymerase Dpo4 incorporated the size-augmented nucleotides relatively more efficiently than the more selective KF exo-. DNA polymerases are assumed to form nucleotide binding pockets that differ in properties like shape and tightness. Thus, high-fidelity DNA polymerases are believed to form more rigid binding pockets tolerating less geometric deviation, while low-fidelity enzymes exhibit more flexibility leading to decreased fidelity [*Goodman*, 2002, *Prakash* et al., 2005]. Therefore, our experimental data were in agreement with these earlier findings [*Kim* et al., 2005, 2006, *Mizukami* et al., 2006, *Sintim and Kool*, 2006, *Silverman* et al., 2007].

Secondly, for both enzymes, the incorporation of unmodified dA was more efficient than was dT. However, the opposite was found for the size-augmented probes. It appeared that the bulkier purine **dA^{R}** nucleotides were subjected to more steric constraints within the active site of the enzymes than were the **dT^{R}** pyrimidines. These different properties might well be the cause for the observation that the selectivity of nucleotide incorporation might vary depending on the nascent nucleotide pair orientation [*Kunkel and Bebenek*, 2000, *Minnick* et al., 2002].

This assumption was further corroborated by the finding that the size-augmented **dT^{R}TPs** were more efficiently incorporated opposite non-canonical template nucleotides than their adenosine counterparts. These findings provide experimental evidence that packing of the nucleotide sugar residue varies within the orientation of the nascent nucleotide pair as well as in different polymerase families. They also support

the model of varied active site tightness as a cause for the varied selectivity observed among different DNA polymerases. Structural investigations showed that the sugar moiety of the incoming dNTP is fully embedded within the substrate binding pockets of DNA polymerases and an integral part of substrate recognition processes [*Johnson and Beese*, 2004, *Rothwell and Waksman*, 2005]. Hence, editing of the incoming dNTP sugar might provide the enzyme with additional paths to achieve canonical base pair formation through indirect readout of aberrant sugar conformations.

The results of the triphosphate effect and the synthesis of the 4'-alkylated triphosphates have been published in Streckenbach, F., Rangam, G., Moller, H.M. & Marx, A. Steric constraints dependent on nucleobase pair orientation vary in different DNA polymerase active sites. *Chembiochem* **10**, 1630-3 (2009).

3.1.10 Discussion Template Effect

The effects observed for 4'-alkylated nucleotides could be further confirmed by gradual expanded constraints on the opposite site of the binding pocket. Once more, Dpo4 processed the size-augmented nucleotides even opposite a modified coding nucleotide relatively more efficiently within one template than the more selective KF exo- (4'-alkyl/H in **Table 3.1-4** and **Table 3.1-5**). At the same time, the natural dATP was incorporated again more efficiently than the dTTP by both enzymes. In almost the same manner as above, the bulkier purine **dA^{R}** nucleotides were subject to more steric constraints within the active site of the enzymes than were the **dT^{R}** pyrimidines for both KF exo- and Dpo4.

DNA polymerase	Nucleotide	Template Base N*	rel. efficiency (Alkyl/H)	Nucleotide	Template Base N*	rel. efficiency (Alkyl/H)
KF exo-	dTTP	A	**1**	dATP	T	**1**
		A^{Me}	**0.12**		T^{Me}	**0.10**
		A^{Et}	**0.14**		T^{Et}	**0.12**
	$dT^{Me}TP$	A	**1**	$dA^{Me}TP$	T	**1**
		A^{Me}	**0.72**		T^{Me}	**0.56**
		A^{Et}	**0.16**		T^{Et}	**0.14**
	$dT^{Et}TP$	A	**1**	$dA^{Et}TP$	T	**1**
		A^{Me}	**0.52**		T^{Me}	**0.63**
		A^{Et}	**0.08**		T^{Et}	**0.28**
Dpo4	dTTP	A	**1**	dATP	T	**1**
		A^{Me}	**0.09**		T^{Me}	**0.09**
		A^{Et}	**0.02**		T^{Et}	**0.03**
	$dT^{Me}TP$	A	**1**	$dA^{Me}TP$	T	**1**
		A^{Me}	**0.11**		T^{Me}	**0.20**
		A^{Et}	**0.01**		T^{Et}	**0.02**
	$dT^{Et}TP$	A	**1**	$dA^{Et}TP$	T	**1**
		A^{Me}	**0.09**		T^{Me}	**0.26**
		A^{Et}	**0.01**		T^{Et}	**0.02**

Table 3.1-6 *Template effect: A comparison of the relative efficiencies $(K_D / k_{cat})_{Alkyl} / (K_D / k_{cat})_H$ for KF exo- and Dpo4.*

**Primer-template substrates used:*
5'-GTG GTG CGA AAT TTC TGA CAG ACA *primer (24nt)*
*3'-CAC CAC GCT TTA AAG ACT GTC TGT **N**CT GTC TGC GTG* *template (36nt)*

Additionally, the effect of size-augmentation within the coding nucleotide could be measured. The template effect with the same triphosphate was more pronounced for Dpo4 than for KF exo-. Introduction of one methyl group in the templates caused a drop in the efficiencies by a factor of four to ten for the respective nucleotides for Dpo4. Upon further augmentation to ethyl the efficiencies dropped again threefold to tenfold (see **Table 3.1-6**). In case of KF exo- this decrease around tenfold could only be observed for the unmodified dNTP. Here, the differences between 4'-methyl and 4'-ethyl were only small. Astonishingly, a partly different picture was observed for modified **dN^{R}TP** by KF exo-. Upon introduction of one methyl group in the coding

nucleotide, the efficiency decreased only by a factor of less than two. Size-augmentation to an ethyl group led to a further twofold to fivefold drop (see **Table 3.1-6**).

Taken together, the results derived from size-augmentation on both ends of the active site of DNA polymerases strongly support the model of active site tightness [*Kool* et al., 2000]. Moreover, they also support the proposed flexibility that TLS polymerases should possess to accommodate certain DNA lesions [*Mizukami* et al., 2006]. Base pair orientation caused different behavior by both enzymes. Upon additional augmentation in the template strand, the flexibilities of the binding pockets of both enzymes reached their limits. Incorporation efficiencies of the bulkiest pairs (**dN^{Et}-$dN^{Et}TP$**) in Dpo4 even reached the level of the investigated mismatched cases (dT-dTTP and dG-dTTP). Unfortunately, steady-state kinetics allowed only limited interpretations of the precise reaction mechanisms.

3.2 *KlenTaq* DNA Polymerase Probed by Size-Augmented Nucleotides in Transient Kinetic Studies

3.2.1 Introduction

The results from investigation of KF exo- and Dpo4 corroborated active site tightness. As presteady-state kinetics deliver precise parameters of nucleotide binding and incorporation, following experiments were based on this technique.

As DNA polymerase I of *Thermus aquaticus* (*Taq* polymerase) and its N-terminally truncated form called *KlenTaq* polymerase are well studied family A polymerases [*Barnes*, 1992], *KlenTaq* was chosen as new model of investigations because studies on its mechanism of nucleotide binding and incorporation exist [*Rothwell* et al., 2005, *Rothwell and Waksman*, 2007]. Furthermore, structural information on *Taq* and *KlenTaq* polymerase are available, that allow more detailed descriptions [*Kim* et al., 1995, *Li* et al., 1998, *Li and Waksman*, 2001]. A crystallization strategy, adapted from this reports, has been established in our group and has already resulted in first structures by Dr. Andreas Schnur, AG Welte/Marx [Schnur, 2009].

Previous structural investigations by *Waksman* and colleagues on *KlenTaq* DNA polymerase showed that the sugar moiety of the incoming dNTP is fully embedded within the substrate binding pocket of DNA polymerases and is an integral part of substrate recognition processes. Nevertheless, detailed studies on interaction of amino acids with the 2'-deoxyribose of the nucleoside triphosphate have not yet been performed.

3.2.2 Functional Studies

As presteady-state kinetics offer data on binding of substrates and their incorporation, *KlenTaq* wild type (wt) DNA polymerase should be probed by 4'-alkylated thymidine-5'-triphosphates (**$dT^{R}TP$**) in transient enzyme kinetics by the quench flow technology. Adopting recently published crystallization techniques on *KlenTaq*, Karin Betz, in a corporation of AG Marx and AG Welte, used these probes for crystallization trials. Functional and structural results together should provide new mechanistic details on the substrate processing and the involvement of sugar readout through amino acid contacts by *KlenTaq* wt DNA polymerase.

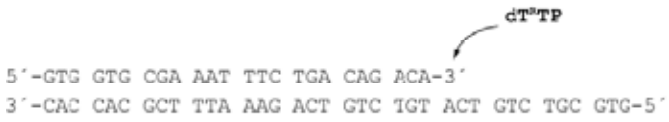

Figure 3.2-1 *24 nt primer and 36 nt template sequence context used in the transient kinetic assay.*

Transient kinetic studies were performed under presteady-state *single turnover conditions* at 37°C in RQF Buffer [*Rothwell* et al., 2005]. A rapid quench flow machine enables measurements of reaction times in millisecond intervals. Time series for different dNTP concentrations were measured. Therefore, a designed 24 nt primer was hybridized with a 36 nt template strand that codes for a dA adjacent at the primer 3'-end (**Figure 3.2-1**). The primer-template complex was pre-incubated with an excess of *KlenTaq* wt DNA polymerase. *KlenTaq* wt DNA polymerase was expressed and purified by Dr. Christian Glöckner, AG Marx [Glöckner, 2008]. The rapid quench flow apparatus starts the reaction by rapid mixing of a reaction volume of primer-template-enzyme complex solution with the dNTP solution in an appropriate buffer and subsequently quenches the reaction at defined time intervals by EDTA solution. In this way, time series for several dNTP concentrations were measured. Converted primer was separated from unreacted primer on a denaturating PAGE. The ratio of conversion (I_{ext}/I_{prim} in %) was plotted against the reaction time and fitted to an exponential equation. Each obtained catalytic rates (k_{obs}) were then plotted against the corresponding dNTP concentration used and fitted to a hyperbolic equation to determine the K_D and k_{cat} of the incoming nucleotide (see **Chapter 1.1.6**, details on calculations in **Chapter 6.3.13**).

dT^RTP	K_D (µM)	k_{pol} (s^{-1})	k_{pol} / K_D ($M^{-1} \cdot s^{-1}$)	rel. eff. [a]
dTTP	25.0 ± 3.4	8.80 ± 0.37	352,000	1
$dT^{Me}TP$	119 ± 21	0.17 ± 0.01	1,430	0.0041
$dT^{Et}TP$	115 ± 18	0.13 ± 0.01	1,130	0.0032

[a] rel. eff.: relative efficiency; efficiency: k_{pol} / K_D

Table 3.2-1 *Transient kinetic parameters for nucleotide incorporation by the KlenTaq wt DNA polymerase.*

The overall reaction efficiency (k_{pol} / K_D) for the natural substrate dTTP was 352,000 $M^{-1}s^{-1}$. dTTP bound to the primer-template-enzyme complex with an dissociation constant K_D of 25.0 µM and was incorporated at a rate k_{pol} of 8.80 s^{-1}.

However, *KlenTaq* wt incorporated the size-augmented nucleotides with reduced efficiencies compared to their natural counterpart. The efficiencies dropped 250-fold for

dT^{Me}TP and 300-fold for **dT^{Et}TP**. While the effect on the K_D was only fourfold and fivefold, a 51- and 67-fold reduction was observed for k_{pol} (**Table 3.2-1** and **Figure 3.2-2**). All three parameters showed no great change upon size-augmentation from 4'-methyl to 4'-ethyl residue.

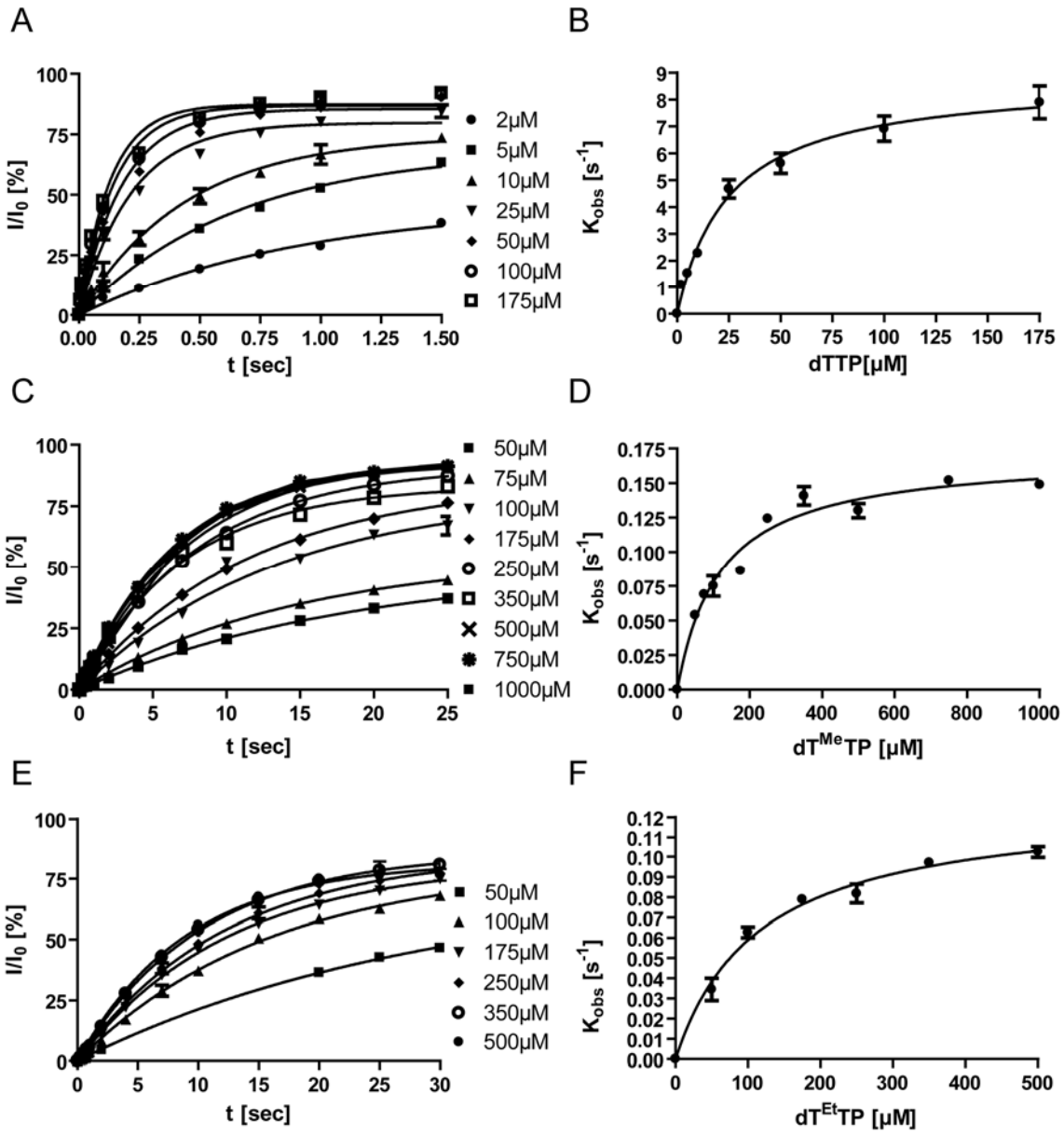

Figure 3.2-2 *Presteady-state kinetics of* ***dT^{R}TP*** *incorporation in a 24mer/36mer primer-template complex (50 nM) by KlenTaq wt (500 nM). (A, C, and E) Graphical plot of product formation in percent as a function of time. The curves show the best fit of the data to a single exponential equation. A preformed complex of polymerase, primer and template was rapidly mixed with different concentrations of dTTP (A),* ***dT^{Me}TP*** *(C), and* ***dT^{Et}TP*** *(E) as indicated in the figure. (B, D, and F) Dependence of the pre-steady state rates on the dTTP (B),* ***dT^{Me}TP*** *(D), and* ***dT^{Et}TP*** *(F) concentrations. The k_{obs} values were plotted versus the* ***dT^{R}TP*** *concentration and fitted to a hyperbolic equation.*

3.2.3 Structural Studies

To get further mechanistic insights into nucleotide incorporation, M.Sc. Karin Betz, AG Marx/Welte, crystallized a ternary complex of *KlenTaq* wt, primer-template and incoming 4'-alkylated triphosphate. Using a crystallization strategy reminiscent to the one reported by *Waksman* and coworkers [*Li* et al., 1998], she was able to obtain several crystals with the 4'-alkylated dNTPs and could solve their structures [*Betz* et al., 2010, *Betz*, 2009].

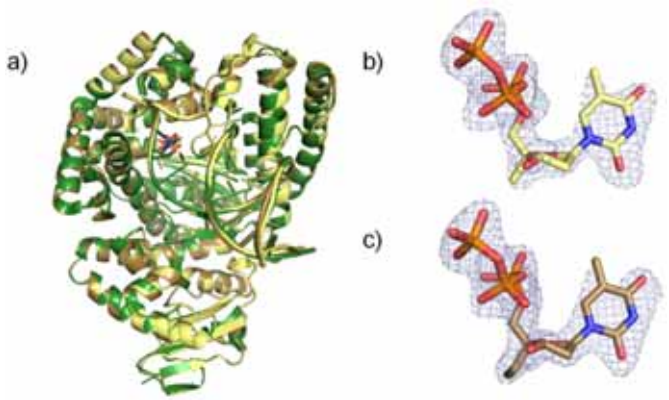

Figure 3.2-3 *Structures of KlenTaq wt ternary complexes. a) Overall structures of KlenTaq wt containing primer, template,* ***dT^{Me}TP*** *(yellow), and* ***dT^{Et}TP*** *(bronze), respectively, superimposed to the known structure containing ddTTP (green, pdb: 1QTM). b) Close-up view of* ***dT^{Me}TP*** *in the complex. The nucleotide is shown as stick model with carbon atoms in yellow, oxygen atoms in red, nitrogen atoms in blue and phosphorus atoms in orange, and is superimposed with the final refined mFo-DFc simulated annealing omit map at 4σ. c) Same as in b) for complex containing* ***dT^{Et}TP****; carbon atoms are shown in bronze [Betz et al., 2010].*

The structures of *KlenTaq* wt in complex with **dT^{Me}TP** and **dT^{Et}TP** superimposed very well with the known structure containing ddTTP by *Waksman* [*Li* et al., 1998] (0.34 Å and 0.31 Å root mean square deviation for Cα atoms, **Figure 3.2-3**, [*Betz* et al., 2010]).

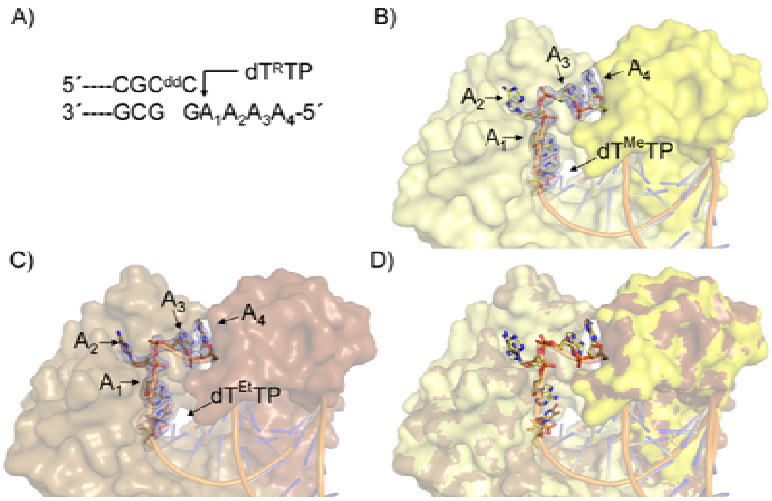

Figure 3.2-4 *Orientation of single-stranded template strand. a) Numbering template nucleotides A_1-A_4. b) Model of structure derived from ternary complex of KlenTaq, primer, template, and* ***dT^{Me}TP****. The respective nucleotides are shown as stick model with carbon atoms in yellow, oxygen atoms in red, nitrogen atoms in blue and phosphorous atoms in orange, and are superimposed with the final refined mFo-DFc simulated annealing omit map. The protein is shown as Connolly surface. c) Same as in b) for complex containing* ***dT^{Et}TP****. d) Superposition of structures depicted in b) and c) using the same colour code [Betz et al., 2010].*

The same held true for the primer and template DNA strand. The online tool PROSIT was used to calculate the conformation (for details see **Appendix 7.5**) [*Sun* et al., 2004]. The DNA was mostly in the B-form, except for the three base pairs at the end of the duplex DNA adjacent to the active site, which were A-form. The entire template was resolved in these structures. The two 5'-terminal nucleotides (A_3 and A_4) of the template strand point towards the thumb domain of the polymerase and adopt slightly different orientations comparing both structures (see **Figure 3.2-4**).

The difference electron density maps at the nucleotide binding site indicated that **dT^{Me}TP** and **dT^{Et}TP** were indeed trapped in the structure. The best fit of the model to the electron density indicated that the 2'-deoxyribose of the nucleotides were puckered in the N-conformation (**Figure 3.2-3**, b and c). Calculations by PROSIT substantiated these assumptions (for details see **Appendix 7.5**) [*Sun* et al., 2004].

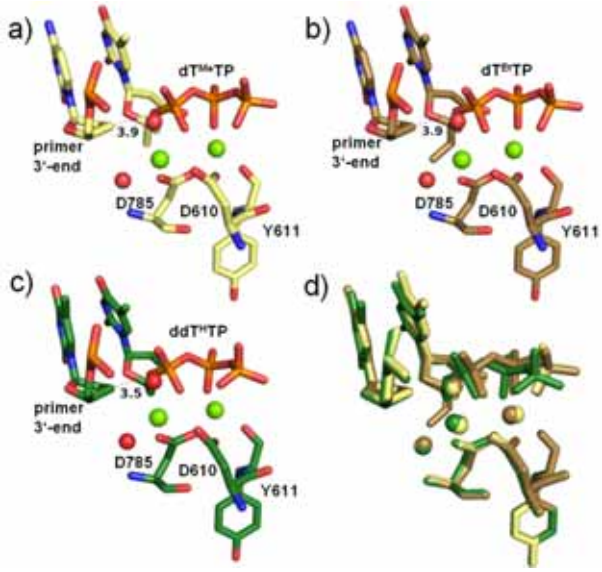

Figure 3.2-5 *Close-up views on primer 3'-end, incoming nucleotide and amino acids complexing divalent cations. a) Stick model from structure derived from ternary complex of KlenTaq, primer, template, and* ***dT^{Me}TP****. Water molecules (red) and magnesium ions (green) are indicated as spheres. The indicated distance was determined by PyMOL and is shown in Å. b) Same as in a) for complex containing* ***dT^{Et}TP****. c) Same as in a) using the reported data containing ddTTP. d) Superposition of structures depicted in a)-c) using the colour code of* ***Figure 3.2-3*** *[Betz et al., 2010].*

Only subtle differences in terms of alignment of the incoming nucleotides, magnesium ions and water molecules were observed (**Figure 3.2-5**). The **dT^{Me}TP** and **dT^{Et}TP** trapped structures as well as the ddTTP superimposed well. Distances of 3.9 Å between C3' of the primer end and the phosphorus atom of the α-phosphate were observed in the structures that contained **dT^{Me}TP** and **dT^{Et}TP**, respectively. A shorter distance of 3.5 Å was found in the ternary structure of *KlenTaq* wt complexed with ddTTP reported previously [*Li* et al., 1998].

3.2.4 Discussion

The overall efficiency for the natural substrate dTTP was in the same order of magnitude as in previously reported data for dATP from *KlenTaq* wt by Dr. Christian Glöckner, AG Marx (352,000 $M^{-1}s^{-1}$ compared to 337,000 $M^{-1}s^{-1}$). The dissociation constant K_D for dTTP was marginal higher (25.0 µM compared to 15.3 µM for dATP), but dTTP was incorporated at a little higher rate k_{pol} (8.80 s^{-1} compared to 5.16 s^{-1}) [*Glöckner*, 2008].

The transient kinetic data showed that *KlenTaq* wt incorporated the size-augmented nucleotides with reduced efficiencies compared to their natural counterpart. The efficiencies dropped 250-fold for **dT^{Me}TP** and 300-fold for **dT^{Et}TP**. While the effect on the K_D was only fourfold to fivefold, a 51- and 67-fold reduction was observed for k_{pol} (**Table 3.2-1**). Interestingly, both nucleotides yielded similar kinetic constants. Thus, the effect on incorporation efficiency by introducing one additional methylene residue in the natural nucleotide was by far larger as the difference between the methyl and ethyl modifications. Similar effects were observed in studies of enzymes from the same sequence family [*Streckenbach* et al., 2009, *Summerer and Marx*, 2001, *Strerath* et al., 2002, *Di Pasquale* et al., 2008]. The effect that size-augmentation was more prominent for the incorporation rate k_{pol} than for the dissociation constant K_D leads to the assumption that structural hindrance acting on the sugar residue plays a major role during the catalysis transition state.

A first insight on the structural environment of 4'-modified **dN^{R}TP** in the active site of *KlenTaq* DNA polymerase could be deduced from the crystal structures obtained by M.Sc. Karin Betz, AG Marx / AG Welte [*Betz* et al., 2010]. The overall structures of *KlenTaq* in complexes containing **dT^{Me}TP** and **dT^{Et}TP** were very similar to the *KlenTaq* structure (1QTM) described earlier with complexed ddTTP, indicating that the modifications had only little effect on the overall enzyme conformation [*Li and Waksman*, 2001]. Especially in the active site, the amino acid backbone showed only minimal deviations. Furthermore, primer and template DNA strand of the structures fit very well. The DNA was mostly in the B-form, except for the three base pairs at the end of the duplex DNA adjacent to the active site, which were A-form. The same was reported in the structures containing non-modified nucleotides [*Li* et al., 1998, 1999].

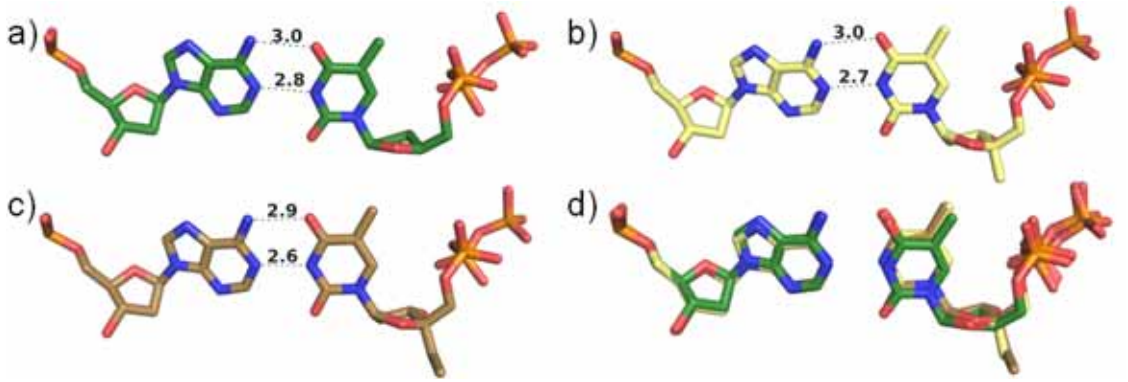

Figure 3.2-6 *Close-up view on coding adenosine and incoming thymidine analogue. a) Stick model of structure derived from ternary complex of KlenTaq, primer, template, and ddTTP (pdb: 1QTM). The indicated distances were determined by PyMOL and are shown in Å. b) Same as in a) for complex containing* ***dT^{Me}TP****. c) Same as in a) for complex containing* ***dT^{Et}TP****. d) Superposition of structures depicted in a)-c) using the colour code of* ***Figure 3.2-3*** *[Betz et al., 2010].*

The best fit of the model to the electron density indicated that the 2'-deoxyribose of the nucleotides were puckered in the N-conformation (**Figure 3.2-3** b, c) similar to the structure obtained for ddTTP (see **Figure 3.2-6**). Distances between nucleobases of modified nucleotides are comparable to the ones for the reported structure with dTTP (3.0 Å and 2.7 Å for **dT^{Me}TP**, 2.9 Å and 2.6 Å for **dT^{Et}TP** versus 3.0 Å and 2.8 Å for ddTTP). Thus, hydrogen bonding pattern was not altered through the 4'-modification. Binding of the nucleotide triphosphate by the enzyme was accompanied with structural reorganizations. In particular, in the structures obtained for **dT^{Me}TP** and **dT^{Et}TP** the closing motion of the finger domain could fully take place, which has been discussed to be crucial to promote catalysis [*Pelletier* et al., 1994, *Doublié* et al., 1998, *Huang* et al., 1998, *Franklin* et al., 2001, *Ling* et al., 2001, 2003]. All components of the active site were correctly aligned to allow the enzyme to catalyze the phosphodiester bond formation. Only subtle differences in terms of alignment of the incoming nucleotides, magnesium ions and water molecules were observed (**Figure 3.2-5**). The **dT^{Me}TP** and **dT^{Et}TP** trapped structures as well as the ddTTP superimposed well, suggesting that the enzyme employs similar mechanistic routes for nucleotide incorporation. However, our kinetic studies showed that the phosphodiester bond to the incoming **dT^{R}TP** analogues was formed with significantly lower efficiency (**Table 3.2-1**). Nevertheless, the effect of 4'-alkylation is less pronounced for the dissociation constant, which is reflected in minor deviations within the structures of **dT^{Me}TP** and **dT^{Et}TP** compared to ddTTP. Distances of 3.9 Å between C3' of the primer end and the phosphorus atom of the α-phosphate were observed in the structures that contained **dT^{Me}TP** and **dT^{Et}TP**, respectively. A shorter distance of 3.5 Å was found in the ternary structure of *KlenTaq*

complexed with ddTTP reported previously [*Li and Waksman*, 2001]. Even if this increase in distances correlates with the decrease in reaction rates, one has to note that the structural variations are within the error of model refinement at this resolution.

Recent studies showed that the closing of the finger domain occurs too fast to be rate limiting [*Rothwell* et al., 2005]. Thus, other steps occurring after the closing and the correct placement of the nascent nucleobase are supposed to be rate limiting. Since it is not possible to experimentally trap additional intermediates of the chemical reaction, the reasons for the different kinetics remain speculative. Previously, *Warshel* et al. performed empirical valence bond calculations on T7 DNA polymerase showing that the nucleophilic attack, and not the formation of the ternary complex, is time limiting [*Florián* et al., 2002, 2003, 2005]. The simulations also suggested that minor conformational differences introduced by the mismatched base pairs could result in increased reaction barriers. Studies on DNA polymerase β came to the same conclusion: changes in the binding patterns of the substrate can lead to profound changes in the reaction mechanism [*Radhakrishnan and Schlick*, 2004, 2005, *Arora* et al., 2005]. In a similar way, the steric hindrance introduced by the additional alkyl groups of the probes could force the reaction to follow a route with increased reaction barrier. Finally, also the opening step could be influenced by the modified steric demands [*Yang* et al., 2002].

Since the kinetics of nucleotide incorporation differed significantly between the natural and size-augmented nucleotides the finding of nearly identical enzyme and substrate conformations suggested mechanistic steps that were not resolved by the crystal structures to be rate limiting. Thus, further studies were carried out using mutated enzymes. Findings there were expected to give hints on participation of certain protein contacts.

3.3 Rational Design of a DNA Polymerase Mutant with Enhanced Acceptance for 4'-Alkylated Nucleotide Probes

3.3.1 Introduction

Preceding results showed that 4'-alkyl modifications were buried in a cavity within the nucleotide binding pocket (**Figure 3.3-1**).

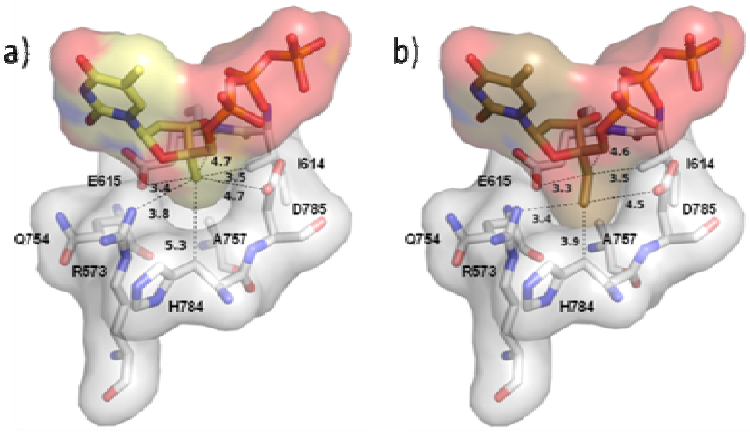

Figure 3.3-1 *Close-up views of amino acid residues closest to the 4'-modifications of* ***dT^{Me}TP*** *(a) and* ***dT^{Et}TP*** *(b), respectively. The stick models are within transparent Connolly surfaces. Indicated distances were determined by PyMOL and are shown in Å [Betz et al., 2010].*

The shortest distances for the respective modification to amino acid residues were measured from the 4'-methyl group and the methylene moiety of the 4'-ethyl group to amino acids I614 (3.5 Å for **dT^{Me}TP** and **dT^{Et}TP**, respectively) and E615 (3.4 Å and 3.3 Å) rendering these residues prime targets for mutational analysis. Recent results highlight the necessity of a carboxylate at position 615 for enzyme catalysis [*Patel and Loeb*, 2000]. Thus, further investigations focused on I614, which had been discussed to be involved in selectivity and sugar recognition before for *Taq* DNA polymerase [*Patel and Loeb*, 2000, *Patel* et al., 2001].

Furthermore, the position H784 was considered to be mutated. This histidine residue of motif C is known to form close contact to the sugar part of the primer end after incorporation [*Summerer* et al., 2005, *Strerath* et al., 2007b]. Motif C was recently suggested to be involved in selectivity recognition by members of the family A DNA polymerases, in which mismatches in the primer/template substrate are recognized through indirect H-bonding between the minor groove and the histidine side chain [*Franklin* et al., 2001].

3.3.2 Functional Studies

In each case, amino acids isoleucine 614 and histidine 784 were converted into alanine by site-directed mutagenesis with designed primer pairs on the plasmid *pGDR11:KTQwt*. After transformation of the PCR product in *Escherichia coli BL21 (DE3)* the *KlenTaq* gene plasmid was isolated and sequenced to ensure successful site-directed mutagenesis. Then, the mutated polymerases *KlenTaq* I614A and H784A were expressed and purified using standard protocols (**Figure 3.3-2**) [*Glöckner*, 2008].

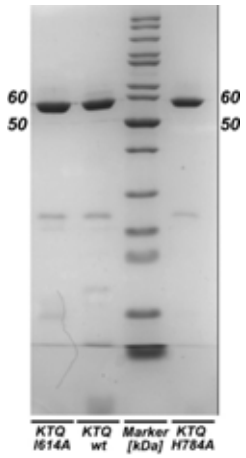

Figure 3.3-2 *SDS-PAGE gel of purified KlenTaq DNA polymerases KlenTaq wt, KlenTaq I614A and KlenTaq H784A.*

Both mutations should reduce steric constraints on the nucleoside triphosphate within the active site of *KlenTaq*. In a first trial single incorporation was studied qualitatively in comparison to the wild type enzyme. Interestingly the mutant I614A showed by far higher acceptance for the size-augmented nucleotides **dT^{Me}TP** and **dT^{Et}TP**, whereas the mutant H784A was less active as the wild type even for the natural substrates dTTP (**Figure 7.5-1** in **Appendix 7.5**).

As a result, the purified mutant I614A was investigated further in a comparison to *KlenTaq* wt (**Figure 3.3-3**). Strikingly, I614A incorporated all three nucleotides almost equally to the 24 nt primer. *KlenTaq* wt processed size-augmented **dT^{R}TPs** distinctly slower.

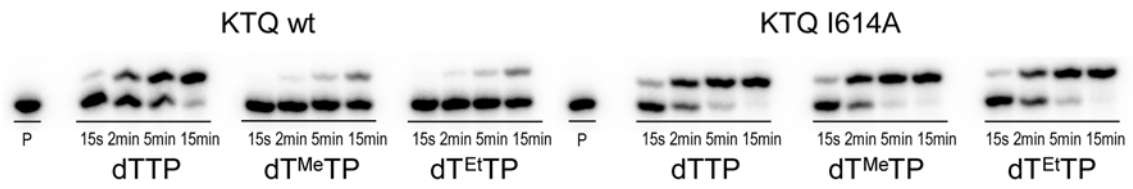

Figure 3.3-3 *Time course of single incorporation of **dT^{R}TP** by KlenTaq wt (left) and mutated KlenTaq I614A (right). The mutant accepted the modified probes significantly better than the wt enzyme. Conditions: 37°C, 5nM polymerase, 150nM primer, 225nM template, 100µM dNTP, RQF-Buffer.*

Transient kinetic analysis should quantify the observed single nucleotide incorporation results (**Table 3.3-1** and **Figure 3.3-4**). As anticipated, the I614A mutant processed the 4'-alkylated nucleotides **dT^{Me}TP** and **dT^{Et}TP** with the same activity as the wild type enzyme processed the unmodified dTTP. This resulted in more than 220-fold increased incorporation efficiencies for the modified nucleotides. Interestingly, this was paralleled by a sixfold increase for the efficiency of processing dTTP by the I614A mutant in comparison to *KlenTaq* wt.

I614A mutant showed comparable dissociation constants for all three dNTP, but all were significant lower than wt K_D for dTTP. Nevertheless, a fourfold and sixfold decreased polymerization rate k_{pol} could be observed for **dT^{R}TPs** compared to natural dTTP.

Poly-merase	dT^{R}TP	K_D (µM)	k_{pol} (s^{-1})	k_{pol} / K_D ($M^{-1}*s^{-1}$)	rel. eff. [a]
wt	dTTP	25.0 ± 3.4	8.80 ± 0.37	352,000	1
	dT^{Me}TP	119 ± 21	0.17 ± 0.01	1,430	0.0041
	dT^{Et}TP	115 ± 18	0.13 ± 0.01	1,130	0.0032
I614A	dTTP	6.83 ± 0.55	13.3 ± 0.30	1,950,000	1
	dT^{Me}TP	10.4 ± 0.80	3.62 ± 0.08	350,000	0.18
	dT^{Et}TP	4.44 ± 0.37	2.01 ± 0.04	450,000	0.22

[a] rel. eff.: relative efficiency; efficiency: k_{pol} / K_D.

Table 3.3-1 *Transient kinetic parameters for nucleotide incorporation by the KlenTaq I614A mutant.*

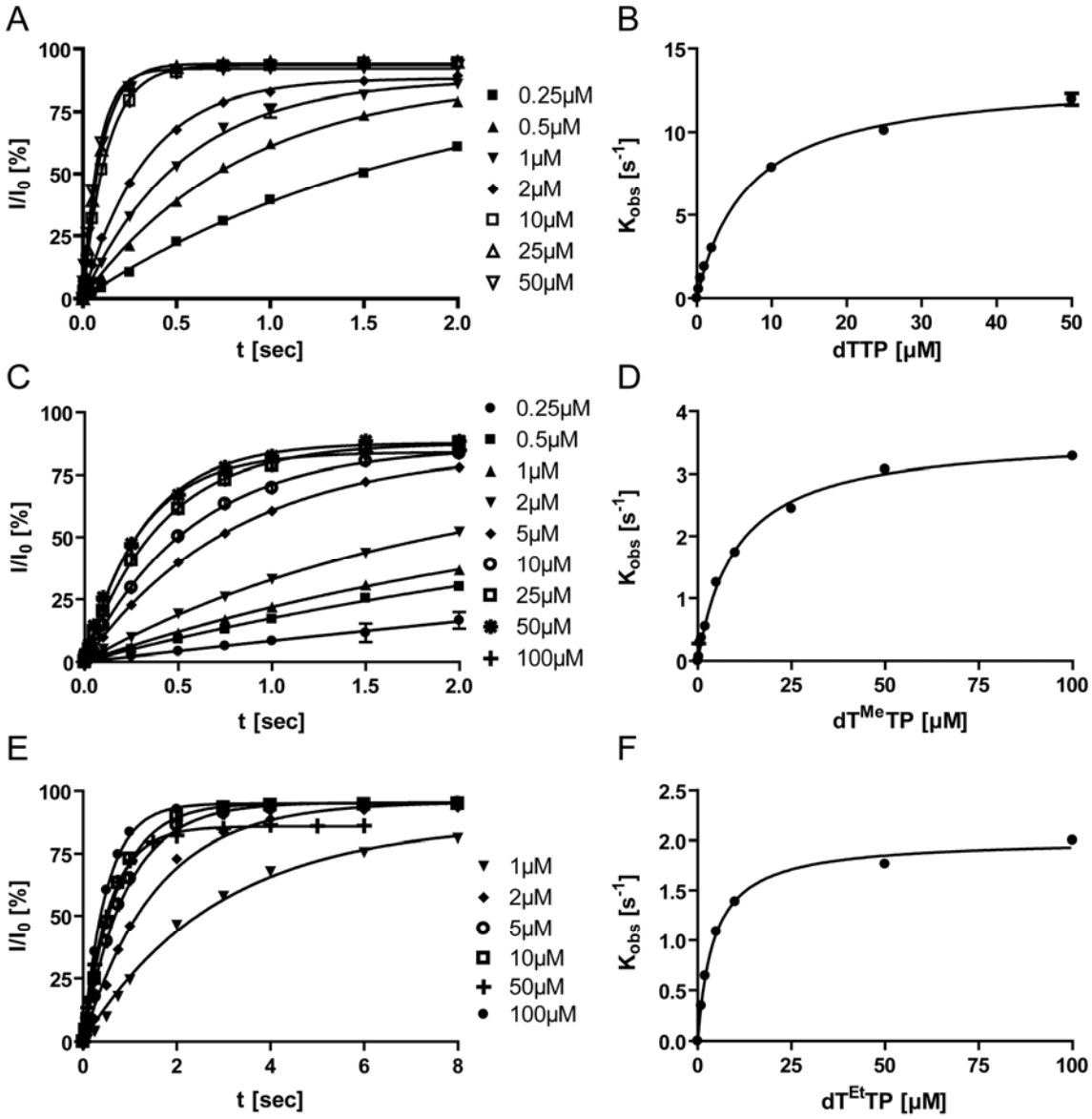

Figure 3.3-4 *Presteady-state kinetics of* ***dT^{R}TP*** *incorporation in a 24mer/36mer primer-template complex (50 nM) by KlenTaq I614A (500 nM). (A, C, and E) Graphical plot of product formation in percent as a function of time. The curves show the best fit of the data to a single exponential equation. A preformed complex of polymerase, primer and template was rapidly mixed with different concentrations of dTTP (A),* ***dT^{Me}TP*** *(C), and* ***dT^{Et}TP*** *(E) as indicated in the figure. (B, D, and F) Dependence of the pre-steady state rates on the dTTP (B),* ***dT^{Me}TP*** *(D), and* ***dT^{Et}TP*** *(F) concentrations. The k_{obs} values were plotted versus the* ***dT^{R}TP*** *concentration and fitted to a hyperbolic equation.*

For further characterization of the mutant, the error spectrum for *KlenTaq* I614A was determined using a PCR based assay described by *Patel* et al. [Patel et al., 2001]. However, no elevated error rate could be determined (**Table 3.3-2**).

Enzyme	Repli-cations	No. of clones	Av. No. of Mutations per clone[a]	Error rate[b]	No. of individual substitutions						No. of deletions	No. of insertions
					Transitions		Transversions					
					AT → GC	*GC → AT*	AT → TA	AT → CG	GC → TA	GC → CG		
***KTQ* wt** [c]	7.7	32	0.4	8.8×10^{-5}	5	4	0	0	1	0	3	0
***KTQ* I614K**	11.6	41	0.3	6.1×10^{-5}	5	4	0	0	1	0	1	0

[a] Number of mutations per 381 bases sequenced per clone (600 bases for wt).

[b] Error rate equals number of mutations per base per division.

[c] Data were taken from [*Glöckner*, 2008].

Table 3.3-2 *Error spectrum of KlenTaq I614A and KlenTaq wt.*

3.3.3 Discussion

The *KlenTaq* mutant generated in this work possessed a mutation from the bulky amino acid isoleucine to the smaller alanine. This mutation is proximate to the 4'-alkyl modification of incoming nucleoside triphosphates. Alanine is not only smaller than isoleucine, but it also lacks the β-methyl residue of isoleucine, which is orientated towards the 4'-position of the nucleotide (see **Figure 3.3-1**). This fact generates space for increasing 4'-alkylated residues.

This effect was already visible in a simple time course experiment (**Figure 3.3-3**). The mutant I614A processed size-augmented **dT^{R}TPs** comparable to natural dTTP, whereas *KlenTaq* wt incorporated these nucleotides with prolonged incorporation times (as expected by the results of the preceding studies in **Chapter 3.2**).

The decrease of steric demand in the active site of the enzyme by mutating the amino acid I614 results in steep increases of incorporation efficiencies for the size-augmented nucleotides. Strikingly, the I614A mutant processed the 4'-alkylated nucleotides **dT^{Me}TP** and **dT^{Et}TP** in presteady-state experiments with the same activity as the wild type enzyme processed the unmodified dTTP. The 220-fold increased incorporation efficiencies for the modified nucleotides compared to wild type, resulted from an unhindered binding of the substrates (K_D comparable to dTTPs). More importantly, the polymerization rate k_{pol} only decreased by a factor of four and six. *KlenTaq* wt in contrast did incorporate size-augmented nucleotides with a 51- and 67-fold decrease for k_{pol}. Interestingly, the mutation I614A increased the efficiency of processing dTTP sixfold in comparison to *KlenTaq* wt.

Mutating isoleucine 614 to alanine and binding a 4'-alkylated nucleotide instead of a natural substrate, could be imagined as if the β-alkyl residue of isoleucine has been "grafted" to the nucleotide. Therefore, a comparable dissociation constant to dTTP is not surprising. Then again, the incorporation rate was still reduced compared to dTTP. This decrease indicates that during transitions state of the incorporation reaction 4'-residue of the modified nucleotide is exposed to a steric constraint, which is absent for natural dTTP. Thus, amino acid I614, which is highly conserved from bacteria to humans among DNA polymerases from this sequence family (see **Table 3.3-3**), presumably plays an important role for sugar recognition by *KlenTaq* DNA polymerase [*Patel and Loeb*, 2000, *Patel* et al., 2001]. The same isoleucine to alanine mutation was

reported to increase rNTP incorporation by DNA polymerase I of *Escherichia coli* (I709 in DNA pol I corresponds to I614 in *KlenTaq*) [*Shinkai* et al., 2001].

Thermus aquaticus	**DYSQIELR**
Thermus thermophilus	**DYSQIELR**
Thermus caldophilus	**DYSQIELR**
Thermus filiformis	**DYSQIELR**
Rickettsia felis	**DYSQIELR**
Mycobacterium tuberculosis	**DYSQIEMR**
Homo sapiens (pol theta)	**DYSQIELR**
Escherichia coli (pol I)	**DYSQIELR**
Chlamydia trachomatis (pol I)	**DYSQIELR**
Chlamydia pneumoniae (pol I)	**DYSQIELR**
Treponema pallidum (pol I)	**DYSQIELV**
Methylobacterium (pol I)	**DYSQIELR**
Deinococcus radiodurans (pol I)	**DYSQIELR**
Helicobacter pylori (pol I)	**DYSQIELR**
Borrelia burgdorferi (pol I)	**DYSQIELA**
Bacillus subtilis (pol I)	**DYSQIELR**

Table 3.3-3 *Motif A consensus sequence alignement.*

KlenTaq I614A showed no elevated error rates compared to *KlenTaq* wt DNA polymerase, even though its binding pocket is enlarged. Probably, the nucleobase and the triphosphate moiety are held tight and the size-augmentation on the opposite site is too small to promote non-canonical mispairing. Hence, I614A is able to selectively incorporate nucleotides in PCR reactions.

These and preceding results have been published in Betz[+], K., Streckenbach[+], F., Schnur, A., Exner, T., Welte, W., Diederichs, K. and Marx, A. Structures of DNA polymerase caught processing size-augmented nucleotide probes. *Angew Chem Int Ed Engl accepted* (2010). ([+]equal contribution)

3.4 DNA Polymerase Mutant with Enhanced Processing Ability of Size-augmented Nucleotide Probes

3.4.1 Introduction

Recently, Dr. Christian Glöckner, AG Marx, found a mutation in the *KlenTaq* DNA polymerase (M747K), which led to higher lesion bypass ability, higher processivity and increased PCR activity at lower enzyme concentrations [*Glöckner and Marx*, 2007]. Mutating methionine 747 into the positively charged amino acid lysine, which points towards the template strand, enhanced the affinity of the DNA template strand to the enzyme. Throughout this stabilization, the *KlenTaq* mutant was able to read over UV light damaged DNA.

Furthermore, *Loeb* et al. reported that mutating isoleucine 614 of full-length *Taq* DNA polymerase to lysine enhanced DNA polymerase lesion bypass [Patel et al., 2001]. The isoleucine in position 614 is in close contact to the 4'-position of the 2'-deoxyribose of the incoming nucleoside triphosphate. *Loeb* et al. already suggested that this mutation opens the active site pocket to accommodate damaged templates, non-Watson-Crick base pairs, and diverse nucleotide analogues.

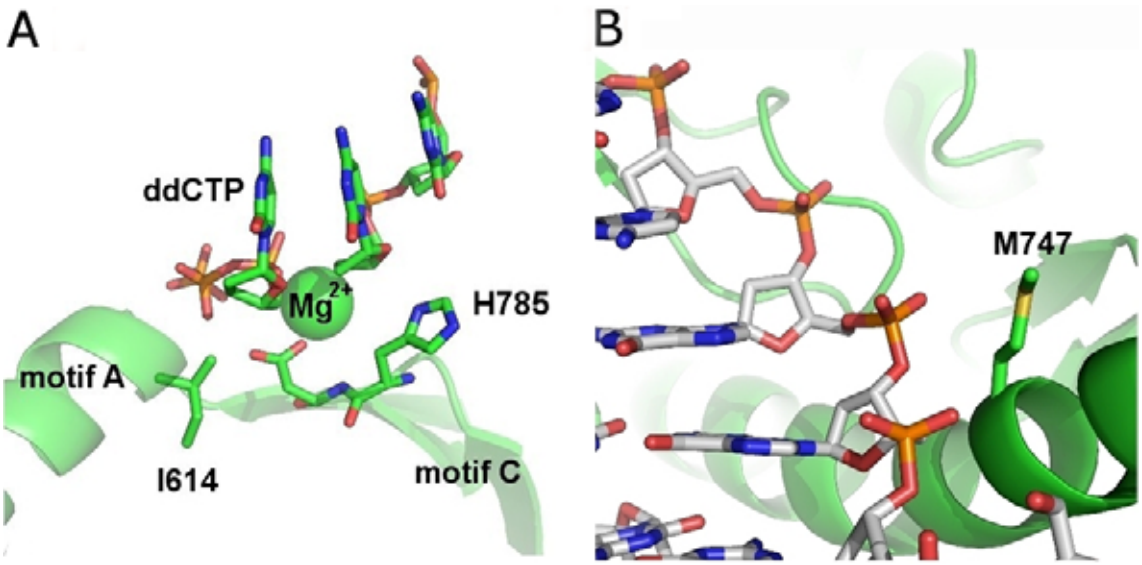

Figure 3.4-1 *Mutation sites of KlenTaq double mutant M747K I614K. A) Isoleucine at position 614 in motif A. B) Methionine at position 747 [adapted from Schnur, 2009].*

A combination of both mutations into one *KlenTaq* double mutant (DM KK) by Dr. Christian Glöckner, AG Marx, resulted in a highly efficient DNA polymerase (**Figure 3.4-1**). The double mutations M747K and I614K increased the ability to overread abasic site and 8-oxoguanine or 8-oxoadenine lesions. Presteady-state kinetics

demonstrated an over tenfold increased incorporation efficiency for the natural dATP opposite template dT compared to *KlenTaq* wt DNA polymerase [*Glöckner*, 2008]. Moreover, Dr. Andreas Schnur, AG Welte, could already report first crystal structures of the DM KK in complex with primer, template and ddCTP [*Schnur*, 2009].

As demonstrated in the preceding project, the exchange of I614 of *KlenTaq* DNA polymerase to the amino acid alanine enabled the mutated DNA polymerase to accept 4'-alkylated thymidine probes as efficient as the wild type enzyme accepted natural dTTP. Driven by these results, the *KlenTaq* DM KK seemed to be another ideal enzyme for revealing the functional and structural basis for processing size-augmented **dT^{R}TPs**. The mutation I614K, like I614A, lacks the β-methyl residue of the isoleucine, which makes room for increasing 4'-alkylated residues. To further tighten steric constraints in the binding pocket, bulkier **dT^{iP}TP** have been used. These probes have shown before to be poor substrates for polymerases [*Summerer and Marx*, 2001; *Strerath* et al., 2002]. The additional space in the binding pocket should help processing these kinds of probes.

The functional studies again were accompanied by structural investigations. Karin Betz employed the steric probes in crystallization trials.

The results from both functional and structural investigations should also be compared to results reported by Dr. Christian Glöckner and Dr. Andreas Schnur to discuss the contribution of protein-DNA contacts by the amino acid mutations on the elevated incorporation efficiency [*Glöckner*, 2008, *Schnur*, 2009].

3.4.2 Functional Studies

First, a radiometric assay was set up to probe processing of 4'-alkylated dTTPs by *KlenTaq* DM KK, expressed and purified by Dr. Christian Glöckner, AG Marx, compared to *KlenTaq* wt enzyme [*Glöckner*, 2008]. Not only the reported higher efficiency of the mutated enzyme should affect the processing of steric increased probes, but also more interestingly the exchange of the amino acid at position 614 should give an additional positive effect by providing a larger binding pocket.

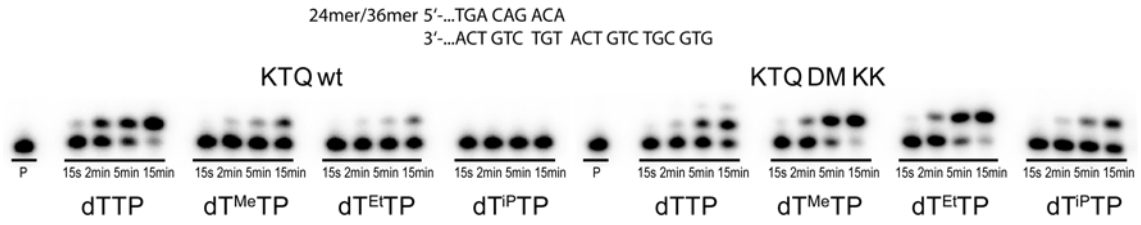

Figure 3.4-2 *Single incorporation studies comparing Klentaq wt and DM KK in a time course experiment. Conditions: 37°C, 5 nM polymerase, 150 nM primer, 225 nM template, 100 µM dNTP, RQF-Buffer.*

To gain initial ideas on how the highly efficient polymerase mutant behaves on size-augmentation of substrates, single incorporation studies of **dT^{R}TPs** in a time course experiment were performed (**Figure 3.4-2**). Indeed, qualitatively *KlenTaq* DM KK processed modified **dT^{R}TPs** considerably better than the wild type enzyme. After 15 minutes reaction time, the nucleotide probes **dT^{Me}TP** and **dT^{Et}TP** showed only minor incorporation for *KlenTaq* wt, whereas the huge **dT^{iP}TP** was not processed at all by the wild type enzyme. However, *KlenTaq* DM KK was able to synthesize significant amounts of extension product for all three modified **dT^{R}TPs**.

In order to quantify the observed increased efficiencies, the single incorporation studies were then performed under presteady-state conditions by rapid quench flow technology (**Table 3.4-1** and **Figure 3.4-3**). Additionally the transient kinetic parameters of the processing of **dT^{iP}TP** by *KlenTaq* wt were measured.

Enzyme	Template:dNTP	k_{pol} (s^{-1})	K_D (µM)	k_{pol} / K_D (M^{-1} s^{-1})	Rel. Eff.
wild type	A : dTTP	8.80 ± 0.34	25.0 ± 3.1	352,000	1
wild type	A : $dT^{Me}TP$	0.17 ± $0.08*10^{-1}$	119 ± 20	1,430	$4.1*10^{-3}$
wild type	A : $dT^{Et}TP$	0.13 ± $0.06*10^{-1}$	115 ± 16	1,130	$3.2*10^{-3}$
wild type	A : $dT^{iP}TP$	$0.04*10^{-1}$ ± $0.05*10^{-2}$	488 ± 146	8.20	$2.3*10^{-5}$
M747K I614K	A : dTTP	5.51 ± 0.14	0.83 ± 0.10	6,640,000	1
M747K I614K	A : $dT^{Me}TP$	1.05 ± 0.04	4.48 ± 0.83	230,000	$3.5*10^{-2}$
M747K I614K	A : $dT^{Et}TP$	1.17 ± 0.02	4.36 ± 0.28	260,000	$3.9*10^{-2}$
M747K I614K	A : $dT^{iP}TP$	0.26 ± 0.02	130 ± 32	2,000	$3.0*10^{-4}$

Table 3.4-1 *Transient kinetic parameters under single turnover conditions measured on a rapid quench flow machine.*

KlenTaq wt showed a 40,000-fold lower overall efficiency (k_{pol} / K_D) for **$dT^{iP}TP$** compared to the natural substrate dTTP. At the same time, the dissociation constant of **$dT^{iP}TP$** (K_D) was only increased 20-fold compared to the natural substrate. However, the incorporation rate k_{pol} underwent a drop of around 2,200-fold.

Compared to transient kinetic parameters of *KlenTaq* wt, around 20-fold increase in efficiency was observed for *KlenTaq* DM KK when incorporating dTTP. Interestingly, the effect on the nucleotide incorporation efficiency only results from decreased dissociation constant K_D. Coincidently, the *KlenTaq* DM KK processed 4'-alkylated nucleoside probes **$dT^{Me}TP$** and **$dT^{Et}TP$** with only 25-fold and 30-fold reduced efficiencies compared to dTTP. Thereby, K_D increased by almost the same factor that k_{pol} decreased (approximately fivefold). Even more interestingly, the *KlenTaq* DM KK also incorporated the bulkiest thymidine analogue, **$dT^{iP}TP$,** with a considerable efficiency of 2,000 $M^{-1}s^{-1}$, which correlated to a reduction of around 3,000-fold in relation to the efficiency of dTTP. As observed upon size-augmentation from dTTP to **$dT^{Me}TP$** and **$dT^{Et}TP$**, the size-augmentation to **$dT^{iP}TP$** led to an approximately fivefold decrease of k_{pol} compared to **$dT^{Me}TP$** and **$dT^{Et}TP$**. The dissociation constant of **$dT^{iP}TP$** increased 30-fold compared to **$dT^{Me}TP$** and **$dT^{Et}TP$** and even 150-fold compared to dTTP.

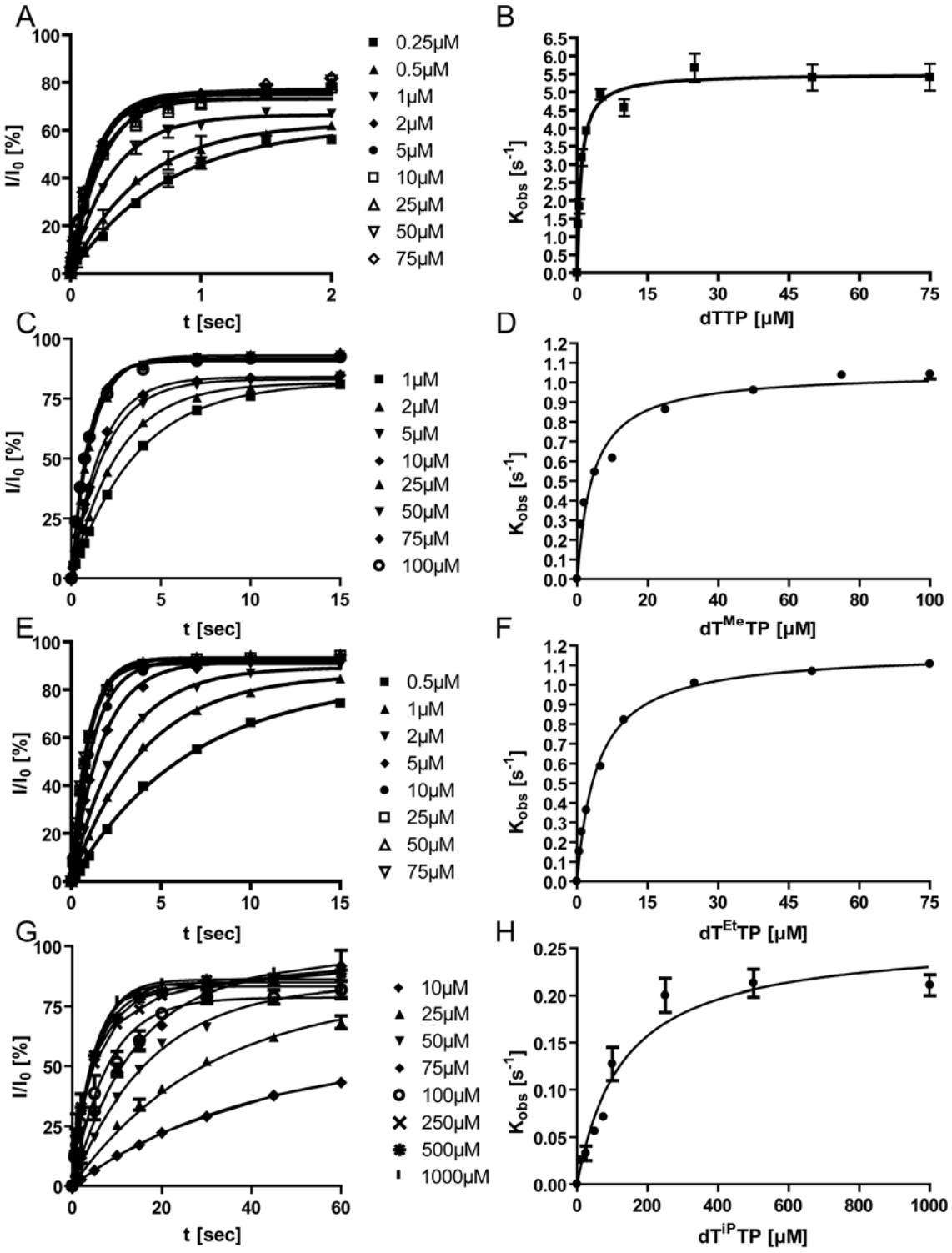

Figure 3.4-3 *Presteady-state kinetics of* ***dT^{R}TP*** *incorporation in a 24mer/36mer primer-template complex (50 nM) by KlenTaq DM KK (500 nM). (A, C, E, and G) Graphical plot of product formation in percent as a function of time. The curves show the best fit of the data to a single exponential equation. A preformed complex of polymerase, primer and template was rapidly mixed with different concentrations of dTTP (A),* ***dT^{Me}TP*** *(C),* ***dT^{Et}TP*** *(E), and* ***dT^{iP}TP*** *(G) as indicated in the figure. (B, D, F, and H) Dependence of the pre-steady state rates on the dTTP (B),* ***dT^{Me}TP*** *(D),* ***dT^{Et}TP*** *(F), and* ***dT^{iP}TP*** *(H) concentrations. The k_{obs} values were plotted versus the* ***dT^{R}TP*** *concentration and fitted to a hyperbolic equation.*

3.4.3 Structural Investigations

In order to interpret the functional results further, the previously reported crystallization strategy for *KlenTaq* wt was adapted to the *KlenTaq* DM KK. Indeed Karin Betz, AG Marx, could report not only crystal structures of *KlenTaq* variant I614K M747K in complex with primer, template, and incoming **dT^{Me}TP** and **dT^{Et}TP**, but also with the larger **dT^{iP}TP** [*Betz*, 2009]. Crystallization trials with **dT^{iP}TP** for the wild type enzyme failed. The crystal structures of this *KlenTaq* DNA polymerase mutant in complex with 4'-alkylated structures gave the first structural insights on how the enlarged binding pocket accommodates the 4'-residue.

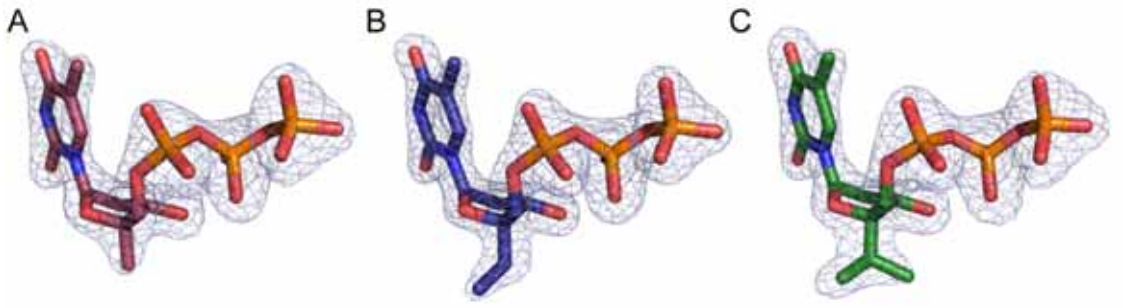

Figure 3.4-4 *Electron density of **dT^{Me}TP** (A), **dT^{Et}TP** (B) and **dT^{iP}TP** (C) in the waiting position of the KTQ DM. The 2mFo-DFc map of the nucleoside triphosphate is shown in grey with a sigma level of 1, the omit maps of the three different modifications are shown in dark green with a sigma level of 4 [Betz, 2009].*

The overall structures of *KlenTaq* DM KK in complex with 4'-alkylated thymidine triphosphates showed low root mean square deviation (RMSD) of 0.28 Å, 0.26 Å and 0.34 Å respectively [*Betz*, 2009]. Comparing the amino acid backbone of the active site to the wild type structure only marginal deviations could be observed between these structures. The same held true for the primer and template strands, which were mostly in the B-Form, again except for the last base pairs at the end of the duplex adjacent the active site, that are A-Form (see **Appendix 7.6**). The difference electron density map for each nucleotide at the binding side clearly showed the three different modifications in the respective crystal structure (**Figure 3.4-4**). All sugar rings of the nucleoside triphosphates were puckered in the N-conformation as calculated by PROSIT [*Sun* et al., 2004]. Noteworthy, the incoming nucleotide base thymine orientated towards the coding adenine as well as the triphosphate moiety arranged in the anticipated position.

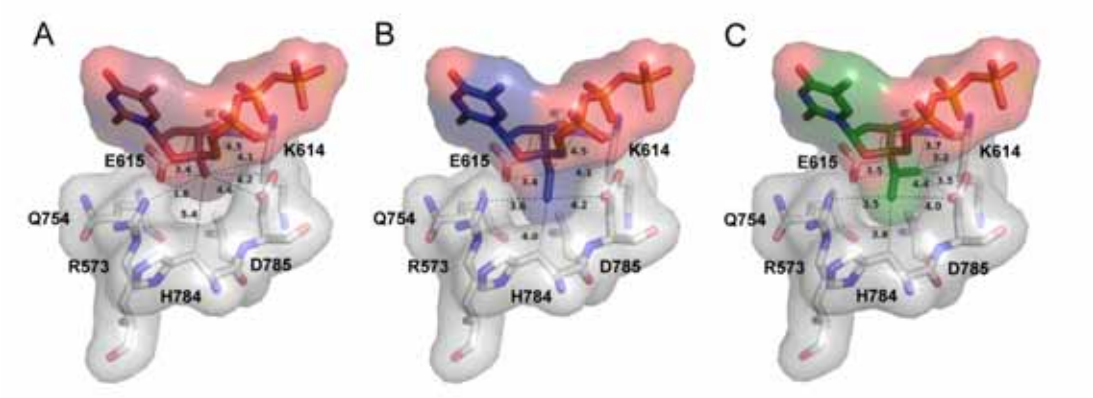

Figure 3.4-5 *Surface and distances of the steric probes and near protein residues of $dT^{Me}TP$ (A), $dT^{Et}TP$ (B) and $dT^{iP}TP$ (C) trapped KlenTaq DM KK structures. Protein residues and nucleoside triphosphates are shown as sticks and surface. Protein residues are coloured grey;* ***$dT^{Me}TP$****,* ***$dT^{Et}TP$*** *and* ***$dT^{iP}TP$*** *are colored red, blue and green, respectively. Nearest distances to protein residues are shown as dashes and are labeled in Å [Betz, 2009].*

In the obtained crystals the distances between the 4'-methyl and the 4'-methylene of the 4'-ethyl group to the K614 were measured to be 4.2 Å and 4.1 Å, respectively (***Figure 3.4-5***). The closest distance from K614 to the 4'-isopropyl fork was 3.2 Å. Distances of approximately 3.8 - 4.1 Å between the C3' of the primer end and the phosphorous atom of the α-phosphate are observed for all three structures (data in [Betz, 2009]).

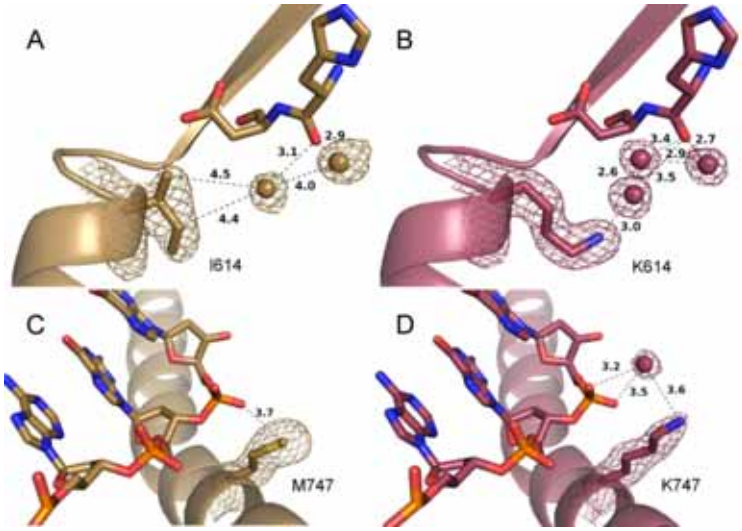

Figure 3.4-6 *Mutation sites of the* ***$dT^{Me}TP$*** *trapped structures of KlenTaq DM (colored in red) and KlenTaq wt (colored in sand). Water molecules are shown as spheres. The electron densities of the side chains and the water molecules are shown with a sigma level of 1 and in the respective color. All distances are given in Å. For the amino acid K614 a possible hydrogen bonding network to motif C is shown (B). The distances of the corresponding amino acid I614 in the wt to near water molecules are indicated (A). For M747 the direct distance to the template backbone is shown (C), for K747 the distances to the backbone over a near water molecule are shown (D) [Betz, 2009].*

Dr. Christian Glöckner and Dr. Andreas Schnur have discussed the participation of the positively charged amino acids and possible water bridges to stabilize the DNA backbone [*Glöckner*, 2008, *Schnur*, 2009]. The mutation K614 is located in motif A

near the binding pocket and is orientated along $C^{\gamma 1}$ and $C^{\delta 1}$ of the I614 side chain of the wt structure. Dr. Andreas Schnur could observe a water bridge between K614 and motif C [*Schnur*, 2009]. He suspected that stabilization of the binding pocket by this water bridge might lead to a higher substrate tolerance. Apart from that, the higher positive charge in the binding pocket could also be responsible for the higher substrate tolerance by reducing the activation energy for incorporation of unfavorable substrates. Furthermore, he found a water bridge (two water molecules) from K747 located in the Q-helix to the backbone oxygen of the first new synthesized base pair on the template. This water bridge should mediate additional stabilization of the template strand.

All *KlenTaq* DM KK structures reported by Karin Betz showed water bridges to Motif C. The two mutation sites of the **dT^{Me}TP** trapped *KlenTaq* wt and DM KK structures are depicted in **Figure 3.4-6**. Near position 614 an additional water molecule in the **dT^{Me}TP**-trapped structure of the *KlenTaq* DM KK compared to the respective wt structure was found. A water bridge mediated by one or two water molecules would be possible. For I614 in the wt structure the distances to the next water molecule are shown in **Figure 3.4-6**.

Stabilization of the template backbone through a water bridge from K747 could be revealed only in the **dT^{Me}TP** trapped *KlenTaq* DM KK structure. No clear spherical electron density for a water molecule was visible in the other structures. At position 747 a possible hydrogen bonding bridge from lysine to the OH group of the template dG could be observed although the distance of 3.7 Å to the OH group is not in the range of normal hydrogen bonding distances (between 2.6 and 3.1Å).

3.4.4 Discussion

Presteady-state kinetic data of the *KlenTaq* wt enzyme on the natural substrate dTTP as well as on **dT^{Me}TP** and **dT^{Et}TP** have been discussed in the chapter 3.2. Additionally, the transient kinetic parameters of the processing of **dT^{iP}TP** showed that this probe is a poor substrate for the wild type DNA polymerase. In fact, the binding of **dT^{iP}TP** (K_D) was only diminished by a factor of 20 compared to the natural substrate. However, the incorporation rate k_{pol} underwent a drop of around 2,200-fold, which lead to a 40,000-fold lower overall efficiency (k_{pol} / K_D). Comparing the two transient kinetic parameters K_D and k_{pol} further corroborates the previously stated assumption that I614, which is conserved from bacteria to humans among DNA polymerases, is involved in sugar recognition at 4'-position of nucleoside triphosphates. Nevertheless, due to flexibility of the amino acid residue the binding of 4'-alkylated 2'-deoxynucleoside triphosphates is only slightly affected. When it comes to incorporation of these substrates, the enzyme seems to undergo a transition in a way that the amino acid isoleucine contacts closer to the sugar residue. This transition raises the energy barrier, which results in a drastically reduced incorporation rate k_{pol}.

By conversion of isoleucine into lysine, the steric constraints on the sugar ring within the active site of *KlenTaq* are lowered due to the absence of a β-alkyl side chain. This leads to enough space even for 4'-isopropyl residues. Transient kinetic studies of the *KlenTaq* DM KK yielded higher overall efficiencies k_{pol} / K_D for dTTP as well as for the three modified substrates compared to the wild type. The almost 20-fold increased efficiency ($6.6 \cdot 10^6$ M^{-1} s^{-1}) for the natural substrate dTTP was in the range of the value for dATP incorporation which had been reported by Dr. Christian Glöckner, AG Marx ($3.2 \cdot 10^6$ M^{-1} s^{-1}) [*Glöckner*, 2008]. The high nucleotide incorporation efficiency k_{pol} / K_D compared to wild type enzyme only resulted from a decreased dissociation constant K_D. The polymerization rate k_{pol} of 5.51 s^{-1} was comparable to 8.80 s^{-1} of *KlenTaq* wt. This stronger binding presumably originates from the introduction of the two positively charged amino acids holding the primer-template-triphosphate complex tight (for a graphical summary of k_{pol} / K_D: **Figure 3.4-7**). As for dTTP steric constraints to the position 614 lack, the reaction could proceed almost not affected, which was represented by a similar k_{pol}.

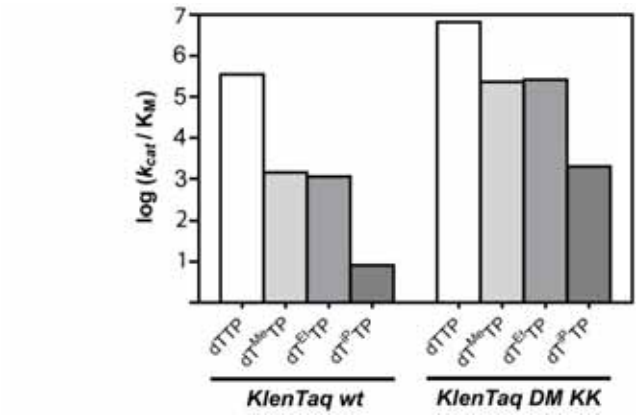

Figure 3.4-7 *Representation of the incorporation efficiencies of* ***dT^{R}TP*** *into a 24nt/36nt primer template by KlenTaq wt and KlenTaq DM KK.*

Concordantly to the parameters of the mutant I614A the double mutant incorporated the **dT^{Me}TP** and **dT^{Et}TP** with efficiencies almost as high as the wild type processed dTTP (230,000 M^{-1} s^{-1} / 260,000 M^{-1} s^{-1} compared to 352,000 M^{-1} s^{-1}, **Table 3.4-1**). However, the efficiencies are lower than the ones for mutant I614A due to the enlarged steric bulk of lysine compared to the small alanine (for parameters of *KlenTaq* I614A see **Table 3.3-1**). The efficiencies for **dT^{Me}TP** and **dT^{Et}TP** are a result of a fivefold increased K_D and a fivefold decreased k_{pol}. The same factor in increase for K_D was observed before for the *KlenTaq* wt, where as for I614A mutant almost no effect on the binding of the substrate could be measured. *KlenTaq* wt showed a 200-fold decreased incorporation rate k_{pol} upon size-augmentation from dTTP to **dT^{Me}TP** and **dT^{Et}TP**, whereas the fivefold reduction for *KlenTaq* DM KK was the same factor, which could be measured for mutant I614A. The fivefold lower k_{pol} for both mutants leads to the assumption that the β-alkyl chain of isoleucine, which is absent in both mutants, closely contacts the 4'-position of the nucleotide during the transition state of the reaction and thus is involved in the sugar recognition during replication [*Patel* et al., 2001]. There again, the unaffected K_D for mutant I614A compared to a fivefold reduced one for *KlenTaq* DM KK and *KlenTaq* wt could be explained by the larger active site. In fact, the K_D for *KlenTaq* DM KK were lower than for *KlenTaq* wt in absolute values, which could be explained by stronger binding through positively charged amino acids. Nevertheless, the same fivefold reduction for **dT^{Me}TP** and **dT^{Et}TP** compared to dTTP suggested that the isoleucine in *KlenTaq* wt could avoid the steric clash upon binding by a simple rotation.

KlenTaq wt only marginal processed the bulky **dT^{iP}TP**, whereas the *KlenTaq* DM KK was able to incorporate this substrate with efficiencies slightly higher than the wild

type incorporated the smaller substrates **dT^{Me}TP** and **dT^{Et}TP** (~2,000 M^{-1} s^{-1} to ~1,000 M^{-1} s^{-1}). Furthermore, K_D and k_{pol} were also in the range of the ones for **dT^{Me}TP** / **dT^{Et}TP** for *KlenTaq* wt (~130 µM to ~120 µM and 0.26 s^{-1} to 0.17 s^{-1} / 0.13 s^{-1}).

The drop in efficiency for *KlenTaq* DM KK was around 3,000-fold compared to around 40,000-fold of the wild type enzyme (dTTP versus **dT^{iP}TP**). Interestingly the K_D for the *KlenTaq* DM KK dropped by around 150-fold, whereas for *KlenTaq* wt only a 20-fold drop was measured (0.8 µM to 130 µM versus 25 µM to ~500 µM). It remained unclear, why the binding of **dT^{iP}TP** compared to dTTP is less affected for *KlenTaq* wt than for *KlenTaq* DM KK. One explanation might be that the binding of **dT^{iP}TP** in *KlenTaq* wt is strongly hindered and results in a complex rearrangement of the proximate amino acids as well as of the nucleotide. This might explain why no crystal structure could be obtained for *KlenTaq* wt in complex with **dT^{iP}TP**. However, the larger active site is reflected in the higher incorporation rate k_{pol} for **dT^{iP}TP** of *KlenTaq* DM KK compared to *KlenTaq* wt, giving a hint on the situation during the transition state. The k_{pol} for the wild type enzyme is insignificant compared to the one for the *KlenTaq* DM KK (0.004 s^{-1} to 0.26 s^{-1}). The mutation I614K leads to a larger active site and, hence, to less steric constraints during the transition state.

Taken together, the functional studies of the *KlenTaq* DM KK in comparison to *KlenTaq* wt confirmed the reported higher efficiency [Glöckner, 2008] not only for natural dTTP, but also for the size-augmented **dT^{R}TPs**. Moreover, the active site of the *KlenTaq* DM KK is enlarged through one of the mutations (I614K). This led to a better acceptance of the 4'-alkylated nucleotides.

As mentioned before, crystallization gives a snapshot on the binding situation and thus is related to the dissociation constant K_D. Thus, the crystal structures obtained by Karin Betz, AG Marx / AG Welte, could help elucidating the functional data. The protein conformation in the crystal structures showed almost no deviation to the wt structures, as the root mean square deviations for all structures were below 0.3 Å. Moreover, the calculations by PROSIT revealed no rearranged DNA structure of primer and template. Again, like for wt structures, the sugar puckering was not disturbed by the 4'-modification. Therefore, the small structural deviations appeared only in the binding pocket.

In the obtained crystals the distances between the 4'-methyl and the 4'-methylene of the 4'-ethyl group to the K614 were measured with 4.2 Å and 4.1 Å. This increase of

0.6 - 0.7 Å compared to the wt structures (3.5 Å for 4'-methyl and 4'-methylene of 4'-ethyl) is smaller than the proposed size of one C-C bond (length 1.5 Å), but nevertheless reflects an enlarged active site. Thus, this gap helps the enzyme to deal with the size-augmentation at the 4'-residue of the nucleoside triphosphates. The comparable kinetic parameters of **dT^{iP}TP** for *KlenTaq* DM KK and of **dT^{Me}TP** and **dT^{Et}TP** for *KlenTaq* wt became apparent through the distance between 4'-isopropyl to I614K, which is similar to the distances between 4'-methyl (**dT^{Me}TP**) and 4'-methylene (**dT^{Et}TP**) and I614 of the *KlenTaq* wt structures (**Figure 3.4-5** and **Figure 3.3-1**: 3.2 Å versus 3.5 Å). The distances between the C3' of the primer end and the phosphorous atom of the α-phosphate for all three structures are similar to the ones observed in the wt structure for **dT^{Me}TP** and **dT^{Et}TP** nucleotides, thus comparable reaction mechanisms for *KlenTaq* wt and DM KK can be assumed (data in [*Betz*, 2009]).

As mentioned before kinetic data confirmed the reported higher efficiency [Glöckner, 2008] not only for natural dTTP, but also for the size-augmented **dT^{R}TPs** (besides the effect of the larger binding pocket). Whether this effect could be explained by stabilization through water bridges in the *KlenTaq* DM KK remained controversially through the structures by Karin Betz, AG Marx / AG Welte. The mutation K614 is located in motif A near the binding pocket and orientates along $C^{\gamma 1}$ and $C^{\delta 1}$ of the I614 side chain of the wt structure (**Figure 3.4-6**). All *KlenTaq* DM KK structures showed water bridges to motif C, which provide additional stability of the binding pocket and increased substrate tolerance. At position 747, a hydrogen bonding bridge from lysine to the OH group of the template dG could be observed only for the **dT^{Me}TP** structure. However, the distance of 3.7 Å to the OH group is not in the range of normal hydrogen bonding distances (between 2.6 Å and 3.1 Å). Therefore, stabilization of the DNA backbone through a water bridge from K747 to dG in the double mutant is unlikely. The effects observed in the M747K mutation rather rely on the discussed direct electrostatic effects of the additional positively charged amino acid [Glöckner, 2008, Schnur, 2009]. Taken together, the additional water bridge to motif C plus the additional electrostatic effect of the two positively charged amino acids might explain the high efficiency of the *KlenTaq* DM I614K M747K for both dTTP and **dT^{R}TPs**. The higher acceptance of **dT^{R}TPs** compared to dTTP however correlated to the larger active site through the mutation I614K.

4 Summary and Outlook

In this work the synthesis of 4'-alkylated 2'-deoxyadenosine and thymidine nucleosides and their corresponding 5'-*O*-triphosphates and 3'-*O*-phosphoramidites could be successfully performed starting from 1,2:5,6-di-*O*-isopropylidene-α-D-glucofuranose. The synthesis strategy for this purpose was developed by Dr. Gopinath Rangam, AG Marx. The obtained phosphoramidites have been used in an automated DNA synthesis to synthesize modified oligonucleotide templates.

The modified templates as well as the complementary nucleoside triphosphates have then been used in single incorporation studies as substrates for two different polymerases. The relative high-fidelity enzyme Klenow Fragment exo- of DNA polymerase I from *Escherichia coli*, a family A polymerase, has been compared to the translesion polymerase Dpo4 of family Y. Through steady-state enzyme kinetics under *single completed hit conditions,* the processing of both enzymes on these probes has been measured quantitatively.

The results obtained are interesting in many respects. First, the error-prone TLS DNA polymerase Dpo4 incorporated the size-augmented nucleotides more efficiently than the more selective KF exo-. This observation is along the line of the model that high fidelity DNA polymerases form more rigid binding pockets tolerating less geometric deviation, while low fidelity enzymes exhibit more flexibility leading to decreased fidelity. This is in agreement with earlier findings [*Kool*, 2002]. Second, for both enzymes the incorporation of unmodified dATP was more efficient than of dTTP. However, the opposite was found for the size-augmented probes. It appears that the bulkier purine nucleotides $\mathbf{dA^R}$ were subject to more steric constraints within the active site of the enzymes than the pyrimidines $\mathbf{dT^R}$. These different properties might well be the causative for the observation that the selectivity of nucleotide incorporation might vary depending of the nascent nucleotide pair orientation [*Minnick* et al., 2002]. This

assumption was further corroborated by the finding that the size-augmented **dT^{R}TPs** are, relative to their unmodified analogue, more efficiently incorporated opposite non-canonical template nucleotides than their adenosine counterparts. Structural investigations showed that the sugar moiety of the incoming dNTP is fully embedded within the substrate binding pockets of DNA polymerases and an integral part of substrate recognition processes [*Johnson and Beese*, 2004, *Rothwell and Waksman*, 2005]. Hence, editing of the incoming dNTP sugar might provide the enzyme with additional paths to achieve canonical base pair formation through indirect readout of aberrant sugar conformations.

Following the preceding studies, the active sites of the polymerases were then subjected to additional steric constraints through modified template nucleotides. A less pronounced influence of the size-augmentation in the template strand on the incorporation efficiency was observed for KF exo- than for Dpo4. For both enzymes, the triphosphate effect observed for unmodified templates could also be measured within modified templates. However, comparing the different modified templates for the same nucleoside triphosphate, it attracted attention that the template effect was less pronounced than the triphosphate effect in case of KF exo-. In case of Dpo4 in contrast it was more pronounced than the triphosphate effect. Astonishingly, in case of KF exo- the template effect on modified nucleoside triphosphates was even less than on unmodified nucleoside triphosphates, whereas for Dpo4 the effect was almost equal for all triphosphates. Nevertheless, the flexibilities of the binding pockets of both enzymes reached their limits. In Dpo4 for example, the incorporation efficiencies of the bulkiest pairs (**dN^{Et}-dN^{Et}TP**) even reached the level of mismatched cases (dT-dTTP and dG-dTTP).

Taken together, the results derived from size-augmentation on both ends of the active site of the DNA polymerases strongly agree with the model of *active site tightness* [*Kool*, 2002]. Moreover, they support the reported flexibility that TLS polymerases should possess to accommodate certain DNA lesions [*Mizukami* et al., 2006]. Furthermore, the different behavior on the base pair orientation by both enzymes is along the lines with earlier findings [*Minnick* et al., 2002]. Additonally, it was observed that the influence on the incorporation efficiency through sterically enlarged probes is stronger for purine nucleotides than for pyrimidine nucleotides.

The second project concerns transient kinetics on *KlenTaq* DNA polymerase and two mutants with 4'-alkylated thymidine nucleotides. These functional studies have been accompanied by structural investigations of M.Sc. Karin Betz in a collaboration of AG Marx and AG Welte. The studies on the wild type enzyme delivered structural snapshots of size-augmented nucleotide probes bound to the active site of a DNA polymerase. The nucleotide probes adopted nearly identical conformation as reported earlier for the unmodified substrates. The same held true for the protein side chains. Since the kinetics of nucleotide incorporation differed significantly between the natural and size-augmented nucleotides, the finding of nearly identical enzyme and substrate conformations suggested mechanistic steps that are not resolved by the crystal structures to be rate-limiting. The interplay with distinct enzyme side chains may account for this observation.

Indeed, upon these results site-directed mutagenesis of a single side chain most proximate to the 4'-modification in *KlenTaq* DNA polymerase increased nucleotide incorporation efficiencies for the size-augmented nucleotides to the level found for the unmodified substrate in the wild type enzyme. The mutation from an isoleucine at position 614 to a smaller alanine opened space for the 4'-alkyl residue of the modified dNTP. Interestingly, the dissociation constants of the modified substrates did not differ from the natural one assuming unaffected binding. However, the incorporation rate of natural dTTP was around threefold higher leading to an increased incorporation efficiency of the natural substrate. The results corroborate the assumption that during the transition state the amino acid side chain at position 614 closely contacts the sugar ring to read out aberrant sugar conformations.

Motivated by these results, a highly efficient *KlenTaq* mutant evolved by Dr. Christian Glöckner, AG Marx, bearing two mutations M747K and I614K has been probed by the 4'-modified dTTP in presteady-state kinetics. Again, M.Sc. Karin Betz performed crystallization trials with the **dN^{R}TP** to give additional structural insights on the binding interaction of these substrates by the double mutant polymerase. Besides the 4'-methylated and 4'-ethylated thymidine triphosphates, which showed similar kinetic parameters in preceding experiments, 4'-isopropylated thymidine triphosphates were applied in addition. As observed before from Dr. Christian Glöckner, AG Marx, for unmodified dATP, higher incorporation efficiencies could also be reported for the unmodified thymidine triphosphates, but also for the modified ones. Additionally,

4'-alkylated probes were significantly better incorporated relatively to unmodified substrates by the double mutant than by the wild type. The *KlenTaq* DM KK could even process the bulky **dT^{iP}TP**, which is a poor substrate for the *KlenTaq* wt DNA polymerase. Once more, M.Sc. Karin Betz could report crystal structures of the polymerase in complex with DNA and 4'-methylated and 4'-ethylated dTTP. Moreover, as the *KlenTaq* DM KK binding pocket is large enough to accommodate **dT^{iP}TP**, she could also report a structure for this substrate, which was not accessible for the wild type enzyme. Like in the wt structures, protein, DNA and nucleotide in the *KlenTaq* DM KK structures did not differ noticeably from the structures of the wild type in complex with ddTTP. However, the distances between 4'-methyl and 4'-ethyl residue, respectively, and the side chain of amino acid K614 were, as expected, larger than the distances of these residues to the side chain of I614 in the wt structures. For the 4'-isopropyl residue the distance to the side chain of K614 of the *KlenTaq* DM KK structure was comparable to the distances measured for 4'-methyl and 4'-ethyl residue, respectively, to the side chain of amino acid I614 in the wt structure. This again explained the comparable kinetic parameters.

Summarized the results from functional and structural studies delivered new insights on the processing of 4'-*C*-alkylated nucleotides and on the interaction of DNA polymerases with the sugar part of nucleotides. First, the findings are in the line with previous results that geometrical factors are mainly the reason for gaining selectivity [*Kool*, 2002]. Second, the transient kinetics showed that 4'-alkylation of dNTP mostly influences the incorporation rate, whereas the binding constant is less affected. Structural results from M.Sc. Karin Betz corroborate these findings. Third, the results from mutating position 614 suggest that this amino acid plays an important role in recognition of aberrant sugar conformations and constitutions. Possibly, during transition state this amino acid closely contacts the sugar ring.

Altogether, the results of this work confirm the model of *active site tightness* [*Kool*, 2002]. The kinetic parameters helped to give quantitative conclusions of the incorporation efficiencies obtained for 4'-modified nucleotides. Steady-state kinetics of two complementary, 4'-modified nucleotide base pair yielded incorporation efficiencies that allowed conclusions on the influence of 4'-modifications on the incorporation efficiency of the orientation of the nucleobase pairs (dA-template:dTTP compared to dT-template:dATP). It was observed that the size-augmentation at the 4'-position influenced the incorporation efficiency of the purine nucleotide more than of the

pyrimidine nucleotide. This was further corroborated by the misincorporation of the **dT^{R}TPs** opposite dT and dG by the TLS DNA polymerase Dpo4. Furthermore, the results for Dpo4 on the sterically enlarged probes indicated that TLS polymerases posses a flexible active site [*Mizukami* et al., 2006].

The presteady-state kinetics of *KlenTaq* DNA polymerase and two mutants on 4'-alkylated dTTP delivered the first kinetic parameters of the incorporation of these probes by these enzymes. It was observed that the influence of 4'-modifications is much higher on the incorporation rate k_{pol} than the binding (K_D). Accompanying structural investigations by M.Sc. Karin Betz gave an insight on the binding situation of **dT^{R}TPs** in the active site. Due to these results the amino acid I614 could be identified, which was discussed to be directly involved in the recognition process of ribonucleotides [*Patel and Loeb*, 2000, *Patel* et al, 2001]. Through site-directed mutagenesis, the amino acid was exchanged to the smaller amino acid alanine, resulting in an almost unaffected acceptance of the modified substrates. Similar results could be obtained for the DM KK of *KlenTaq* DNA polymerase, which has the non-branched amino acid lysine at this position. This mutant also showed an increased acceptance for 4'-modified nucleotides.

It remains unclear, how the recognition step by I614 proceeds in detail. The same isoleucine to alanine mutation was reported to increase rNTP incorporation by DNA polymerase I of *Escherichia coli* (I709 in DNA pol I corresponds to I614 in *KlenTaq*) [*Shinkai* et al., 2001]. Moreover, further side chains of other amino acids might be crucial for the recognition of the substrates during transition state. Unfortunatelly, until now no transition state analogues for crystallization of DNA polymerases exist. Vanadate modified nucleotides are currently intensively discussed for this purpose [*Borden* et al., 2006]. Moreover, it is not known, why 4'-modifications interfere further extension after the incorporation of 4'-alkylated substrates. To clarify this and to better understand the reaction pathway, the crystallization of primer probes already bearing the incorporated 4'-alkylated nucleotide at the primer end would be helpful. Primer probes for crystallization generally contain dideoxynucleotides, to prevent further incorporation at the primer end. However, deoxygenation of the C3'-OH would influence the 2'-endo conformation of the sugar, leading to an abnormal orientation of the 4'-modification. Non-hydrolizable triphosphates, which have recently been used for crystallization [*Upton* et al., 2009], could help to solve this problem. The structural investigations should be accompanied by site-directed mutagenesis along with enzyme

kinetics, which through the exchange of further amino acids in the active site might deliver supplementing insights on substrate recognition. Through transferring the concept to other DNA polymerases, especially of different families, additional results about the influence of these positions on the substrate recognition process might explain, why selectivity varies within different DNA polymerases and which amino acids are crucial.

Until now, it is still not yet completely clarified, which amino acid has which function through contacts with the substrates during the nucleotidyl transfer. As could be shown in this work, even non-polar amino acids, which are part of the developing binding pocket, can influence selectivity. Studies on the recently proposed extended 2-metal-ion mechanism could reveal different acidic amino acids as proton donors for the pyrophosphate leaving group, which are involved in the nucleotidyl transfer in different DNA polymerases [*Castro* et al., 2009]. At the same time, the authors postulate that an unidentified basic amino acid should promote the deprotonation of the C3'-OH of the primer terminus. The participation of individual amino acids on the functionality and selectivity of different DNA polymerases is a complex mechanism and remains a challenge to be revealed. The selectivity of processes involving DNA polymerases was recently reported to be significant influenced even by auxiliary proteins [*Maga* et al., 2007]. Even if we are far from understanding the complex mechanisms of these enzymes in detail and in which way whole protein-ensembles are involved, it can be mentioned as a concluding remark, that chemically tailor-made probes can help to gain detailed insights in biological processes, like in this case the DNA synthesis.

5 Zusammenfassung und Ausblick

Im Rahmen dieser Arbeit wurde die Synthese von 4'-alkylierten 2'-Desoxyadenosin und Thymidin Nukleosiden und den entsprechenden 5'-*O*-Triphosphaten sowie 3'-*O*-Phosphoramiditen ausgehend von 1,2:5,6-Di-*O*-isopropyliden-α-D-glucofuranose erfolgreich durchgeführt. Die Synthesestrategie hierfür wurde von Dr. Gopinath Rangam, AG Marx, entwickelt. Die erhaltenen Phosphoramidite wurden anschließend in einer automatisierten DNA-Synthese verwendet um modifizierte Oligonukleotid-Template zu synthetisieren.

Die modifizierte Template sowie die komplementären Nukleosidtriphosphate wurden anschließend in Einzeleinbaustudien als Substrate für zwei verschiedene Polymerasen eingesetzt. Das Klenow Fragment exo- der DNA-Polymerase I aus *Escherichia coli*, einem relativ genauen Enzym der Polymerasenfamilie A, wurde mit der Transläsionspolymerase Dpo4 der Familie Y verglichen. Die Einbauverhalten beider Enzyme mit obengenannten Sonden wurden mittels Steady-State Enzymkinetiken unter *single completed hit* Bedingungen quantitativ ermittelt.

Die erhaltenen Ergebnisse lieferten interessante neue Aspekte. Erstens, bestätigte die Tatsache, dass die fehleranfällige TLS DNA-Polymerase Dpo4 die vergrößerten Nukleotide effizienter einbaut als die selektivere KF exo-, das Modell, dass DNA-Polymerasen, welche eine hohe Genauigkeit aufweisen, starrere Bindungstaschen ausbilden und somit weniger geometrische Variation zulassen, während weniger genaue Enzyme größere Flexibilität zeigen, was wiederum zu geringerer Genauigkeit führt. Dieses Ergebnis bekräftigt frühere Forschungsergebnisse [*Kool*, 2002, *Mizukami* et al., 2006]. Zweitens, bauten beide Enzyme unmodifiziertes dATP effizienter ein als dTTP. Das Gegenteil konnte jedoch für vergrößerte Sonden beobachtet werden. Scheinbar sind die sperrigeren Purin-Nukleotide $\mathbf{dA^R}$ größeren sterischen Zwängen im Aktiven Zentrum des Enzyms ausgesetzt als die Pyrimidine $\mathbf{dT^R}$. Diese unterschiedlichen

Eigenschaften könnten ein Grund dafür sein, dass die Selektivität des Nukleotideinbaus je nach Orientierung des sich ausbildenden Nukleotidpaares variiert [*Minnick* et al., 2002]. Diese Annahme wird unterstützt von der Tatsache, dass die vergrößerten **dT^{R}TP** relativ zu ihrem unmodifizierten Analoga effizienter gegenüber nicht-kanonischen Templat-Nukleotiden eingebaut werden als im Vergleich dazu ihre Adenosin Pendants. Frühere Strukturuntersuchungen zeigten, dass der Zuckerrest des eintretenden dNTPs vollständig in der Substratbindetasche der DNA-Polymerase eingebettet ist und ein wichtiger Bestandteil des Substraterkennungsprozesses darstellt [*Johnson and Beese*, 2004, *Rothwell and Waksman*, 2005]. Demzufolge, scheint das Erkennen des eintretenden dNTP-Zuckers dem Enzym zusätzliche Möglichkeiten zu bieten, um kanonische Basenpaarformation durch indirektes Ablesen von abweichenden Zuckerkonformationen zu ermöglichen.

Anschließend an die vorherigen Ergebnisse, wurde das Aktive Zentrum der Polymerasen durch modifizierte Templatnukleotide weiteren sterischen Wechselwirkungen ausgesetzt. Dabei konnte beobachtet werden, dass durch die sterische Vergrößerung im Templatstrang ein geringerer Einfluss auf die Einbaueffizienz des KF exo- als der Dpo4 ausgeübt wird. Für beide Enzyme konnte der für unmodifizierte Template beobachtete Triphosphateffekt auch für modifizierte beobachtet werden. Wenn man jedoch die verschiedenen modifizierten Template für das gleiche Nukleosidtriphosphat vergleicht, fällt im Falle der KF exo- auf, dass der Templateffekt geringer ausfiel als der Triphosphateffekt. Im Falle von Dpo4 dagegen war der Templateffekt stärker als der Triphosphateffekt. Überraschenderweise war der Templateffekt für modifizierte Nukleosidtriphosphate in der KF exo- geringer als für unmodifizierte Nukleosidtriphosphate, wohingegen für Dpo4 der Effekt für alle Triphosphate ähnlich war. Ungeachtet dessen erreichte die Flexibilität der Bindungstasche bei beiden Enzymen ihre Grenze. Einbaueffizienzen der sperrigsten Paare (**dN^{Et}-dN^{Et}TP**) erreichte beispielsweise in Dpo4 die Größenordnung der untersuchten Fehlpaarungseinbauten (dT-dTTP und dG-dTTP).

Zusammengefasst lässt sich sagen, dass die Ergebnisse, welche durch die Vergrößerung der Substrate an beiden Enden des Aktiven Zentrums der DNA-Polymerasen erhalten wurden, mit dem *sterischen Modell der selektiven Substratauswahl* übereinstimmten [*Kool*, 2002]. Desweiteren bestätigten sie auch die postulierte Flexibilität, welche TLS DNA-Polymerasen besitzen müssen, um DNA-Schäden überlesen zu können [*Mizukami* et al., 2006]. Auch das unterschiedliche

Verhalten beider Enzyme auf die Basenpaarorientierung war im Einklang mit früheren Beobachtungen [*Minnick* et al., 2002]. Zusätzlich konnte gezeigt werden, dass bei sterisch vergrößerten Sonden der Einfluss auf die Einbaueffizienz für das Purinnukleotid stärker ausfällt als für das Pyrimidinnukleotid. Die größeren Purinnukleotide scheinen im Aktiven Zentrum stärkeren Zwängen hinsichtlich geometrischer Abweichungen ausgesetzt zu sein. Dieses wiederum zeigte auch der beobachtete Fehleinbau von **dT^{R}TP** gegenüber dT- und dG-Templatnukleotiden durch Dpo4.

Im zweiten Projekt wurden Transient-Kinetiken der *KlenTaq* DNA-Polymerase und zweier Mutanten mit 4'-alkylierten Thymidinnukleotiden gemessen. Diese funktionalen Studien wurden durch strukturelle Untersuchungen von M.Sc. Karin Betz in einer Kooperation der AG Marx und Welte vervollständigt. Die Ergebnisse aus den Strukturuntersuchungen am *KlenTaq* Wildtyp Enzym ergaben strukturelle Momentaufnahmen von vergrößerten Nukleotidsonden, die im Aktiven Zentrum der DNA-Polymerase gebunden waren. Die Nukleotidsonden lagen dabei in fast identischer Konformation wie in früher publizierte Strukturen mit unmodifizierten Substraten vor. Das galt auch für die Proteinseitenketten. Da die Kinetiken der Nukleotideinbauten zwischen natürlichen und vergrößerten Nukleotiden signifikant voneinander abwichen, ließen die fast identischen Enzym- und Substratkonformationen vermuten, dass mechanistische Abläufe geschwindigkeitsbestimmend sind, welche nicht durch die Kristallstrukturen aufgelöst werden können. Die Wechselwirkungen mit einzelnen Enzymseitenketten könnten hierbei eine große Rolle spielen.

Tatsächlich erhöhte aufgrund dieser strukturellen Ergebnisse eine ortsgerichtete Mutagenese einer einzelnen Seitenkette in unmittelbarer Nähe zur 4'-Modifikation in der *KlenTaq* DNA-Polymerase die Nukleotideinbaueffizienzen für die vergrößerten Nukleotide auf die Größenordnung der Effizienz des unmodifizierten Substrates im Wildtyp Enzym. Die Mutation von einem Isoleucin an der Position 614 zu einem kleineren Alanin schafft Platz für den 4'-Alkylrest der modifizierten dNTP. Interessanterweise, unterscheiden sich die Dissoziationskonstanten der modifizierten Substrate nicht von dem natürlichen, was eine unbeeinflusste Bindung vermuten lässt. Jedoch, war die Einbaurate des natürlichen dTTP dreimal höher, was zu einer deutlich vergrößerten Einbaueffizienz des natürlichen Substrates führte. Die Ergebnisse bestätigen die Annahme, dass während des Übergangszustandes die Aminosäure-

seitenkette an der Position 614 dem Zuckerring sehr nahe kommt, um möglicherweise abweichende Zuckerkonformationen zu erkennen.

Motiviert durch diese Ergebnisse, wurde eine hoch effiziente *KlenTaq* Mutante, welche von Dr. Christian Glöckner, AG Marx, im Rahmen seiner Dissertation hergestellt wurde und die zwei Mutationen M747K und I614K beinhaltet, mit 4'-modifizierten dTTP in Presteady-State Kinetiken untersucht. Auch an dieser Stelle führte M.Sc. Karin Betz Kristallisierungsstudien mit den **dN^{R}TP** durch, um zusätzliche strukturelle Einblicke in das Bindungsverhalten dieser Substrate mit der Doppelmutante zu erhalten. Neben 4'-methylierten und 4'-ethylierten Thymidintriphosphaten, die ähnliche kinetische Parameter in vorherigen Experiment zeigten, wurden zusätzlich 4'-isopropylierte Thymidintriphosphate untersucht. Wie schon von Dr. Christian Glöckner für das unmodifizierte dATP beschrieben, konnten höhere Einbaueffizienzen für das unmodifizierte dTTP, aber auch für die modifizierten Thymidintriphosphate beobachtet werden. 4'-Alkylierte Sonden wurden von der Doppelmutante auch relativ zum unmodifizierten Substrat signifikant besser eingebaut als vom Wildtyp. Die *KlenTaq* DM KK war sogar in der Lage das sperrigere **dT^{iP}TP** einbauen, welches ein schlechtes Substrat für die *KlenTaq* wt DNA-Polymerase ist. Auch hier konnte M.Sc. Karin Betz Kristallstrukturen der Polymerase im Komplex mit DNA und 4'-methylierten und 4'-ethylierten dTTP erhalten. Da die Bindungstasche der *KlenTaq* DM KK groß genug für das **dT^{iP}TP** ist, konnte sie außerdem Strukturen von diesem Substrat erhalten, was mit der Wildtyp Polymerase nicht gelang. Wie in den Wildtyp Strukturen, unterscheiden sich auch in den *KlenTaq* DM KK Strukturen das Protein, die DNA sowie die jeweiligen Nukleotide nicht wesentlich von den Strukturen des Wildtyps im Komplex mit ddTTP. Es konnten jedoch Abstände zwischen den 4'-Methyl- und 4'-Ethylresten zur Seitenkette der Aminosäure K614 gemessen werden, welche wie erwartet größer waren als die Abstände der Reste zur Seitenkette der I614. Für den 4'-Isopropylrest zur Seitenkette der K614 wurde ein vergleichbarer Abstand gemessen wie für 4'-Methyl- und 4'-Ethylreste zur Seitenkette I614 in der Wildtyp Struktur. Das wiederum erklärte die vergleichbaren kinetischen Parameter.

Zusammenfassend liefern die Ergebnisse der funktionalen und strukturellen Studien mehrere neue Einblicke in das Einbauverhalten der 4'-alkylierten Nukleotide und in die Interaktion der DNA-Polymerase mit den Zuckerresten der Nukleotide. Erstens, bestätigen die Ergebnisse frühere Erkenntnisse, dass geometrische Faktoren der Hauptgrund für die erlangte Selektivität sind [*Kool*, 2002]. Zweitens, zeigten die

Transient-Kinetiken, dass die 4'-Alkylierung des dNTP hauptsächlich die Einbaurate beeinflusst, wohingegen die Bindungskonstante weniger stark beeinflusst wird. Strukturergebnisse von M.Sc. Karin Betz bestätigen diese Ergebnisse. Drittens, suggerieren die Ergebnisse der Mutation an der Position 614, dass diese Aminosäure eine wichtige Rolle im Erkennen von abweichenden Zuckerkonformationen und -konstitutionen spielt. Möglicherweise kommt diese Aminosäure während des Übergangszustandes in starke räumliche Nähe zum Zuckerring.

Insgesamt lässt sich sagen, dass die Ergebnisse dieser Arbeit das *sterische Modell der selektiven Substratauswahl* durch funktionelle Kinetikstudien an verschiedenen DNA-Polymerasen bestätigen konnten [*Kool*, 2002]. Die kinetischen Parameter erlauben quantitative Aussagen über Einbaueffizienzen von 4'-modifizierten Nukleotiden. Steady-State Kinetiken ergaben Einbaueffizienzen zweier komplementärer, 4'-modifizierter Nukleotidbasenpaare, welche Schlussfolgerungen über den Einfluss der 4'-Modifikation auf die Einbaueffizienz der zwei Orientierung des Basenpaares erlaubten (dA-Templatnukleotid:dTTP im Vergleich zu dT-Templatnukleotid:dATP). Es konnte festgestellt werden, dass Vergrößerungen an der 4'-Position des Purinnukleotids stärker die Effizienz beeinflussen als entsprechende Modifikationen des kleineren Pyrimidinnukleotids. Dies zeigten auch die erhaltenen Fehleinbauten der **dT^{R}TP** gegenüber dT und dG durch die TLS DNA-Polymerase Dpo4. Desweiteren konnten die Ergebnisse für die Dpo4 mit den sterisch anspruchsvollen Sonden weitere Indizien liefern, dass Transläsionspolymerasen eine erhöhte Flexibilität der Bindungstasche aufweisen [*Mizukami* et al., 2006].

Die Presteady-State Kinetiken mit 4'-alkylierten dTTP an der *KlenTaq* DNA-Polymerase und zweier Mutanten ergaben die ersten kinetischen Daten zum Einbau dieser Sonden durch die *KlenTaq* DNA-Polymerase. Es konnte gezeigt werden, dass der Einfluss der 4'-Modifikation in größerem Maße die Einbaurate k_{pol} beeinträchtigt und geringfügiger die Bindung (K_D). Begleitende Strukturuntersuchungen durch M.Sc. Karin Betz halfen einen Einblick in die Bindungssituation der **dT^{R}TP** im Aktiven Zentrum zu erhalten. Es konnte aufgrund dieser Strukturen die Aminosäure I614 identifiziert werden, deren Beteiligung im Erkennungsprozess von Ribonukleotiden eine entscheidende Rolle spielt [*Patel and Loeb*, 2000, *Patel* et al., 2001]. Durch ortsgerichtete Mutagenese wurde diese Aminosäure durch die kleinere Aminosäure Alanin ausgetauscht, was zu einer fast unbeeinflussten Akzeptanz der

modifizierten Substrate führte. Ähnliche Ergebnisse wurden mit einer Doppelmutante der *KlenTaq* DNA-Polymerase erhalten, welche an der gleichen Position die nichtverzweigte Aminosäure Lysin trägt. Auch diese zeigte eine verbesserte Akzeptanz 4‘-modifizierter Nukleotide.

Weiterhin unklar bleibt, wie genau der Erkennungsschritt durch I614 abläuft. Die gleiche Isoleucin zu Alanin Mutation erhöhte einer Studie zufolge die Einbaurate von rNTP durch die DNA-Polymerase I von *Escherichia coli* (I709 in der DNA pol I entspricht I614 in *KlenTaq*) [*Shinkai* et al., 2001]. Zusätzlich könnten noch weitere Seitenketten anderer Aminosäuren am Substraterkennungsprozess im Übergangszustand entscheidend sind. Leider existieren noch keine Übergangszustandsanaloga zur Kristallisation von DNA-Polymerasen. Vanadat-modifizierte Nukleotide wurden kürzlich für diesen Zweck vorgeschlagen [*Borden* et al., 2006]. Es ist außerdem noch nicht klar, weshalb 4‘-Modifikationen eine Verlängerung nach dem Einbau der 4‘-alkylierten Substrate behindern. Zur Klärung dieses Verhaltens und auch um den Reaktionsverlauf besser zu verstehen, wäre die Kristallisation von Primersonden von Vorteil, welche schon eingebaute 4’-alkylierte Nukleotide am Primerende besitzen. Primersonden zur Kristallisation besitzen meistens Didesoxynukleotide für diesen Zweck, um weiteren Einbau am Primerende zu verhindern. Jedoch würde die Reduktion der C3’-OH Gruppe die C2’-endo Konformation des Zucker beeinflussen, was zu einer unnatürlichen Orientierung der 4’-Modifikation führen würde. Durch nicht-hydrolysierbare Triphosphate, welche kürzlich zur Kristallisation von DNA-Polymerasen verwendet wurden, könnte dieses Problem umgangen werden [*Upton* et al., 2009]. Die Strukturuntersuchungen müssten durch zielgerichtete Mutationsstudien der *KlenTaq* DNA-Polymerase und deren enzymkinetischer Untersuchung begleitet werden, welche durch den Austausch weiterer Aminosäuren im Aktiven Zentrum ergänzende Einblicke liefern würden. Der Einfluss relevanter Positionen auf die Substraterkennung könnte durch Übertragung der Erkenntnisse auf andere DNA-Polymerasen, besonders aus anderen Familien, weitere Informationen liefern, warum die Selektivität zwischen einzelnen DNA-Polymerasen variiert und welche Aminosäuren dafür entscheidend sind.

Bis jetzt ist weiterhin noch nicht vollständig geklärt, welche Aminosäure welche Funktion während des Nukleotideinbaus durch Kontakte mit den Substraten besitzt. Wie in dieser Arbeit gezeigt wurde, können auch nicht-polare Aminosäuren, welche Teil der sich ausbildenden Bindungstasche sind, Einfluss auf die Selektivität haben. Arbeiten

zum kürzlich vorgeschlagenen erweiterten 2-Metal-Ionen-Mechanismus konnten verschiedene saure Aminosäuren als Protonendonatoren für das austretende Pyrophosphat identifizieren, welche in verschiedenen Enzymen am Nukleotidtransfer beteiligt sind [*Castro* et al., 2009]. Gleichzeitig postulieren die Autoren, dass auch eine bis jetzt nicht identifizierte basische Aminosäure als Protonenakzeptor der C3‘-OH des Primerterminus beteiligt sein muss. Die Beteiligung einzelner Aminosäuren an der Funktionsweise als auch an der Selektivität verschiedener DNA-Polymerasen ist ein komplexer Mechanismus und es bleibt weiterhin eine Herausforderung diese aufzudecken. Die Selektivität von Prozessen, an denen DNA-Polymerasen beteiligt sind, wird wie kürzlich berichtet auch möglicherweise durch Hilfsproteine von außen beeinflusst [*Maga* et al., 2007]. Auch wenn weiterhin noch viele Unklarheiten bestehen, wie der äußerst komplexe Mechanismus der DNA-Polymerasen funktioniert und inwiefern ganze Protein-Ensemble diesen beeinflussen, kann abschließend gesagt werden, dass chemisch maßgeschneiderte Sonden helfen können, detaillierte Einblicke in biologischen Prozesse, wie in diesem Fall die DNA-Synthese, zu erhalten.

6 Experimentals

6.1 General Equipment, Reagents and Instruments

All chemicals were - if not stated otherwise - of p.a. or of molecular biology quality grade. Chemicals for synthesis were bought from Acros, Sigma Aldrich or Carbosynth. Purified water was drawn from a combined reverse osmosis/ultrapure water system (Sartorius stedim biotech, arium-series).

Chemicals used for Biochemical Assays:

Acrylamid	Roth
Agar	Roth
Agarose	Invitrogen
Ammonium hydroxide solution (33%)	Riedel de Haën
Ammonium peroxodisulfate	Fluka
β-Mercaptoethanol	Roth
Boric Acid	Fluka
Bromphenol Blue	Fluka
Bovine Serum Albumin Standard (2mg/ml)	Pierce
Carbenicilline disodium salt	Roth
Chelating Sepharose Fast Flow	GE Healthcare
Coomassie Brillant Blau G 250	Roth
1,4-Dithiothreitol	Roth
Ethanol (100%)	Roth
Ethidiumbromide (0.1%)	Roth

Ethylendiamintetraacetat (EDTA)	Roth
Formamide	Merck
Glycerol	Prolabo
Imidazole	Merck
Isopropyl β-D-1-thiogalactopyranoside (IPTG)	Roth
LB broth (Lennox)	Roth
Magnesium chloride	Acros Organics
N,N,N‘,N‘-Tetramethylenethylendiamin (TMEDA)	Roth
Sodium acetate trihydrate	Merck
Sodium chloride	Roth
Sodium dodecylsulfate (SDS)	Roth
Natriumhydroxid	Merck
Ni-NTA-Agarose	Roth
Sephadex G50	Amersham Pharmacia Biotech
Tris-(hydroxymethyl)-aminomethan (Tris)	Roth
Triton X-100	Roth
Urea	Roth

Nucleotides and Radiochemicals:

dNTPs	Roche, Fermentas
[γ-^{32}P]-ATP	Hartmann Analytik

Biochemical Reagents, Enzymes and Kits:

DpnI	New England Biolabs/Fermentas
Gene Ruler 1 kp DNA Ladder	Fermentas
Gene Ruler DNA Ladder Mix	Fermentas
High Pure PCR Cleanup Micro Kit	Roche
High Pure Plasmid Isolation Kit	Roche
Lysozyme	Sigma
PageRuler Unstained Protein Ladder	Fermentas

Phusion DNA Polymerase	Finnzyme
QIAquick Gel Extraction Kit	Qiagen
Rapid DNA Ligation Kit	Fermantas
T4 Polynucleotide kinase	New England Biolabs

Bacterial Strains and Plasmids

E. coli BL21-Rosetta (DE3) pLysS	Novagen (kindly provided by N. Staiger)
Electro competent *E. coli* XL10-Gold	Stratagene (kindly provided by K. Heintz)
Electro competent *E. coli* BL21 (DE3) Gold	Stratagene (kindly provided by F. Di Pasquale, N. Staiger, M. Drum and N. Blatter)
pGDR11	AG Welte, Universität Konstanz
pQKF-	AG Marx, Universität Konstanz
pET22b(+)	AG Marx, Universität Konstanz

Disposables

96-well plates (200 µl)	ABgene
96-deep well plates (2.2 ml)	Peske
384-deep well plates (300 µl)	Abgene
Adhesive sealing foil	ABgene
Cuvettes (1.5 – 3 ml)	Roth
Diamond sealing foil	ABgene
Electroporation Gene Pulser cuvettes (1/2 mm)	BioRAD
Gas permeable adhesive seals	ABgene
Glass wool	Serva
Injection needles	Braun
Petri dishes	Roth
Reaction tubes (1.5, 2.0 ml)	Peske Laborbedarf

Scalpels	Bayha
Sephadex G-25 columns	GE Healthcare
Tips for pipetting robot	Hamilton Robotics
Tips for multichannel pipettes	Peske
Tips for laboratory pipettes	Peske, Eppendorf
UV-cuvettes	Eppendorf
Vivaspin columns (6, 20 ml) 10.000 MWCO	Sartorius stedim biotech
Whatmanpaper 3mm	Merck Eurolab

Equipment

Agarose gel racks	Fisher Scientific, ABgene
Autoclav	Autoclav Systec 3150 ELV
Electroporator Gene Pulser Xcell	BioRAD
ESI-MS 3000	Bruker Daltonics
Floor centrifuge 5804R	Eppendorf
Freezer (-80°C, -20°C, 4°C)	Thermo Forma, Liebherr, Premium
Gel documentation device, Chemidoc XRS	BioRAD
Gel dryer	BioRAD
GenePix Personal 4100A microarray scanner	Molecular Devices
Heating block	Stuart
Incubation shaker	New Brunswick Scientific
Incubation shaker, Titramax 1000	Heidolph
Laboratory pipettes	Eppendorf
Magnetic stirrer MR 3000 D	Heidolph
Microarray Peltier Thermal Cycler 200	MJ Research
Multifuge KR 4	Heraeus
Multichannel pipettes Transferpette	Brand

Oligonucleotide synthesizer	ABI 392
PAGE electrophoresis racks	BioRAD
PCR-thermocycler	Biometra
pH meter, Seven Easy	Mettler Toledo
Phosphorimager Molecular Imager Chemi-Doc XRS System	BioRAD
Photometer Cary 100 Bio	Varian
Pipetting robot Microlab Star	Hamilton Robotics
Phosphor screens	Fuji
Phosphor screen cassettes BAS-Cassette 2025	Fuji
Plate sealer	Abgene
Power supply Power Pac 3000	BioRAD
Radioactivity counter Contamat FHT111M	Thermo
Reagent dispenser Multidrop	Thermo
Refrigerated centrifuge Biofuge Primo R	Heraeus
Radioactivity shields	Roth
SDS-PAGE racks	BioRAD
Speed-Vac Concentrator 5301	Eppendorf
Sterile bench	HERA safe
Thermomixer, Thermomixer comfort	Eppendorf
Table top centrifuges, MiniSpin	Eppendorf
UV-transilluminator	Bachofer
UV/VIS photometer ND-1000 Nanodrop	Peqlab
Vortexer REAX Control	Heidolph
Water baths	Memmert

Buffers and Solutions

Agarose gel loading buffer	Bromophenol Blue	0.025% (w/v)
	Xylene cyanol FF	0.025% (w/v)
	Glycerol	60%
	EDTA	60 mM
Agarose gel staining solution	Ethidium bromide	0.5 µg/ml in 1x TAE
Coomassie staining solution	Acetic acid	50 ml
	Ethanol	125 ml
	Water	300 ml
	Coomassie Roti Blue	375 mg
Coomassie destaining solution	Acetic acid	10%
	Ethanol	30% (v/v)
10x *KlenTaq* reaction buffer	Tris-HCl pH 9.2	500 mM
	$(NH_4)_2SO_2$	160 mM
	$MgCl_2$	25 mM
	Tween 20	1 % (v/v)
1 x *KlenTaq* lysis buffer	1 x *KlenTaq* reaction buffer	
	Lysozyme	0.1 mg/ml
2 x *KlenTaq* washing buffer (Ni-NTA purification and Vivaspin)	Tris-HCl pH 9.2	100 mM
	$MgCl_2$	25 mM
	Imidazole	various concentrations: (0, 5, 20,200 mM)

1x *KlenTaq* storage buffer	Tris-HCl pH 9.2	50 mM
	$(NH_4)_2SO_2$	16 mM
	$MgCl_2$	2.5 mM
	Tween 20	0.1 % (v/v)
	Glycerole	~ 50% (v/v)
SDS-PAGE stacking gel buffer	Tris-HCl pH 6.8	1 M
SDS-PAGE resolving gel buffer	Tris-HCl pH 8.8	1.5 M
SOB-Medium pH 7.0	Tryptone	2% (w/v)
	Yeast extract	0.5% (w/v)
	NaCl	0.05%(w/v)
	After sterilisation, addition of:	
	$MgCl_2$	0.01M
	$MgSO_4$	0.01M
SOC-Medium pH 7.0	SOB Medium +	
	Glucose 20%(w/v)	2% (v/v)
5x SDS-PAGE loading buffer	Tris-HCl pH 8.0	1 M
	EDTA	0.5 M
	Glycerol	50%
	Bromophenol Blue	0.05% (w/v)
	β-Mercaptoethanol	1% (v/v)
10x SDS-PAGE electrophoresis buffer	Tris-HCl pH 8.9	250 mM
	Glycin	2 M
	SDS	1% (w/v)

10x TBE buffer	Tris	890 mM
	Boric acid	890 mM
	EDTA pH 8.0	20 mM
10x SDS-PAGE electrophoresis buffer	Tris-HCl pH 8.9	250 mM
	Glycin	2 M
	SDS	1% (w/v)
10x TBE buffer	Tris	890 mM
	Boric acid	890 mM
	EDTA pH 8.0	20 mM
Urea-PAGE loading buffer (STOP-solution)	EDTA	20 mM
	Formamide	80%
	Bromophenol Blue	0.025% (w/v)
	Xylene cyanol FF	0.025% (w/v)
Urea-PAGE stock solution 1	Urea	8.3 M in 10x TBE
Urea-PAGE stock solution 2	Acrylamide solution	25%
	Urea	8.3 M
	N,N'-Methylenbisacrylamide	2%
Urea-PAGE stock solution 3	Urea	8.3 M
1x Dpo4 Reaction Buffer	Tris-HCl pH 8.0	50 mM
	$MgCl_2$	10 mM
	KCl	20 mM
	DTT	2 mM
	BSA	100 µg/ml
	Glycerol	10%

1x KF exo- Reaction Buffer	Tris-HCl pH 7.3	50 mM
	$MgCl_2$	10 mM
	DTT	1 mM
1x RQF Reaction Buffer	Tris-HCl pH 7.5	20 mM
	NaCl	50 mM
	$MgCl_2$	2 mM

6.2 Chemical Methods

6.2.1 Synthesis of Nucleoside 5'-*O*-Triphosphates

The synthesis of the nucleoside 5'-*O*-triphosphates has been published in Streckenbach, F., Rangam, G., Moller, H.M. & Marx, A. *Chembiochem* **10**, 1630-3 (2009). 4'-Isopropylated thymidine 5'-*O*-triphosphates have been available in our group.

6.2.2 Synthesis of Phosphoramidite Building Blocks

Thymidine building blocks have already been synthesized during my Diploma work [*Streckenbach*, 2006].

2'-Deoxy-6-*N*-formamidine-5'-*O*-(4,4-dimethoxytrityl)-4'-*C*-methyl adenosine

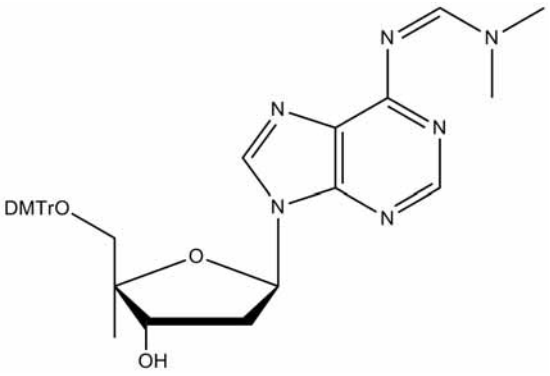

6a-A

The compound **2'-deoxy-4'-*C*-methyl adenosine (1a)** (100 mg, 0.377 mmol) was dissolved in methanol (4 ml) and *N*,*N*-dimethylformamide dimethylacetal (200 µl, 1.5 mmol) was added and the reaction mixture was stirred at 40 °C for 4 h. After completion of the reaction, the mixture was concentrated to dryness and dried overnight at vacuum.

The residue was coevaporated thrice with pyridine and afterwards dissolved in pyridine (4 ml). 4,4'-dimethoxytrityl chloride (193 mg, 0.57 mmol) and a catalytic amount of DMAP were then added under argon atmosphere at ice-cool condition. After removing of the icebath the reaction was stirred for 4 h and the mixture was quenched with MeOH (0.5 ml). After diluting with DCM (4 ml) the mixture was then poured onto aq. sat. $NaHCO_3$ solution and extracted thrice with DCM (3x5ml). The combined extracts were dried ($MgSO_4$), concentrated and purified by silica gel column chromatography [EtOAc-petroleum ether, 3:1 → EtOAc-MeOH, 96:4 (containing 1% Et_3N)] to yield **6a-A** (83%, 195 mg, 0.313 mmol) as a colorless foam.

Rf 0.50 (EtOAc-MeOH, 5:1).

^{1}H NMR (600.1 MHz, d_6-acetone): δ = 1.43 (s, *4'-Me*; 3 H), 2.58-2.60 (m, *2'-H*; 1 H), 2.94-2.96 (m, *2''-H*; 1 H), 3.10-3.26 (m, 5'+5''-*H* + $Me_{formamidine}$; 8 H), 3.74 (s, DMTr-O*Me*; 3 H), 3.75 (s, DMTr-O*Me*; 3 H), 4.75 (t, J = 6 Hz, *3'-H*; 1 H), 6.46 (t, J = 6 Hz, *1'-H*; 1 H), 6.77-6.83 (m, H_{Ar}; 4 H), 7.15-7.35 (m, H_{Ar}; 7 H), 7.44 (d, J = 6 Hz, H_{Ar}; 2 H), 8.15 (s, *8-H*; 1 H), 8.33 (s, *2-H*; 1 H), 8.93 (s, $H_{formamidine}$; 1 H).

^{13}C NMR (151 MHz, d_6-acetone): δ = 19.1, 39.9, 41.0, 55.4, 69.2, 73.1, 83.6, 86.7, 87.9, 113.8, 127.4, 128.4, 128.5, 129.0, 130.8 130.9, 131.0, 136.8, 136.9, 141.5, 146.2, 152.5, 152.8, 158.9, 159.4, 159.5, 160.5.

ESI MS (positive mode):

m/z calc. = 623.7 $[M + H]^+$.

m/z found = 623.4 $[M + H]^+$, 645.4 $[M + Na]^+$, 661.3 $[M + K]^+$.

2'-Deoxy-6-*N*-formamidine-5'-*O*-(4,4-dimethoxytrityl)-4'-*C*-ethyl adenosine

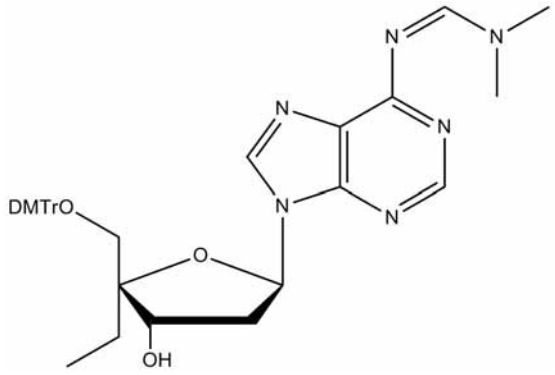

6b-A

The compound **2'-deoxy-4'-*C*-ethyl adenosine (1b)** (35 mg, 0.125 mmol) was dissolved in methanol (4 ml) and *N,N*-dimethylformamide dimethylacetal (200 µl, 0.5 mmol) was added and the reaction mixture was stirred at 40 °C for 2.5 h. After

completion of the reaction, the mixture was concentrated to dryness and dried overnight at vacuum.

The residue was coevaporated thrice with pyridine and afterwards dissolved in pyridine (4 ml). 4,4'-dimethoxytrityl chloride (63.5 mg, 0.19 mmol) and a catalytic amount of DMAP were then added under argon atmosphere at ice-cool condition. After removing of the icebath the reaction was stirred for 16 h and the mixture was quenched with MeOH (0.5 ml). After diluting with DCM (4 ml) the mixture was then poured onto aq. sat. $NaHCO_3$ solution and extracted thrice with DCM (3x5ml). The combined extracts were dried ($MgSO_4$), concentrated and purified by silica gel column chromatography [EtOAc-petroleum ether, 1:1 → EtOAc-petroleum ether, 4:1 (containing 1% Et_3N)] to yield **6b-A** (94%, 75 mg, 0.118 mmol) as a colorless foam.

Rf 0.55 (EtOAc-MeOH, 5:1).

^{1}H NMR (400 MHz, d_6-acetone): δ = 0.83 (t, J = 7.4 Hz, *4'*-CH_2*Me*; 3 H), 1.89-1.93 (m, *4'*-C*H*$_2$Me; 2 H), 2.45-2.51 (m, *2'-H*; 1 H), 3.02-3.07 (m, *2''-H*; 1 H), 3.18 (s, $Me_{formamidine}$; 1 H), 3.24 (s, $Me_{formamidine}$; 1 H), 3.31 (t, J = 10.3 Hz, 5'+5''-*H*; 2 H), 3.76 (s, DMTr-O*Me*; 3 H), 3.77 (s, DMTr-O*Me*; 3 H), 4.79 (dd, J_1 = 6.2 Hz, J_2 = 4.4 Hz, *3'-H*; 1 H), 6.44 (t, J = 6.7 Hz, *1'-H*; 1 H), 6.81 (dd, J_1 = 13.2 Hz, J_2 = 8.9 Hz, H_{Ar}; 4 H), 7.25 (d, J = 7.7 Hz, H_{Ar}; 2 H), 7.31(d, J = 8.9 Hz, H_{Ar}; 5 H), 7.46 (d, J = 7.3 Hz, H_{Ar}; 2 H), 8.13 (s, *8-H*; 1 H), 8.30 (s, *2-H*; 1 H), 8.93 (s, $H_{formamidine}$; 1 H).

^{13}C NMR (101 MHz, d_6-acetone): δ = 8.5, 25.1, 34.9, 40.2, 41.1, 55.5, 64.2, 66.2, 74.0, 88.1, 86.8, 89.9, 113.8, 127.5, 128.5, 129.0, 130.9, 131.1, 136.7, 136.8, 141.8, 146.3, 152.5, 152.8, 158.9, 159.4, 159.5, 160.6.

ESI MS (positive mode):

m/z calc. = 636.3 $[M + H]^+$.

m/z found = 636.4 $[M + H]^+$.

Standard Protocol for Phosphitylation [*Beaucage*, 2001]

The DMTr-protected Nucleosides **6a-A** (75 mg, 0.12 mmol) and **6b-A** (50 mg, (0.07 mmol) were coevaporated with toluene and two times with DCM. After dissolving in DCM (2 ml) huenig base (5 eq) was added under argon atmosphere. The reaction then was cooled to 0 °C and 2-cyanoethyl-N,N-(diisopropylamino)chlorophosphor-amidite (2 eq) was added to give a yellowish solution. Stirring was performed for 30 min at 0 °C. Then the reaction mixture was stirred until complete conversion (1.5 h-5 h) and then quenched by addition of MeOH (0.5 ml). After dilution with DCM (5 ml) the

reaction mixture was poured onto H_2O and extracted thrice with DCM (3x5 ml) and dried over anhydrous $MgSO_4$.

2'-Deoxy-6-*N*-formamidine-5'-*O*-(4,4-dimethoxytrityl)-4'-*C*-methyl adenosine phosphoramidite

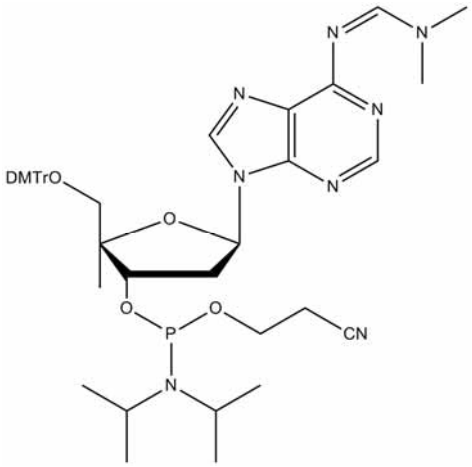

dA^{Me}-PA

Flash chromatography [EE-PE 1:2 -> EE-MeOH 98:2 (containing 1% Et_3N)] yielded 95 mg (0.115 mmol, 96%) of compound **dA^{Me}-PA**.

$Rf_{diast.}$ 0.52 (EtOAc-MeOH, 8:1).

^{1}H NMR (600 MHz, d_6-acetone) (mixture of diastereomeres): δ = 1.19-1.28 (m, N(CH*Me*$_2$)$_2$; 24 H), 1.43-1.44 (m, *4'-Me*; 6 H), 2.67-2.82 (m, *2''-H* + C*H*$_2$CN; 6 H), 3.16-3.23 (m, *2''-H+5'-H+ Me*$_{formamidine}$; 16 H), 3.32-3.35 (m, *5''*-H; 2 H), 3.65-3.69 (m, POC*H*$_2$; 4 H), 3.75 (m, DMTr-O*Me*; 12 H), 3.82-3.96 (m, N(C*H*Me$_2$)$_2$; 4 H); 4.96-5.03 (m, *3'-H*; 1 H$_{diast.A}$), 5.09-5.14 (m, *3'-H*; 1 H$_{diast.B}$), 6.44-6.45 (m, *1'-H*; 2 H), 6.78-6.81 (m, *H*$_{Ar}$; 8 H), 7.18-7.45 (m, *H*$_{Ar}$; 18 H), 8.16 (s, *8-H*; 2 H), 8.33-8.35 (m, *2-H*; 2 H), 8.92 (s, *H*$_{formamidine}$; 2 H).

^{13}C NMR (151 MHz, d_6-acetone) (mixture of diastereomeres): δ = 19.6, 24.9, 25.0, 34.9, 38.3, 38.5, 43.8, 43.9, 44.0, 55.5, 59.3, 59.5, 59.8, 59.9, 68.4, 68.5, 74.5, 74.6, 75.7, 75.8, 83.6, 83.7, 86.8, 87.3, 87.4, 87.5, 113.0, 113.8, 118.8, 119.0, 127.4, 127.6, 128.5, 129.0, 129.1, 130.9, 131.0, 136.7, 136.8, 142.0, 146.1, 146.2, 152.3, 152.4, 152.8, 158.8, 159.5, 160.6, 170.9.

^{31}P NMR (161.85 MHz, d_6-acetone) (mixture of diastereomeres): δ = 145.53, 146.30.

ESI MS (positive mode):

m/z calc. = 823.4 $[M + H]^+$.

m/z found = 823.5 $[M + H]^+$.

6-*N*-Benzoyl-2'-deoxy-5'-*O*-dimethoxytrityl-4'-*C*-ethyl adenosine phosphoramidite

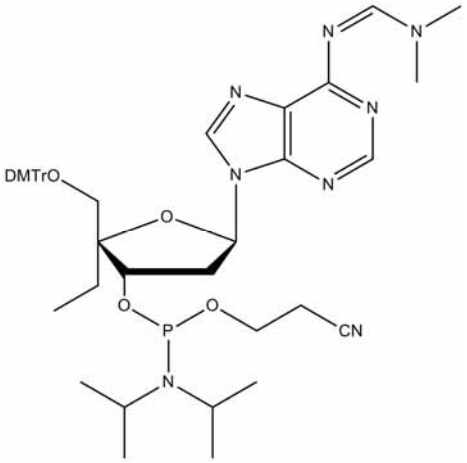

dA^{Et}-PA

Flash chromatography [EE-PE 1:2 -> EE-PE 3:1 (containing1% Et_3N)] yielded 59 mg (0.067 mmol, 91%) of compound **dA^{Et}-PA**.

$Rf_{diast.}$ 0.66/0.68 (EtOAc-PE, 3:1).

^{1}H NMR (600 MHz, d_6-acetone) (mixture of diastereomeres a and b): δ = 0.85-0.92 (m, *4'*-CH_2*Me*; 6 H), 1.21-1.25 (m, N(CH*Me*$_2$)$_2$; 24 H), 1.87-1.97 (m, *4'*-C*H*$_2$Me*;* 4 H), 2.59-2.94 (m, 2'-*H*+*2''*-*H* +C*H*$_2$CN; 8 H), 3.17 (s, *Me*$_{formamidine}$; 3 H), 3.21 (s, *Me*$_{formamidine}$; 3 H), 3.23-3.26 (m, *5'*-*H*; 2 H), 3.37-3.41 (m, *5''*-*H*; 2 H), 3.75 (s, DMTr-O*Me*$_{diast.A}$; 6 H), 3.76 (s, DMTr-O*Me*$_{diast.B}$; 6 H), 3.68-3.87 (m, POC*H*$_2$+N(C*H*Me$_2$)$_2$; 8 H); 4.99-5.04 (m, *3'*-*H*$_{diast.A}$; 1 H), 5.11-5.17 (m, *3'*-*H*$_{diast.B}$; 1 H), 6.44-6.48 (m, *1'*-*H*; 2 H), 6.79-6.84 (m, *H*$_{Ar}$; 8 H), 7.19-7.47 (m, *H*$_{Ar}$; 18 H), 8.16 (s, *8*-*H*$_{diast.A}$; 1 H), 8.17 (s, *8*-*H*$_{diast.B}$; 1 H), 8.32 (s, *2*-*H*$_{diast.A}$; 1 H), 8.33 (s, *2*-*H*$_{diast.B}$; 1 H), 8.92 (s, *H*$_{formamidine}$; 2 H).

^{13}C NMR (151 MHz, d_6-acetone) (mixture of diastereomeres): δ = 8.5, 20.9, 23.0, 25.1, 26.0, 35.0, 38.9, 41.1, 43.9, 44.0, 44.2, 55.6, 59.3, 59.5, 59.8, 60.0, 66.2, 66.2, 75.6, 75.8, 84.2, 84.3, 89.5, 89.6, 89.7, 113.9, 118.9, 119.0, 127.5, 127.7, 128.5, 129.1, 129.2, 131.0, 131.1, 136.7, 136.9, 142.1, 142.2, 146.2, 152.3, 152.4, 152.9, 158.9, 159.5, 159.6, 160.7.

^{31}P NMR (161.85 MHz, d_6-acetone) (mixture of diastereomeres): δ = 148.13, 149.22.

ESI MS (positive mode): *m/z calc.* = 837.4 $[M + H]^+$.

m/z found = 837.6 $[M + H]^+$.

6.2.3 General Method for Coupling of Nucleosides to Solid Supports

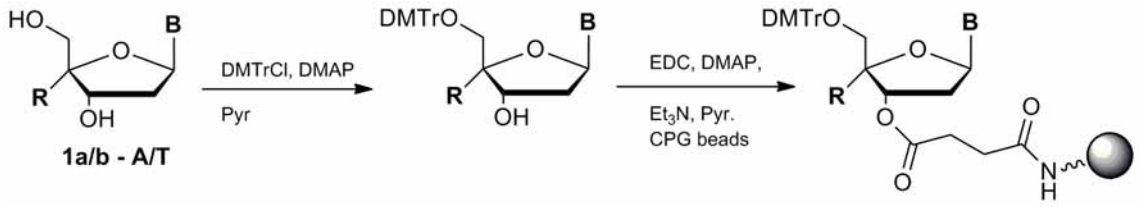

Scheme 6.2-1 *Schematic drawing of the attachment of nucleosides to CPG resin.*

Thymidine solid supports have been available in our research group.

5'-*O*-DMTr protected nucleosides **6a-A** and **6b-A** were coupled to succinylated LCAA-CPG by using standard protocols (**Scheme 6.2-1**) [*Beaucage,* 2001]. Briefly, succinylated LCAA-CPG, the respective nucleosides, DMAP (each 0.1 mmol/1.0 g CPG), and EDC (1.0 mmol/1.0 g CPG), were combined, pyridine (10 ml/1.0 g CPG) and NEt_3 (80 ml/1.0 g CPG) were added, and the reaction mixture was shaken under argon overnight.

Next, 4-nitrophenol (0.5 mmol/1.0 g CPG) was added and shaking was continued for an additional 24 h. Piperidine (5 ml/1.0 g CPG) was added, and shaking was continued for 5 min. The beads were then filtered off and washed successively with pyridine, methanol, and finally with CH_2Cl_2. After drying, the beads were suspended in equal amounts of acetic anhydride/pyridine/THF (Cap A) and 1-methylimidazole/THF (Cap B) capping reagents. After shaking for 2 h, the beads were filtered off and intensively washed as described above. After drying, loading was determined by trityl analysis of a small portion of the collected beads (loading range 10-30 mmol/g).

6.2.4 Oligonucleotide Synthesis

DNA oligonucleotide primers and templates have been synthesized in an automated synthesis on an Applied-Biosystems 392 DNA/RNA synthesizer. Coupling times of and to modified nucleotides were increased to 10 min. For modified primers the respective solid supports were packed into empty, cleaned columns for 200 nmol synthesis (**Figure 6.2-1**).

5'-GTG GTG CGA AAT TTC TGA CAG ACA $\mathbf{A^R}$-3'
5'-GTG GTG CGA AAT TTC TGA CAG ACA $\mathbf{T^R}$-3'
3'-CAC CAC GCT TTA AAG ACT GTC TGT $\mathbf{A^R}$CT GTC TGC GTG-5'
3'-CAC CAC GCT TTA AAG ACT GTC TGT $\mathbf{T^R}$CT GTC TGC GTG-5'

Figure 6.2-1 *Synthesized primer and template sequences (R = Me, Et).*

6.2.5 DNA Thermal Denaturation Studies

Melting curves were recorded on a Cary 100 bio UV/Vis instrument with temperature controller. Data were obtained from three individual cooling/heating cycles. Melting temperatures (T_m values in °C) were obtained from the maximum of the first derivative of the melting curves (absorbance at 260 nm versus temperature). Measurements were conducted in buffer (20 mM Tris-HCl (pH 7.5), 20 mM NaCl) and contained 5 μM duplex DNA. The mixtures were heated at 95°C for 5 min and slowly cooled down to room temperature prior to the melting curve measurements. A measurement of the buffer was conducted separately and subtracted from the spectra resulting from the sample.

6.2.6 Determination of DNA Concentration

Quantification of DNA and RNA was conducted by UV absorption measurements at 260 nm using UV/VIS photometer. Water or the respective buffer was used as a reference. Based on Lambert-Beer's law the DNA concentration could be calculated. Extinction coefficients, as well as molecular weight and melting behavior were determined using the online available “Oligonucleotide Properties Calculator” which is based on specific extinction coefficients of each different nucleobase (http://www.basic.northwestern.edu/biotools/oligocalc.html, 11.07.2010).

6.3 Biochemical Methods

6.3.1 Oligonucleotides

Unmodified oligonucleotides for kinetic studies were synthesized on an Applied-Biosystems 392 DNA/RNA synthesizer and purified by RP-HPLC (DMTr-On) and preparative denaturating PAGE. All other unmodified oligonucleotides were purchased from Metabion international AG (Martinsried, Germany). Templates and cloning primers were used desalted or 1x HPLC purified.

The integrity of all oligonucleotides was confirmed by ESI-MS. Therefore, oligonucleotide samples were diluted (c = 1μM) in a mixture of water (79% v/v), 2-propanol (20% v/v) and triethylamine (1% v/v).

6.3.2 Radioactive Labeling of DNA Oligonucleotides

Oligonucleotides were radioactively labeled by [^{32}P]-ATP using T4 polynucleotide kinase (T4-PNK). The labeling reaction was carried out in 50 μl scale with 400 nM oligonucleotides, 20 μCi [^{32}P]-ATP (2 μl), 0.4 U / μl T4-PNK (2 μl) and 1x T4-PNK reaction buffer. The reaction was incubated at 37°C for 1 h and subsequently stopped by heat-inactivation of T4-PNK at 95°C for 5 min. After gel filtration (G25 sephadex spin column) to remove salt and residual [^{32}P]-ATP, the radioactively labeled oligonucleotide solution was diluted with 19 μl of a 10 μM unlabeled oligonucleotide solution to obtain a final primer concentration of 3 μM.

6.3.3 Agarose Gel Electrophoresis

Agarose gel electrophoresis was performed according to standard procedures. Depending on fragment DNA size a 0.8% or 2.5% agarose in 0.5 x TBE was used. Gels were stained for 5-30 min in 0.01% (w/v) ethidiumbromide (EtBr) in 0.5 x TBE and shortly destained in 0.5 x TBE for further 5 min and documented in a Chemidoc XRS System. For preparative agarose gels it was taken care that UV irradiation of the fragments to be isolated was minimized.

6.3.4 Denaturing Polyacrylamide Gel Electrophoresis

Denaturing polyacrylamide gel electrophoresis (PAGE) was performed according to standard procedures. It was applied for purification of DNA-oligonucleotides and for analytical separation of reaction products. All denaturing polyacrylamide gels (12%) contained urea. Preparative gels had a gauge of 1.5 mm and analytical gels a gauge of 0.4 mm.

After running, analytical gels were transferred onto whatman paper, dried subsequently and exposed to a phosphor screen preferentially overnight.

For DNA-isolation from polyacrylamide-gels the separated DNA was visualized by UV shadowing and the respective bands were excised with a scalpel. Excised gel pieces were crushed by forcing them through a syringe and collected in 2 ml eppendorf tubes.

DNA was eluted from crushed gel pieces by adding H_2O and incubation at 55 °C overnight. Next, the DNA/PAGE mixture was filtrated through silanized glass-fibers wool. The filtrate was dried in a speedvac (Eppendorf) and extracted DNA was purified by ethanol precipitation according to standard procedures.

6.3.5 SDS Polyacrylamide Gel Electrophoresis

Expressed proteins were analyzed by discontinuous glycine SDS-PAGE (12%) according to standard procedures including a stacking- and a resolving-gel. Staining was performed by a Coomassie-staining solution.

6.3.6 Determination of Protein Concentration

Protein samples were loaded in parallel with a BSA standard dilution series. Respective band intensities were quantified on a BioRad Chemidoc XRS System (Quantity One 4.5.0) and protein concentrations could be calculated in comparison with the BSA sample intensities by linear curve analysis.

6.3.7 Site Directed Mutagenesis of *KlenTaq* I614A, Expression and Purification

Mutant I614A was introduced into the *KlenTaq* DNA polymerase ORF via site-directed mutagenesis according to the QuikChange Site-Directed Mutagenesis protocol (Stratagene) with the following modifications: Desalted mutagenesis primers and Phusion DNA Polymerase was used for whole plasmid PCR. Negative controls were performed via plating DpnI digested original plasmid on LB agar plates with 100 ng/µl carbencillin. Following primers have been used:

forward: 5'-d(CCTGGACTATAGCCAGGCAGAGCTCAGGGTGCTG)-3'

reverse: 5'-d(CAGCACCCTGAGCTCTGCCTGGCTATAGTCCAGG)-3'.

The sequence was determined by DNA sequencing. Expression of the *KlenTaq* DNA polymerases wt and I614A (in pGDR11 vector) was conducted in *E. coli* BL21 (DE3) Gold. Expression cultures were inoculated with 2% of an overnight culture grown at 30°C, and expression was induced at OD_{600} = 0.5 with IPTG at a final concentration of 1 mM. After 4 hr of expression, cultures were centrifuged at 4500xg at 4°C for 10 min. All cultures were grown in LB medium (Roth) with 100 mg/l carbenicillin. Collected cell pellets were resuspended in lysis-buffer (10mM Tris-HCl [pH 9.2], 300mM NaCl,

2.5 mM $MgCl_2$, 0.1% Triton X-100, 1 mg/ml lysozyme, 5 ml lysis buffer/50 ml culture) and lysed at 37°C for 10 min. *E. coli* proteins were denaturated through heating to 75°C for 45 min with a subsequent centrifugation at 15,000xg for 30 min at 4°C. Centrifuged expression lysates were incubated with pre-equilibrated (in 10 mM Tris-HCl [pH 9.2], 0.3 M NaCl, 2.5 mM $MgCl_2$, 0.1% Triton X-100) NTA-matrix (QIAGEN, 2–3 ml slurry/20 ml lysate) for 60 min at 4°C in an overhead shaker. The NTA matrix was then washed twice with NTA-wash-buffer (10 mM Tris-HCl [pH 9.2], 0.3 M NaCl, 2.5 mM $MgCl_2$, 0.1% Triton X-100, 20 mM imidazole), and the protein was eluted twice with NTA-elution-buffer (10 mM Tris-HCl [pH 9.2], 0.3 M NaCl, 2.5 mM $MgCl_2$, 0.1% Triton X-100, 200 mM imidazole). The elution buffer was exchanged by storage buffer (elution buffer without imidazole) using VivaSpins. For storage, glycerol was added to 50%, $(NH_4)_2SO_4$ to a final concentration of 16 mM and Tween 20 to 0.1%. Enzyme purity was controlled by SDS-PAGE. Protein concentrations were determined using Bradford assay. Purified enzymes were stored at -20°C.

6.3.8 Transformation of Chemically Competent Cells

Chemically competent *E. coli* cells were transformed as described in the manufacturer's manual (Stratagene) using an electroporator Gene Pulser Xcell.

6.3.9 DNA Sequencing

The prepared DNA samples were sent to a professional sequencing company (GATC Biotech AG, Konstanz). Sequences were analyzed and aligned using Chromas Lite (http://www.technelysium.com.au/chromas_lite.html, 11.07.2010) and SDSC Biology Workbench (http://workbench.sdsc.edu/, 11.07.2010).

6.3.10 Crystal Structure Models

Own DNA and protein crystal structure models were prepared by the respective PDB code using PyMOL Molecular Viewer (http://pymol.sourceforge.net/, 11.07.2010) or Sybyl7.2 package from Tripos for visualization. PDB code of the *KlenTaq* wt structures 3M8S and 3M8R.

6.3.11 Single Nucleotide Incorporation Studies

Appropriate primer/template substrates were annealed by mixing 5'-^{32}P labeled primer with 1.5-fold the amount of template in the specific reaction buffer (see below).

The mixture was heated to 95°C for 5 min and subsequently allowed to cool to room temperature over 1 h. After annealing, the appropriate DNA polymerase amount (see below) was added and the solution was incubated at 0°C for 10 min. DNA/enzyme mixture and dN^RTP solution were incubated at 37°C for 2 minutes. Then the reactions were initiated by addition of the DNA/enzyme mixture (10 µL) to an equal amount of dN^RTP solution in the reaction buffer and incubated at 37°C.

Reactions promoted by the Klenow fragment of *E. coli* DNA polymerase I (*exo*- mutant) were performed in Tris-HCl (pH 7.3, 50 mM), $MgCl_2$ (10 mM), and DTT (1 mM).

Reactions promoted by the DNA Polymerase IV of *Sulfolobus solfataricus* were performed in Tris-HCl (pH 8.0, 50 mM), $MgCl_2$ (10 mM), KCl (20 mM), DTT (2 mM), BSA (100 µg/ml) and Glycerol (10%).

Reactions promoted by the *KlenTaq* DNA polymerase were performed in RQF buffer: Tris-HCl (pH 7.5, 20mM), NaCl (50mM) and $MgCl_2$ (2mM) [*Rothwell* et al., 2005].

Assays included: 150 nM primer and 5-10 nM enzyme for nucleotide insertion. After incubation for the indicated time (15 min matched/ 45 min mismatched) the reactions were quenched by addition of 35 µL of gel loading buffer (80% formamide, EDTA (20 mM)) and subsequently heated to 95°C for 10 min. Reactions were analyzed by 12% polyacrylamide gel electrophoresis containing 8M urea, transferred to filter paper, dried under vacuum, and visualized by phosphor imaging.

6.3.12 Steady-State Enzyme Kinetics

The steady-state kinetic data were obtained from single nucleotide insertion assays as described above except that concentration of nucleotides (at least eight different nucleotide concentrations were used in each investigation), enzyme concentration, and reaction time were adjusted for different reactions to allow 25% or less primer extension ensuring single completed hit conditions according to published procedures [*Creighton* et al., 1995, *Boosalis* et al., 1987]. The reactions were fractionated by 12% denaturing polyacrylamide gel electrophoresis, and the data were quantified by phosphor imager analysis. Relative velocity v was measured as the ratio of the extended product (I_{ext}) to total primer (I_{prim}) as follows $v = I_{ext}/I_{prim}\ t$, where t represents the reaction time, and normalized for the enzyme and primer-template concentration used. The apparent K_M

and k_{cat} values were obtained from Michaelis-Menten kinetics as described [*Creighton* et al., 1995, *Boosalis* et al., 1987]. The data derived from triplet experiments.

6.3.13 Presteady-State Enzyme Kinetics

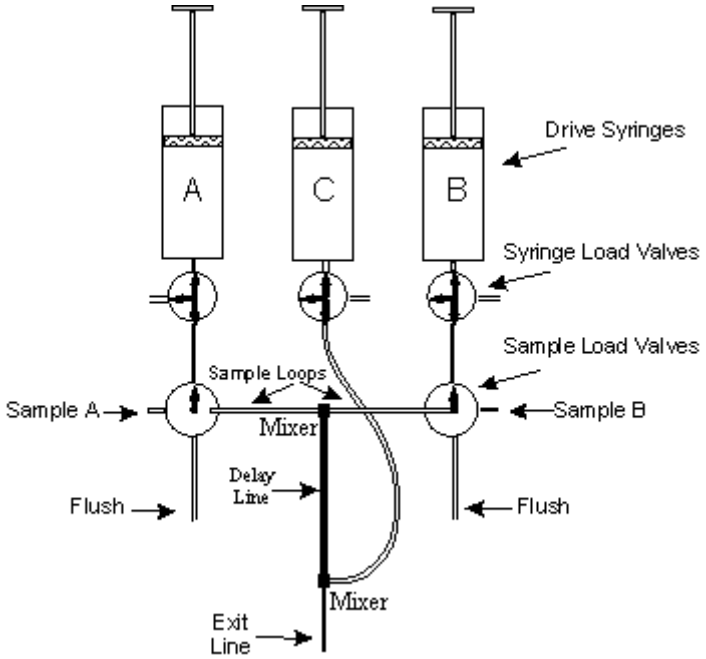

Figure 6.3-1 *Scheme of the RQF-3 from KinTek Corp [Kintek, 2010].*

The rate of single turnover, single nucleotide incorporation was determined using rapid quench flow kinetics on a chemical quench flow apparatus (RQF-3, KinTek Corp., University Park, PA, **Figure 6.3-1**) as previously described [*Di Pasquale* et al., 2008]. In brief, 15 µl of radiolabeled primer/template complex (50 nM) and DNA polymerase (500 nM) in reaction buffer (RQF buffer, Tris-HCl pH 7.5 20mM, NaCl 50mM, $MgCl_2$ 2mM) [*Rothwell* et al., 2005] were rapidly mixed with 15 µl of a dNTP solution in reaction buffer at 37°C. Quenching was achieved by 0.3M EDTA solution (pH 7.0) at defined time intervals. For the investigation of **dT^{R}TP** incorporation a 24nt primer (5'-GTG GTG CGA AAT TTC TGA CAG ACA) and a 36nt template (5'-GTG CGT CTG TC**A** TGT CTG TCA GAA ATT TCG CAC CAC) were applied. Quenched samples were analyzed on a 12% denaturing PAGE followed by phosphor imaging as the ratio of the extended product (I_{ext}) to total primer (I_{prim}).

For kinetic analysis, experimental data (conversion I_{ext}/I_{prim} in % versus reaction time) were fit by nonlinear regression using the program GraphPad Prism 4. The data were fit to a single exponential equation:

$$[\text{conversion}]=A*(1-\exp(-k_{obs}\ t))$$

The observed catalytic rates (k_{obs}) were then plotted against the dNTP concentration used and the data were fitted to a hyperbolic equation:

$$[k_{obs}]=k_{pol}*[\text{dNTP}] / (K_D + [\text{dNTP}])$$

to determine the K_D and k_{pol} of the incoming nucleotide. The incorporation efficiency is given by k_{pol} / K_D. The data derived from double repeated experiments.

7 Appendix

7.1 Abbreviations

°	Degree
°C	Degree Celsius
µg	Microgram
µl	Microliter
µM	Micromolar
10x	Tenfold concentrated
32P	Phosphor ^{32} Isotope
A	Adenosine
Å	Angstrom
AA	Amino acid
Fig.	Figure
Ac_2O	Acetic anhydride
APS	Ammoniumperoxodisulfate
ASA	Allelspecific Amplification
ATP	Adenosin-5'-triphosphat
AZT	3´-Azido-2´-3´-dideoxythymidine
Bst	*Bacillus stearothermophilus*
bp	Base pair
BSA	Bovine serum albumin
Bu_3N	Tributylamine
BuLi	Buthyllithium
BuOK	Potassium butanolate
c	Concentration
C	Cytidine, carbon atom
C_6H_6	Benzene
cDNA	Complementary DNA
CH_2Cl_2	Dichlormethane
$(CH_3O)_3PO$	Trimethylorthophosphate

CH_3OH	Methanol
CPG	Controlled pore glass
CTP	Cytidine-5'-triphosphate
D_2O	Deuteriumoxide
dATP	2´-Deoxyadenosine-5´-triphosphate
TLC	Thin layer chromatography
DCC	Dicyclohexylcarbodiimide
dCTP	2´-Deoxycytidine 5´-triphosphate
ddC	2´-3´-Dideoxycytidine
ddCTP	2',3'-Dideoxycytidine-5´-triphosphate
ddNTP	2',3'-Dideoxynucleoside-5'-triphosphate
dGTP	2'-Deoxyguanosine-5'-triphosphate
DM KK	Double mutant I614K M747K
DMAP	*N,N*-Dimethylaminopyridine
DMF	*N,N*-Dimethylformamide
DMSO	Dimethylsulfoxide
DMT	4,4-Dimethoxytrityl
DNA	Deoxyribonucleic acid
dNTP	Deoxynucleotid-5'-triphosphate
DTT	Dithiotreitol
E. coli	*Escherichia coli*
EDTA	Ethylendiamin tetracetate
EtOAc	Ethylacetate
EtOH	Ethanol
Exo	Exonuclease activity
F	Fluorescence
g	Gram
G	Guanosine
h	Hours
H_2	Molecular hydrogen
HEPES	*N*-(2-Hydroxyethyl)piperazine-*N'*-(2-ethansulfonic acid)
HIV	Human immunodeficiency virus
HPLC	High performance liquid chromatographie
HTS	High throughput screening
HV	High vacuum
I_2	Iodine
IPTG	1-Isopropyl-β-D-1-thiogalaktopyranosid
k	Velocity constant
k_{cat}	Maximum catalytic velocity constant
K_D	Dissociation constant
kD	Kilo Dalton

KF^-	Klenow fragment of *E. coli* DNA polymerase I (3´-5´-exo-)
k_{pol}	Maximum catalytic polymerization rate
K_M	Michaelis-Menten constant
k_{next}	Velocity constant translocation
k_{off}	Velocity constant dissociation
k_{pol}	Maximum catalytic polymerization rate
l	Liter
LCAA	Long chain amino alkyl
M	Molar
Mg	Magnesium
mg	Milligram
$MgCl_2$	Magnesiumchloride
min	Minute
ml	Milliliter
mM	Millimolar
MPLC	Medium performance liquid chromatography
MW	Molecular weight
n.d.	Not detactable
NEt_3	Triethylamine
ng	Nanogram
Ni-NTA	Nickel-Nitrilotetraacetate
nM	Nanomolar
nmol	Nanomol
NMR	Nuclear magnetic resonance
nt	Nucleotide
NTP	Nucleotide-5'-triphosphate
O	Oxygen atom
OD	Optical density
ORF	Open reading frame
p.a.	Per analysii
PAGE	Polyacrylamide gel electrophoresis
PBS	Phosphate buffered saline
PCR	Polymerase chain reaction
Pd	Palladium
pdb	Protein database
PEG	Polyethylene glycol
Ph_3P	Triphenylphosphine
pM	Picomolar
pmol	Picomol
Pol	DNA polymerase
PP	Pyrophosphate

pQKF$^-$	pQ*Klenow*exo-
Q-PCR	Quantitative PCR
Rel.	Relative
RNA	Ribonucleic acid
RP	Reversed-phase
rpm	Rotations per minute
RT	Reverse Transcription
s	Second
SDS	Sodium dodecyl sulfate
SNP	Single nucleotide polymorphism
ssDNA	Single stranded DNA
t	Time
T	Thymidine
Taq	*Thermus aquaticus*
TBAF	t-Butylammoniumfluoride
TBDMS	t-Butyldimethylsilyl
TBE	Tris Borat EDTA-(buffer)
TBME	t-Butylmethylether
TE	Tris-EDTA-buffer
TEAA	Triethylammoniumacetate
TEAB	Triethylammoniumhydrogencarbonate
TEMED	N, N, N', N'-Tetramethylendiamine
THF	Tetrahydrofuran
TM	Melting temperature (of DNA)
Tris	Tris-(hydroxymethyl)-aminomethane
TTP	Thymidin-5'-triphosphate
U	Uridine
UTP	Uridine-5'-triphosphate
UV	Ultraviolet
V	Volt
V_{max}	Maximum catalysis velocity * enzyme concentration
V	Volume
W	Watt
wt	Wild type

7.2 Nomenclature of Natural Amino Acids

Amino acid	*One-letter-code*	*Three-letter-code*
Alanine	A	Ala
Cysteine	C	Cys
Aspartate	D	Asp
Glutamate	E	Glu
Phenylalanine	F	Phe
Glycine	G	Gly
Histidine	H	His
Isoleucine	I	Ile
Lysine	K	Lys
Leucine	L	Leu
Methionine	M	Met
Asparagine	N	Asn
Proline	P	Pro
Glutamine	Q	Gln
Arginine	R	Arg
Serine	S	Ser
Threonine	T	Thr
Valine	V	Val
Tryptophan	W	Trp
Tyrosine	Y	Tyr

7.3 Mass Spectra of Modified Oligonucleotides

4'-methyl Thymidine modified 36mer Template:
3'-CAC CAC GCT TTA AAG ACT GTC TGT **T^{Me}**CT GTC TGC GTG-5'
m/z calc. = 11007

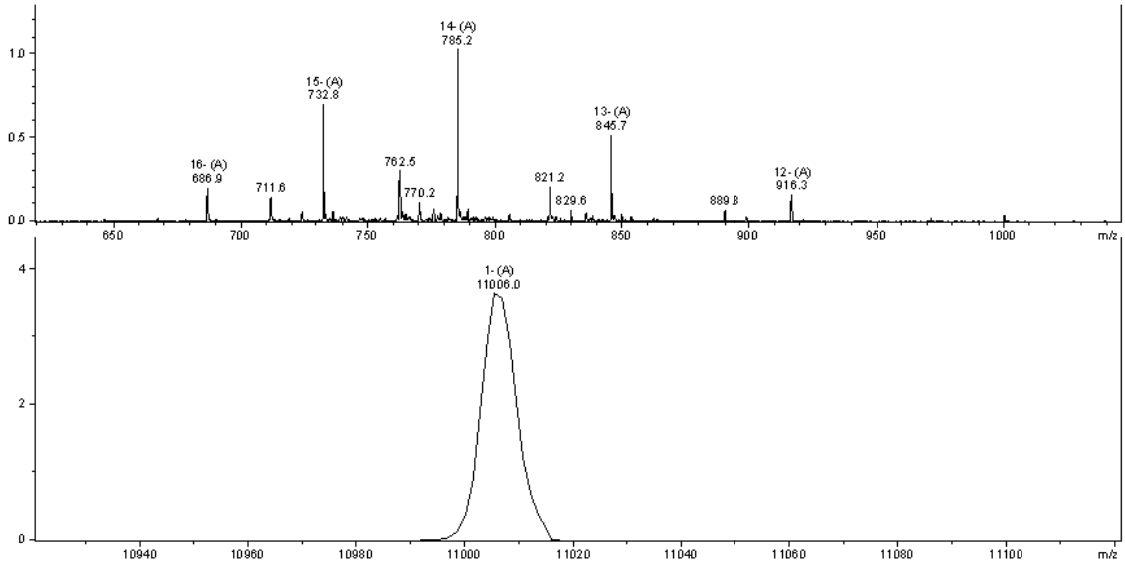

4'-ethyl Thymidine modified 36mer Template:
3'-CAC CAC GCT TTA AAG ACT GTC TGT **T^{Et}**CT GTC TGC GTG-5'
m/z calc. = 11022

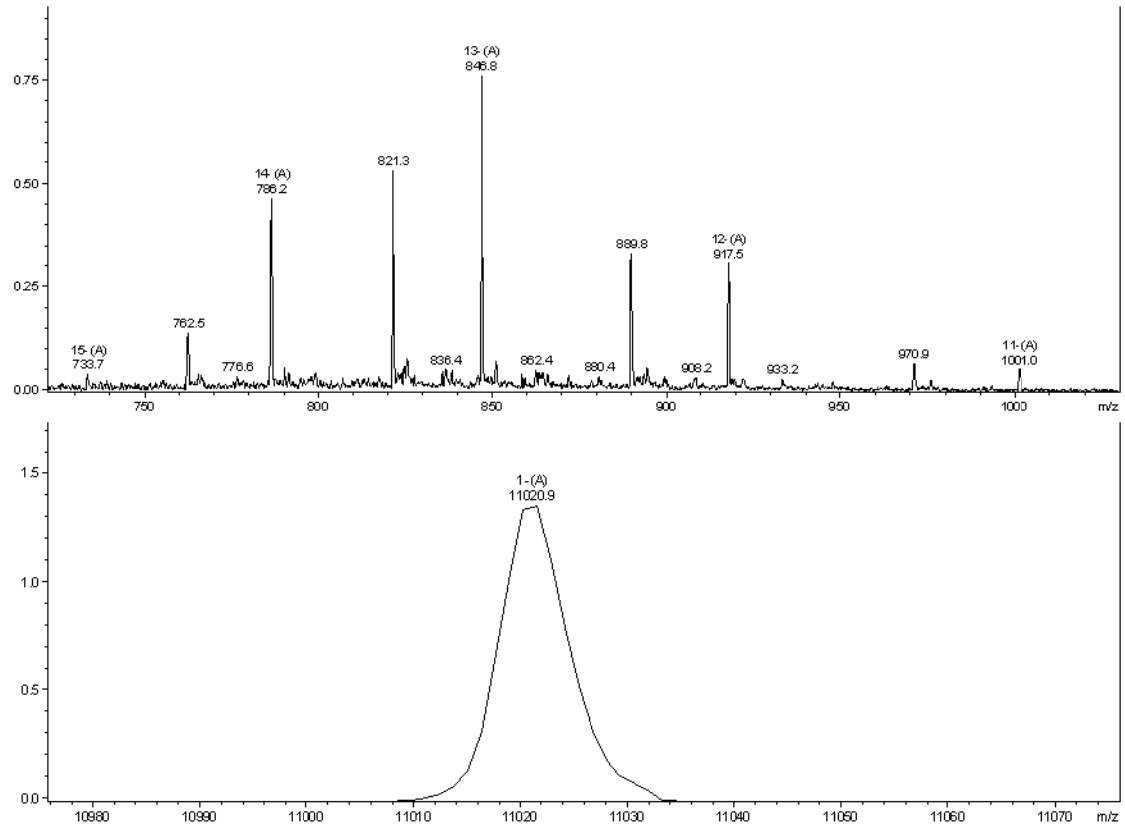

4’-methyl 2’-deoxyadenosine modified 36mer Template:
3'-CAC CAC GCT TTA AAG ACT GTC TGT **A**^{Me}CT GTC TGC GTG-5'
m/z calc. = 11016

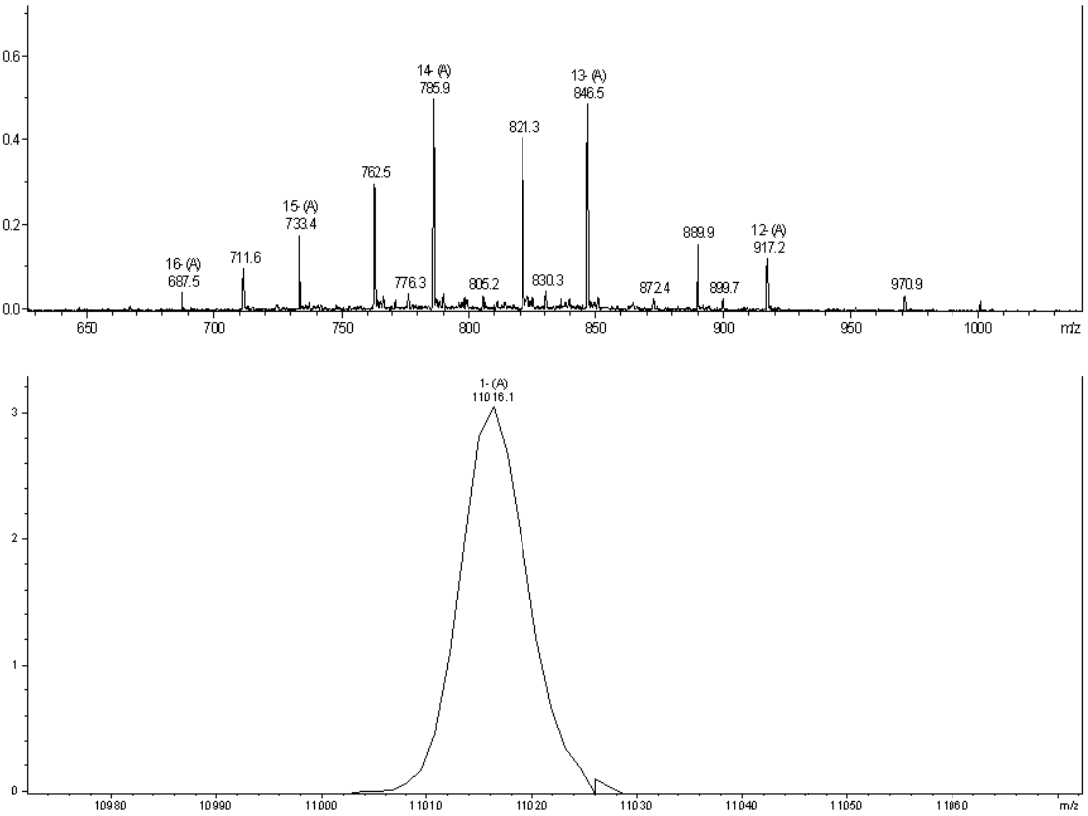

4’-ethyl 2’-deoxyadenosine modified 36mer Template:
3'-CAC CAC GCT TTA AAG ACT GTC TGT **A**^{Me}CT GTC TGC GTG-5'
m/z calc. = 11030

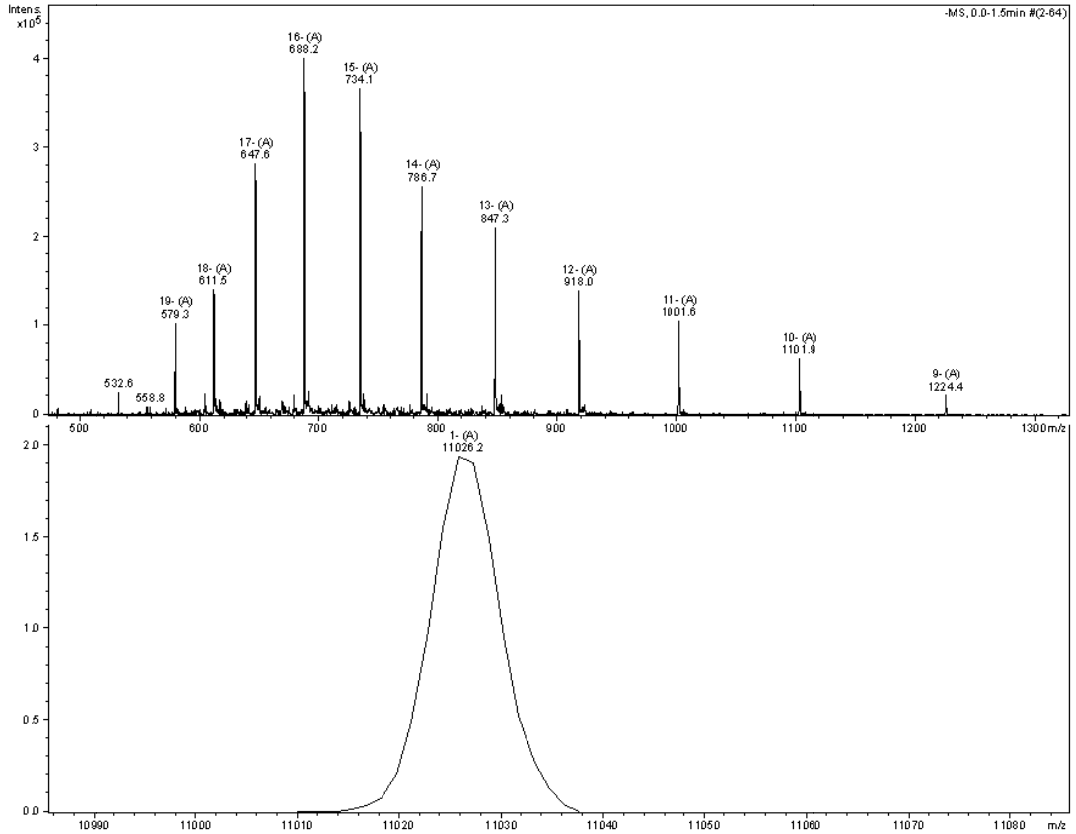

7.4 DNA and Amino Acid Sequences

7.4.1 pQKF⁻::KF exo- ORF and pET22b(t)::Dpo4 ORF

KF exo- ORF in pQKF⁻ plasmid was kindly provided by Francesca Di Pasquale and pET22b(t)::Dpo4 plasmid in *E. coli* BL21-Rosetta (DE3)pLysS was kindly provided by Nadine Staiger. pQKF⁻::KF exo- plasmid was transformed in XL10 Gold as described in **Chapter 6.4.8**.

7.4.2 pGDR11::*KlenTaq* wt ORF

KTQ wt ORF in pGDR11 plasmid was kindly provided by Samra Obeid. Mutation I614A was introduced by changing codon ATA into GCA by site-directed mutagenesis. Mutation H784A was introduced by changing codon CAC into GCC by site directed mutagenesis (see also **Chapter 5.3.7**). Mutation sites are highlighted.

TTGCCCGGCGTCAATACGGGATAATACCGCGCCACATAGCAGAACTTTAAAAGTGCTCATCATTGGAAAA
CGTTCTTCGGGGCGAAAACTCTCAAGGATCTTACCGCTGTTGAGATCCAGTTCGATGTAACCCACTCGTG
CACCCAACTGATCTTCAGCATCTTTTACTTTCACCAGCGTTTCTGGGTGAGCAAAAACAGGAAGGCAAAA
TGCCGCAAAAAAGGGAATAAGGGCGACACGGAAATGTTGAATACTCATACTCTTCCTTTTTCAATATTAT
TGAAGCATTTATCAGGGTTATTGTCTCATGAGCGGATACATATTTGAATGTATTTAGAAAAATAAACAAA
TAGGGGTTCCGCGCACATTTCCCCGAAAAGTGCCACCTGACGTCTAAGAAACCATTATTATCATGACATT
AACCTATAAAAATAGGCGTATCACGAGGCCCTTTCGTCTTCACCTCGAGAAATCATAAAAAATTTATTTG
CTTTGTGAGCGGATAACAATTATAATAGATTCAATTGTGAGCGGATAACAATTTCACACAGAATTCATTA
AAGAGGAGAAATTAACTATGAGAGGATCTCACCATCACCATCACCATACGGATCCGCATGCAGCCCTGGA
GGAGGCCCCCTGGCCCCCGCCGGAAGGGGCCTTCGTGGGCTTTGTGCTTTCCCGCAAGGAGCCCATGTGG
GCCGATCTTCTGGCCCTGGCCGCCGCCAGGGGGGGCCGGGTCCACCGGGCCCCCGAGCCTTATAAAGCCC
TCAGGGACCTGAAGGAGGCGCGGGGGCTTCTCGCCAAAGACCTGAGCGTTCTGGCCCTGAGGGAAGGCCT
TGGCCTCCCGCCCGGCGACGACCCCATGCTCCTCGCCTACCTCCTGGACCCTTCCAACACCACCCCCGAG
GGGGTGGCCCGGCGCTACGGCGGGGAGTGGACGGAGGAGGCGGGGGAGCGGGCCGCCCTTTCCGAGAGGC
TCTTCGCCAACCTGTGGGGGAGGCTTGAGGGGGAGGAGAGGCTCCTTTGGCTTTACCGGGAGGTGGAGAG
GCCCCTTTCCGCTGTCCTGGCCCACATGGAGGCCACGGGGGTGCGCCTGGACGTGGCCTATCTCAGGGCC
TTGTCCCTGGAGGTGGCCGAGGAGATCGCCCGCCTCGAGGCCGAGGTCTTCCGCCTGGCCGGCCACCCCT
TCAACCTCAACTCCCGGGACCAGCTGGAAAGGGTCCTCTTTGACGAGCTAGGGCTTCCCGCCATCGGCAA
GACGGAGAAGACCGGCAAGCGCTCCACCAGCGCCGCCGTCCTGGAGGCCCTCCGCGAGGCCCACCCCATC
GTGGAGAAGATCCTGCAGTACCGGGAGCTCACCAAGCTGAAGAGCACCTACATTGACCCCTTGCCGGACC
TCATCCACCCCAGGACGGGCCGCCTCCACACCCGCTTCAACCAGACGGCCACGGCCACGGGCAGGCTAAG
TAGCTCCGATCCCAACCTCCAGAACATCCCCGTCCGCACCCCGCTTGGGCAGAGGATCCGCCGGGCCTTC
ATCGCCGAGGAGGGGTGGCTATTGGTGGCCCTGGACTATAGCCAG**ATA**GAGCTCAGGGTGCTGGCCCACC
TCTCCGGCGACGAGAACCTGATCCGGGTCTTCCAGGAGGGGCGGGACATCCACACGGAGACCGCCAGCTG
GATGTTCGGCGTCCCCCGGGAGGCCGTGGACCCCCTGATGCGCCGGGCGGCCAAGACCATCAACTTCGGG
GTCCTCTACGGCATGTCGGCCCACCGCCTCTCCCAGGAGCTAGCCATCCCTTACGAGGAGGCCCAGGCCT
TCATTGAGCGCTACTTTCAGAGCTTCCCCAAGGTGCGGGCCTGGATTGAGAAGACCCTGGAGGAGGGCAG
GAGGCGGGGGTACGTGGAGACCCTCTTCGGCCGCCGCCGCTACGTGCCAGACCTAGAGGCCCGGGTGAAG
AGCGTGCGGGAGGCGGCCGAGCGCATGGCCTTCAACATGCCCGTCCAGGGCACCGCCGCCGACCTCATGA
AGCTGGCTATGGTGAAGCTCTTCCCCAGGCTGGAGGAAATGGGGGCCAGGATGCTCCTTCAGGTC**CAC**GA
CGAGCTGGTCCTCGAGGCCCCAAAAGAGAGGGCGGAGGCCGTGGCCCGGCTGGCCAAGGAGGTCATGGAG
GGGGTGTATCCCCTGGCCGTGCCCCTGGAGGTGGAGGTGGGGATAGGGGAGGACTGGCTCTCCGCCAAGG
AGAAAGCTTAATTAGCTGAGCTTGGACTCCTGTTGATAGATCCAGTAATGACCTCAGAACTCCATCTGGA
TTTGTTCAGAACGCTCGGTTGCCGCCGGGCGTTTTTTATTGGTGAGAATCCAAGCTAGCTTGGCGAGATT
TTCAGGAGCTAAGGAAGCTAAAATGGAGAAAAAAATCACTGGATATACCACCGTTGATATATCCCAATGG
CATCGTAAAGAACATTTTGAGGCATTTCAGTCAGTTGCTCAATGTACCTATAACCAGACCGTTCAGCTGG
ATATTACGGCCTTTTTAAAGACCGTAAAGAAAAATAAGCACAAGTTTTATCCGGCCTTTATTCACATTCT
TGCCCGCCTGATGAATGCTCATCCGGAATTTCGTATGGCAATGAAAGACGGTGAGCTGGTGATATGGGAT

AGTGTTCACCCTTGTTACACCGTTTTCCATGAGCAAACTGAAACGTTTTCATCGCTCTGGAGTGAATACC
ACGACGATTTCCGGCAGTTTCTACACATATATTCGCAAGATGTGGCGTGTTACGGTGAAAACCTGGCCTA
TTTCCCTAAAGGGTTTATTGAGAATATGTTTTTCGTCTCAGCCAATCCCTGGGTGAGTTTCACCAGTTTT
GATTTAAACGTGGCCAATATGGACAACTTCTTCGCCCCCGTTTTCACCATGGGCAAATATTATACGCAAG
GCGACAAGGTGCTGATGCCGCTGGCGATTCAGGTTCATCATGCCGTCTGTGATGGCTTCCATGTCGGCAG
AATGCTTAATGAATTACAACAGTACTGCGATGAGTGGCAGGGCGGGGCGTAATTTTTTTAAGGCAGTTAT
TGGTGCCCTTAAACGCCTGGGGTAATGACTCTCTAGCTTGAGGCATCAAATAAAACGAAAGGCTCAGTCG
AAAGACTGGGCCTTTCGTTTTATCTGTTGTTTGTCGGTGAACGCTCTCCTGAGTAGGACAAATCCGCCGC
TCTAGATTACCGTGCAGTCGATGATAAGCTGTCAAACATGAGAATTGTGCCTAATGAGTGAGCTAACTCA
CATTAATTGCGTTGCGCTCACTGCCCGCTTTCCAGTCGGGAAACCTGTCGTGCCAGCTGCATTAATGAAT
CGGCCAACGCGCGGGGAGAGGCGGTTTGCGTATTGGGCGCCAGGGTGGTTTTTCTTTTCACCAGTGAGAC
GGGCAACAGCTGATTGCCCTTCACCGCCTGGCCCTGAGAGAGTTGCAGCAAGCGGTCCACGCTGGTTTGC
CCCAGCAGGCGAAAATCCTGTTTGATGGTGGTTAACGGCGGGATATAACATGAGCTGTCTTCGGTATCGT
CGTATCCCACTACCGAGATATCCGCACCAACGCGCAGCCCGGACTCGGTAATGGCGCGCATTGCGCCCAG
CGCCATCTGATCGTTGGCAACCAGCATCGCAGTGGGAACGATGCCCTCATTCAGCATTTGCATGGTTTGT
TGAAAACCGGACATGGCACTCCAGTCGCCTTCCCGTTCCGCTATCGGCTGAATTTGATTCGAGTGAGATA
TTTATGCCAGCCAGCCAGACGCAGACGCGCCGAGACAGAACTTAATGGGCCCGCTAACAGCGCGATTTGC
TGGTGACCCAATGCGACCAGATGCTCCACGCCCAGTCGCGTACCGTCTTCATGGGAGAAAATAATACTGT
TGATGGGTGTCTGGTCAGAGACATCAAGAAATAACGCCGGAACATTAGTGCAGGCAGCTTCCACAGCAAT
GGCATCCTGGTCATCCAGCGGATAGTTAATGATCAGCCCACTGACGCGTTGCGCGAGAAGATTGTGCACC
GCCGCTTTACAGGCTTCGACGCCGCTTCGTTCTACCATCGACACCACCACGCTGGCACCCAGTTGATCGG
CGCGAGATTTAATCGCCGCGACAATTTGCGACGGCGCGTGCAGGGCCAGACTGGAGGTGGCAACGCCAAT
CAGCAACGACTGTTTGCCCGCCAGTTGTTGTGCCACGCGGTTGGGAATGTAATTCAGCTCCGCCATCGCC
GCTTCCACTTTTTCCCGCGTTTTCGCAGAAACGTGGCTGGCCTGGTTCACCACGCGGGAAACGGTCTGAT
AAGAGACACCGGCATACTCTGCGACATCGTATAACGTTACTGGTTTCATTCACCACCCTGAATTGACTCT
CTTCCGGGCGCTATCATGCCATACCGCGAAAGGTTTTGCACCATTCGATGGTGTCGGAATTTCGGGCAGC
GTTGGGTCCTGGCCACGGGTGCGCATGATCTAGAGCTGCCTCGCGCGTTTCGGTGATGACGGTGAAAACC
TCTGACACATGCAGCTCCCGGAGACGGTCACAGCTTGTCTGTAAGCGGATGCCGGGAGCAGACAAGCCCG
TCAGGGCGCGTCAGCGGGTGTTGGCGGGTGTCGGGGCGCAGCCATGACCCAGTCACGTAGCGATAGCGGA
GTGTATACTGGCTTAACTATGCGGCATCAGAGCAGATTGTACTGAGAGTGCACCATATGCGGTGTGAAAT
ACCGCACAGATGCGTAAGGAGAAAATACCGCATCAGGCGCTCTTCCGCTTCCTCGCTCACTGACTCGCTG
CGCTCGGTCTGTCGGCTGCGGCGAGCGGTATCAGCTCACTCAAAGGCGGTAATACGGTTATCCACAGAAT
CAGGGGATAACGCAGGAAAGAACATGTGAGCAAAAGGCCAGCAAAAGGCCAGGAACCGTAAAAAGGCCGC
GTTGCTGGCGTTTTTCCATAGGCTCCGCCCCCCTGACGAGCATCACAAAAATCGACGCTCAAGTCAGAGG
TGGCGAAACCCGACAGGACTATAAAGATACCAGGCGTTTCCCCCTGGAAGCTCCCTCGTGCGCTCTCCTG
TTCCGACCCTGCCGCTTACCGGATACCTGTCCGCCTTTCTCCCTTCGGGAAGCGTGGCGCTTTCTCAATG
CTCACGCTGTAGGTATCTCAGTTCGGTGTAGGTCGTTCGCTCCAAGCTGGGCTGTGTGCACGAACCCCCC
GTTCAGCCCGACCGCTGCGCCTTATCCGGTAACTATCGTCTTGAGTCCAACCCGGTAAGACACGACTTAT
CGCCACTGGCAGCAGCCACTGGTAACAGGATTAGCAGAGCGAGGTATGTAGGCGGTGCTACAGAGTTCTT
GAAGTGGTGGCCTAACTACGGCTACACTAGAAGGACAGTATTTGGTATCTGCGCTCTGCTGAAGCCAGTT
ACCTTCGGAAAAAGAGTTGGTAGCTCTTGATCCGGCAAACAAACCACCGCTGGTAGCGGTGGTTTTTTTG
TTTGCAAGCAGCAGATTACGCGCAGAAAAAAAGGATCTCAAGAAGATCCTTTGATCTTTTCTACGGGGTC
TGACGCTCAGTGGAACGAAAACTCACGTTAAGGGATTTTGGTCATGAGATTATCAAAAAGGATCTTCACC
TAGATCCTTTTAAATTAAAAATGAAGTTTTAAATCAATCTAAAGTATATATGAGTAAACTTGGTCTGACA
GTTACCAATGCTTAATCAGTGAGGCACCTATCTCAGCGATCTGTCTATTTCGTTCATCCATAGCTGCCTG
ACTCCCCGTCGTGTAGATAACTACGATACGGGAGGGCTTACCATCTGGCCCCAGTGCTGCAATGATACCG
CGAGACCCACGCTCACCGGCTCCAGATTTATCAGCAATAAACCAGCCAGCCGGAAGGGCCGAGCGCAGAA
GTGGTCCTGCAACTTTATCCGCCTCCATCCAGTCTATTAATTGTTGCCGGGAAGCTAGAGTAAGTAGTTC
GCCAGTTAATAGTTTGCGCAACGTTGTTGCCATTGCTACAGGCATCGTGGTGTCACGCTCGTCGTTTGGT
ATGGCTTCATTCAGCTCCGGTTCCCAACGATCAAGGCGAGTTACATGATCCCCCATGTTGTGCAAAAAAG
CGGTTAGCTCCTTCGGTCCTCCGATCGTTGTCAGAAGTAAGTTGGCCGCAGTGTTATCACTCATGGTTAT
GGCAGCACTGCATAATTCTCTTACTGTCATGCCATCCGTAAGATGCTTTTCTGTGACTGGTGAGTACTCA
ACCAAGTCATTCTGAGAATAGTGTATGCGGCGACCGAGTTGCTCTTGCCCGGCGTCAATACGGGATAATA
CCGCGCCACATAGCAGAACTTTAAAAGTGCTCATCATTGGAAAACGTTCTTCGGGGCGAAAACTCTCAAG
GATCTTACCGCTGTTGAGATCCAGTTCGATGTAACCCACTCGTGCACCCAACTGATCTTCAGCATCTTTT
ACTTTCACCAGCGTTTCTGGGTGAGCAAAAACAGGAAGGCAAAATGCCGCAAAAAAGGGAATAAGGGCGA
CACGGAAATGTTGAATACTCATACTCTTCCTTTTTCAATATTATTGAAGCATTTATCAGGGTTATTGTCT
CATGAGCGGATACATATTTGAATGTATTTAGAAAAATAAACAAATAGGGGTTCCGCGCACATTTCCCCGA
AAAGTGCCACCTGACGTCTAAGAAACCATTATTATCATGACATTAACCTATAAAAATAGGCGTATCACGA
GGCCCTTTCGTCTTCACCTCGAGAAATCATAAAAAATTTATTTGCTTTG

7.5 Comparison of Single Incorporation by the different *KlenTaq* mutants

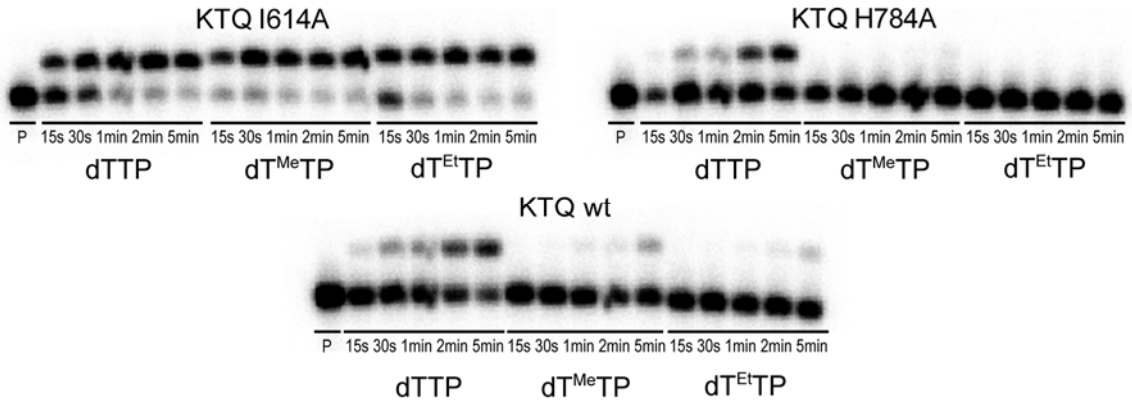

Figure 7.5-1 *Comparison of dT^RTP single incorporation by KlenTaq mutants I614a (top left) and H784 (top right) and KlenTaq wt (bottom). Conditions: 37°C, 12.5nM polymerase, 150nM primer, 225nM template, 100µM dNTP, KTQ-Buffer.*

In a first trial single incorporation was studied qualitatively in comparison to the wild type enzyme. Interestingly the mutant I614A showed by far higher acceptance for the size-augmented nucleotides **$dT^{Me}TP$** and **$dT^{Et}TP$**, whereas the mutant H784A was less active as the wild type even for the natural substrates dTTP

7.6 PROSIT Calculations

P-values of sugar moieties in primer, template and nucleotides of the structures containing **$dT^{Me}TP$** and **$dT^{Et}TP$** and **$dT^{iP}TP$**, respectively determined using the PROSIT server [*Sun* et al., 2005]. It should be noted that the P-value (column 7) was not specifically restrained during refinement in phenix.refine [*Betz* et al., 2010, *Betz*, 2009].

Klentaq wt structures:

dT^{Me}-Template

No.	v_0	v_1	v_2	v_3	v_4	***P***	vmax	χ	γ	TYPE		
A	-13,4	25,0	-26,6	19,4	-3,9	***169,5***	27,0	-127,9	50,8	C2'-endo	B-Form	Southern
A	-31,8	45,2	-40,7	23,8	4,8	***155,2***	44,8	99,3	43,2	C2'-endo	B-Form	Southern
A	-6,5	-17,4	33,2	-37,8	28,0	***28,2***	37,6	4,6	60,3	C3'-endo	A-Form	Northern
A	7,5	-25,1	32,2	-29,0	13,6	***5,7***	32,4	-171,5	177,9	C3'-endo	A-Form	Northern
G	2,7	-27,6	40,0	-39,6	23,5	***14,9***	41,4	-160,0	52,8	C3'-endo	A-Form	Northern
G	-4,1	-22,4	38,7	-42,2	29,1	***24,0***	42,3	-148,7	43,7	C3'-endo	A-Form	Northern
C	-2,2	-17,4	28,9	-30,9	21,1	***22,5***	31,3	-169,5	177,8	C3'-endo	A-Form	Northern
G	-14,1	29,2	-32,3	25,2	-7,2	***173,8***	32,5	-105,6	50,3	C2'-endo	B-Form	Southern
C	-14,0	29,0	-32,2	25,0	-7,1	***173,8***	32,4	-98,7	39,5	C2'-endo	B-Form	Southern
C	-9,1	-9,7	23,5	-29,4	24,3	***36,3***	29,1	-141,9	45,4	C4'-exo	A-Form	Northern
G	-13,8	25,7	-27,4	20,0	-4,1	***169,6***	27,8	-110,6	51,1	C2'-endo	B-Form	Southern
T	-29,6	36,6	-29,9	13,6	9,9	***145,8***	36,1	-110,9	47,5	C1'-exo	B-Form	Southern
G	-34,1	37,7	-27,1	8,3	16,0	***136,3***	37,4	-106,3	43,8	C1'-exo	B-Form	Southern
G	-37,9	34,4	-18,5	-2,8	25,3	***119,5***	37,5	-114,2	36,2	C1'-exo	B-Form	Southern
T	-37,8	38,2	-24,5	3,4	21,5	***128,7***	39,2	-131,2	57,8	C1'-exo	B-Form	Southern
C	-40,4	44,1	-31,3	9,0	19,5	***135,4***	44,0	-117,0	46,9	C1'-exo	B-Form	Southern

dT^{Me}-Primer

No.	v_0	v_1	v_2	v_3	v_4	***P***	vmax	χ	γ	TYPE		
G	-14,8	-11,9	32,1	-41,5	35,5	***39,0***	41,2	-166,7	-10,6	C4'-exo	A-Form	Northern
A	-8,0	-1,6	9,9	-14,8	14,4	***49,4***	15,3	-137,1	46,0	C4'-exo	A-Form	Northern
C	23,2	-30,3	25,7	-13,1	-6,2	***329,5***	29,8	-157,0	-144,9	C2'-exo	A-Form	Northern
C	-21,8	10,9	3,1	-15,7	23,7	***82,5***	23,6	-138,1	38,9	O4'-endo	A-Form	Northern
A	-9,5	28,4	-35,8	31,1	-13,8	***183,7***	35,8	-102,8	46,7	C3'-exo	B-Form	Southern
C	-34,8	23,0	-3,5	-16,6	32,5	***95,8***	34,9	-118,7	43,8	O4'-endo	B-Form	Southern
G	-30,8	36,1	-28,0	11,1	12,2	***141,7***	35,6	-106,3	49,1	C1'-exo	B-Form	Southern
G	-38,7	28,0	-7,4	-14,8	33,6	***101,1***	38,1	-120,9	44,2	O4'-endo	B-Form	Southern
C	-34,7	44,5	-37,0	18,1	10,2	***147,9***	43,6	-96,0	50,5	C2'-endo	B-Form	Southern
G	3,1	-27,3	39,4	-38,7	22,8	***14,4***	40,7	-149,6	38,0	C3'-endo	A-Form	Northern
C	-3,8	-18,7	32,6	-35,8	25,1	***24,7***	35,9	-151,6	49,2	C3'-endo	A-Form	Northern
ddC	8,5	-21,3	25,3	-21,2	8,1	***359,6***	25,3	-149,5	73,0	C3'-endo	A-Form	Northern
dT^{Me}TP	21,7	-37,2	38,0	-24,7	1,2	***344,3***	39,5	-138,0	63,4	C2'-exo	A-Form	Northern

dT^{Et}-Template

No.	v_0	v_1	v_2	v_3	v_4	***P***	vmax	χ	γ	TYPE		
A	-19,8	33,0	-33,0	22,5	-1,9	***164,4***	34,3	-114,9	49,3	C2'-endo	B-Form	Southern
A	-33,6	47,3	-42,4	24,5	5,5	***154,6***	47,0	90,3	45,5	C2'-endo	B-Form	Southern
A	26,9	-31,6	24,5	-9,6	-10,7	***321,7***	31,2	171,1	-40,7	C2'-exo	A-Form	Northern
A	4,4	-23,4	32,3	-30,7	16,7	***11,1***	32,9	-174,6	179,2	C3'-endo	A-Form	Northern
G	0,3	-25,0	38,8	-40,0	25,0	***18,4***	40,9	-161,2	53,2	C3'-endo	A-Form	Northern
G	-3,1	-22,2	37,3	-40,1	27,3	***22,8***	40,4	-149,7	45,1	C3'-endo	A-Form	Northern
C	-7,5	-13,7	28,1	-33,2	26,0	***31,5***	33,0	-173,6	178,5	C3'-endo	A-Form	Northern
G	-14,9	28,8	-30,9	23,3	-5,6	***171,2***	31,3	-104,9	51,9	C2'-endo	B-Form	Southern
C	-19,6	29,9	-28,3	17,8	1,0	***159,4***	30,2	-106,9	44,2	C2'-endo	B-Form	Southern
C	-12,4	-5,9	20,5	-28,3	25,7	***43,8***	28,4	-142,8	42,2	C4'-exo	A-Form	Northern
G	-12,7	23,1	-24,4	17,8	-3,3	***168,8***	24,9	-107,6	47,8	C2'-endo	B-Form	Southern
T	-33,2	35,1	-24,4	6,0	17,0	***133,4***	35,5	-118,5	53,6	C1'-exo	B-Form	Southern
G	-34,5	32,1	-18,1	-1,3	22,4	***121,7***	34,4	-113,4	41,6	C1'-exo	B-Form	Southern
G	-35,5	34,3	-20,4	0,5	21,9	***124,6***	36,0	-117,9	49,7	C1'-exo	B-Form	Southern
T	-43,8	35,7	-14,9	-10,0	33,6	***110,4***	42,7	-136,4	58,9	O4'-endo	B-Form	Southern
C	-37,1	46,7	-38,0	17,9	11,8	***146,4***	45,6	-108,9	46,3	C2'-endo	B-Form	Southern

dT^{Et}-Primer

No.	v_0	v_1	v_2	v_3	v_4	***P***	vmax	χ	γ	TYPE		
G	-11,8	-13,4	31,6	-39,5	32,2	***35,8***	39,0	-161,0	-15,3	C3'-endo	A-Form	Northern
A	-1,0	-16,6	26,6	-27,9	18,3	***20,4***	28,4	-148,0	52,8	C3'-endo	A-Form	Northern
C	25,1	-29,9	23,2	-9,4	-9,8	***322,2***	29,4	-146,5	-103,5	C2'-exo	A-Form	Northern
C	-27,4	27,5	-17,5	2,2	15,7	***128,2***	28,3	-127,5	46,4	C1'-exo	B-Form	Southern
A	-13,6	29,5	-33,4	26,4	-8,2	***175,3***	33,5	-104,3	37,3	C2'-endo	B-Form	Southern
C	-37,6	24,5	-3,6	-18,0	35,1	***95,4***	37,6	-121,9	45,7	O4'-endo	B-Form	Southern
G	-30,8	35,7	-27,1	10,1	12,9	***140,3***	35,3	-107,3	52,0	C1'-exo	B-Form	Southern
G	-42,6	32,7	-10,9	-13,4	35,0	***105,2***	41,6	-120,8	41,8	O4'-endo	B-Form	Southern
C	-34,5	45,8	-39,1	20,6	8,5	***150,5***	44,9	-91,4	46,8	C2'-endo	B-Form	Southern
G	2,0	-27,2	40,2	-40,0	24,4	***15,9***	41,8	-151,4	37,4	C3'-endo	A-Form	Northern
C	-7,5	-16,5	32,5	-37,8	28,7	***29,9***	37,5	-149,9	54,2	C3'-endo	A-Form	Northern
ddC	10,4	-25,6	29,4	-25,1	9,3	***359,0***	29,4	-149,2	56,2	C2'-exo	A-Form	Northern
dT^{Et}TP	20,3	-38,2	40,9	-28,2	4,5	***348,4***	41,7	-139,2	66,3	C2'-exo	A-Form	Northern

Klentaq DM KK structures:

dT^{Me}-Template

No.	v_0	v_1	v_2	v_3	v_4	***P***	vmax	χ	γ	TYPE		
A	-19,3	30,5	-29,6	19,2	-0,1	***161,4***	31,2	-121,6	51,8	C2'-endo	B-Form	Southern
A	-18,0	33,2	-35,1	25,6	-5,0	***169,3***	35,7	-87,8	59,7	C2'-endo	B-Form	Southern
A	24,5	-17,1	4,0	10,0	-21,7	***279,4***	24,2	128,4	-107,9	O4'-exo	A-Form	Northern
A	4,8	-24,2	33,2	-31,5	16,9	***10,8***	33,8	-172,2	-179,7	C3'-endo	A-Form	Northern
G	4,7	-28,0	38,9	-37,3	20,8	***12,0***	39,8	-160,3	48,7	C3'-endo	A-Form	Northern
G	-3,8	-21,7	37,5	-40,8	28,0	***23,8***	41,0	-147,9	42,7	C3'-endo	A-Form	Northern
C	2,5	-19,2	27,6	-26,9	15,6	***13,8***	28,4	-169,6	-174,6	C3'-endo	A-Form	Northern
G	-15,5	28,7	-30,5	22,4	-4,6	***169,6***	31,0	-107,2	56,3	C2'-endo	B-Form	Southern
C	-18,0	31,0	-31,7	22,2	-2,9	***166,3***	32,7	-102,6	41,1	C2'-endo	B-Form	Southern
C	-13,4	-1,8	15,2	-23,4	23,1	***51,2***	24,2	-137,1	40,5	C4'-exo	A-Form	Northern
G	-16,1	27,7	-28,3	19,8	-2,4	***166,1***	29,2	-109,5	49,2	C2'-endo	B-Form	Southern
T	-30,2	35,9	-28,1	11,5	11,6	***142,6***	35,3	-116,3	48,4	C1'-exo	B-Form	Southern
G	-34,5	37,6	-26,7	7,7	16,7	***135,4***	37,6	-106,2	42,7	C1'-exo	B-Form	Southern
G	-36,0	28,2	-10,4	-10,1	28,8	***107,3***	35,1	-117,1	45,4	O4'-endo	B-Form	Southern
T	-40,6	38,3	-21,8	-1,0	26,0	***122,4***	40,7	-134,3	56,4	C1'-exo	B-Form	Southern
C	-40,9	43,0	-29,0	6,3	21,5	***132,0***	43,3	-115,6	42,9	C1'-exo	B-Form	Southern

dT^{Me}-Primer

No.	v_0	v_1	v_2	v_3	v_4	***P***	vmax	χ	γ	TYPE		
G	-18,0	-5,9	25,8	-36,9	34,7	**46,5**	37,5	-162,3	55,9	C4'-exo	A-Form	Northern
A	-13,7	-2,0	15,6	-23,8	23,7	**51,0**	24,8	-141,5	48,2	C4'-exo	A-Form	Northern
C	26,2	-28,0	19,2	-4,7	-13,3	**313,3**	28,0	-148,7	-114,1	C1'-endo	A-Form	Northern
C	-22,7	11,2	3,5	-16,6	24,7	**81,8**	24,7	-137,7	41,8	O4'-endo	A-Form	Northern
A	-10,5	27,4	-33,1	27,7	-11,1	**180,5**	33,1	-100,9	40,2	C3'-exo	B-Form	Southern
C	-36,9	23,1	-1,7	-19,6	35,6	**92,6**	37,5	-125,8	49,5	O4'-endo	B-Form	Southern
G	-33,0	37,3	-27,5	9,2	14,8	**138,1**	36,9	-111,6	58,9	C1'-exo	B-Form	Southern
G	-43,5	35,1	-14,3	-10,4	33,9	**109,7**	42,4	-115,3	39,9	C1'-exo	B-Form	Southern
C	-35,4	44,7	-36,7	17,5	11,0	**146,9**	43,8	-92,9	54,4	C2'-endo	B-Form	Southern
G	2,5	-26,8	39,3	-38,9	23,3	**15,3**	40,7	-149,6	39,1	C3'-endo	A-Form	Northern
C	-4,8	-17,5	31,7	-35,3	25,4	**26,3**	35,3	-149,9	60,4	C3'-endo	A-Form	Northern
ddC	27,1	-37,3	32,4	-16,3	-7,0	**331,2**	37,0	-135,1	71,4	C2'-exo	A-Form	Northern
dT^{Me}TP	19,0	-40,1	45,2	-34,5	9,0	**353,6**	45,5	-144,7	60,5	C2'-exo	A-Form	Northern

dT^{Et}-Template

No.	v_0	v_1	v_2	v_3	v_4	***P***	vmax	χ	γ	TYPE		
A	-21,8	31,6	-28,9	17,1	2,8	***156,2***	31,6	-121,6	52,7	C2'-endo	B-Form	Southern
A	-34,3	37,3	-26,6	7,6	16,7	***135,4***	37,3	81,4	50,3	C1'-exo	B-Form	Southern
A	12,6	-30,3	35,4	-29,2	10,7	***358,4***	35,4	-150,0	47,6	C2'-exo	A-Form	Northern
A	11,0	-28,4	34,0	-29,0	11,5	***0,6***	34,0	-174,7	178,5	C3'-endo	A-Form	Northern
G	5,6	-28,2	38,3	-36,4	19,7	***10,7***	39,0	-160,9	53,5	C3'-endo	A-Form	Northern
G	-4,7	-20,9	36,9	-40,9	28,7	***25,2***	40,7	-148,8	46,8	C3'-endo	A-Form	Northern
C	-3,4	-14,7	26,2	-29,0	20,5	***25,4***	29,0	-169,6	-179,6	C3'-endo	A-Form	Northern
G	-17,4	28,7	-28,7	19,2	-1,3	***163,8***	29,8	-107,5	58,3	C2'-endo	B-Form	Southern
C	-19,6	34,1	-35,0	24,6	-3,4	***166,5***	35,9	-103,3	40,7	C2'-endo	B-Form	Southern
C	-17,3	2,3	12,6	-23,0	25,2	***60,3***	25,4	-134,5	40,2	C4'-exo	A-Form	Northern
G	-15,0	26,3	-27,1	19,2	-2,8	***167,0***	27,8	-110,3	56,8	C2'-endo	B-Form	Southern
T	-29,8	34,5	-26,3	9,9	12,4	***140,4***	34,1	-114,6	49,7	C1'-exo	B-Form	Southern
G	-30,6	38,4	-31,5	14,7	9,8	***146,6***	37,7	-96,7	48,6	C2'-endo	B-Form	Southern
G	-38,7	24,2	-1,6	-20,7	37,2	***92,3***	39,3	-126,5	41,8	O4'-endo	B-Form	Southern
T	-32,1	39,6	-32,1	14,6	10,8	***145,5***	39,0	-125,9	55,9	C2'-endo	B-Form	Southern
C	-37,9	42,2	-30,7	9,8	17,5	***137,1***	41,9	-107,9	38,6	C1'-exo	B-Form	Southern

dT^{Et}-Primer

No.	v_0	v_1	v_2	v_3	v_4	***P***	vmax	χ	γ	TYPE		
G	-27,7	12,6	6,0	-22,0	31,4	***78,9***	31,0	-157,3	64,2	O4'-endo	A-Form	Northern
A	-30,8	21,0	-4,3	-13,3	27,7	***98,1***	30,5	-133,8	50,6	O4'-endo	A-Form	Northern
C	-27,6	12,5	6,1	-22,1	31,3	***78,7***	31,0	-140,5	54,7	O4'-endo	A-Form	Northern
C	-22,5	5,3	12,5	-25,5	30,3	***65,4***	29,9	-140,4	44,1	C4'-exo	B-Form	Southern
A	-8,3	26,0	-33,1	29,0	-13,3	***184,5***	33,2	-99,1	43,3	C3'-exo	B-Form	Southern
C	-38,0	25,5	-4,3	-17,6	35,0	***96,5***	37,9	-127,2	49,2	O4'-endo	B-Form	Southern
G	-32,7	35,3	-24,8	6,7	16,2	***134,5***	35,3	-110,2	56,8	C1'-exo	B-Form	Southern
G	-46,4	35,3	-11,7	-14,7	38,3	***105,0***	45,3	-121,5	45,5	O4'-endo	B-Form	Southern
C	-34,5	45,6	-38,5	20,2	8,6	***150,0***	44,5	-89,7	44,7	C2'-endo	B-Form	Southern
G	3,1	-27,9	40,3	-39,7	23,3	***14,5***	41,6	-149,6	42,7	C3'-endo	A-Form	Northern
C	-6,2	-18,1	33,8	-38,4	28,2	***27,7***	38,2	-154,9	60,6	C3'-endo	A-Form	Northern
ddC	-11,5	-6,1	19,9	-27,4	24,5	***43,1***	27,3	-153,0	58,7	C4'-exo	A-Form	Northern
dT^{Et}TP	17,6	-40,6	47,1	-37,2	11,7	***356,3***	47,2	-142,5	60,1	C2'-exo	A-Form	Northern

dT^{iP}-Template

No.	v_0	v_1	v_2	v_3	v_4	***P***	vmax	χ	γ	TYPE		
A	-14,0	28,7	-31,6	24,4	-6,7	***173,2***	31,8	-113,1	44,5	C2'-endo	B-Form	Southern
A	7,7	-8,0	5,4	-1,1	-4,1	***311,4***	8,1	-82,9	34,2	C1'-endo	B-Form	Southern
A	-15,6	0,2	14,0	-23,4	24,8	***56,1***	25,1	85,8	39,0	C4'-exo	A-Form	Northern
A	12,4	-27,4	31,2	-25,1	8,1	***356,1***	31,2	-172,8	-176,7	C2'-exo	A-Form	Northern
G	7,0	-29,7	39,4	-36,9	19,1	***9,0***	39,9	-162,1	50,5	C3'-endo	A-Form	Northern
G	-4,8	-20,4	36,6	-40,4	28,3	***25,3***	40,5	-150,3	44,9	C3'-endo	A-Form	Northern
C	4,0	-18,1	24,5	-23,0	12,1	***9,8***	24,9	-168,0	-172,2	C3'-endo	A-Form	Northern
G	-15,5	29,4	-31,5	23,3	-5,2	***170,5***	31,9	-105,9	53,0	C2'-endo	B-Form	Southern
C	-19,9	32,4	-32,4	21,7	-1,3	***163,6***	33,7	-102,9	44,0	C2'-endo	B-Form	Southern
C	-10,8	-9,1	24,1	-31,2	26,4	***38,6***	30,8	-140,9	39,2	C4'-exo	A-Form	Northern
G	-15,9	28,3	-29,4	21,0	-3,4	***167,7***	30,1	-111,2	49,6	C2'-endo	B-Form	Southern
T	-34,4	35,0	-22,8	3,7	19,2	***129,5***	35,8	-122,7	52,2	C1'-exo	B-Form	Southern
G	-31,1	36,9	-28,9	11,8	12,0	***142,5***	36,4	-108,2	45,5	C1'-exo	B-Form	Southern
G	-39,9	33,9	-15,8	-6,7	29,1	***113,9***	38,9	-113,5	41,8	C1'-exo	B-Form	Southern
T	-49,4	40,8	-17,3	-10,6	37,2	***111,2***	48,1	-146,5	73,2	C1'-exo	B-Form	Southern
C	-39,3	42,4	-29,9	8,3	19,2	***134,8***	42,4	-105,5	33,8	C1'-exo	B-Form	Southern

dT^{iP}-Primer

No.	v_0	v_1	v_2	v_3	v_4	***P***	vmax	χ	γ	TYPE		
G	-5,0	-19,7	35,2	-39,2	27,9	***25,8***	39,1	-170,2	57,4	C3'-endo	A-Form	Northern
A	-2,9	-17,3	29,4	-31,8	22,0	***23,5***	32,1	-148,4	49,1	C3'-endo	A-Form	Northern
C	-6,3	-13,8	27,3	-31,7	24,1	***29,9***	31,5	-143,9	50,9	C3'-endo	A-Form	Northern
C	-19,6	31,9	-31,5	21,1	-1,1	***163,2***	32,9	-116,6	45,3	C2'-endo	B-Form	Southern
A	-13,8	27,3	-29,9	22,6	-5,7	***172,1***	30,2	-98,2	33,2	C2'-endo	B-Form	Southern
C	-35,6	22,0	-1,2	-19,4	34,9	***91,9***	36,4	-124,0	45,8	O4'-endo	B-Form	Southern
G	-30,0	35,3	-27,4	10,9	11,9	***141,9***	34,9	-109,7	59,0	C1'-exo	B-Form	Southern
G	-42,6	36,2	-16,5	-7,6	31,3	***113,4***	41,6	-115,0	41,1	C1'-exo	B-Form	Southern
C	-34,9	43,4	-35,0	16,2	11,4	***145,7***	42,4	-94,3	48,2	C2'-endo	B-Form	Southern
G	2,8	-25,9	37,5	-37,0	21,8	***14,7***	38,7	-148,3	39,2	C3'-endo	A-Form	Northern
C	-7,0	-14,2	28,4	-33,3	25,5	***30,5***	33,0	-148,0	52,1	C3'-endo	A-Form	Northern
ddC	8,4	-18,1	20,4	-15,7	4,4	***354,2***	20,5	-144,2	63,6	C2'-exo	A-Form	Northern
dT^{iP}TP	19,4	-37,7	40,7	-29,0	5,9	***350,0***	41,3	-141,9	58,2	C2'-exo	A-Form	Northern

8 References

1. Arora, K., Beard, W.A., Wilson, S.H. & Schlick, T. Mismatch-induced conformational distortions in polymerase beta support an induced-fit mechanism for fidelity. *Biochemistry* **44**, 13328-41 (2005).
2. Barman, T.E., Bellamy, S.R., Gutfreund, H., Halford, S.E. & Lionne, C. The identification of chemical intermediates in enzyme catalysis by the rapid quench-flow technique. *Cell Mol Life Sci* **63**, 2571-83 (2006).
3. Barnes, W.M. The fidelity of Taq polymerase catalyzing PCR is improved by an N-terminal deletion. *Gene* **112**, 29-35 (1992).
4. Bartek, J. & Lukas, J. DNA damage checkpoints: from initiation to recovery or adaptation. *Curr Opin Cell Biol* **19**, 238-45 (2007).
5. Barton, D.H.R. & Motherwell, W.B. New and Selective Reactions and Reagents in Carbohydrate-Chemistry. *Pure and Applied Chemistry* **53**, 15-31 (1981).
6. Beaucage, S.L. Current protocols in nucleic acid chemistry. (Wiley, New York, 2001).
7. Beese, L.S., Derbyshire, V. & Steitz, T.A. Structure of DNA polymerase I Klenow fragment bound to duplex DNA. *Science* **260**, 352-5 (1993a).
8. Beese, L.S., Friedman, J.M. & Steitz, T.A. Crystal structures of the Klenow fragment of DNA polymerase I complexed with deoxynucleoside triphosphate and pyrophosphate. *Biochemistry* **32**, 14095-101 (1993b).
9. Berdis, A.J. Mechanisms of DNA polymerases. *Chem Rev* **109**, 2862-79 (2009).
10. Betz, K. Structural Snapshots of KlenTaq DNA polymerase processing 4'-alkylated substrates. *Master Thesis* (2009).
11. Betz, K., Streckenbach, F., Schnur, A., Exner, T., Welte, W., Diederichs, K. and Marx, A. Structures of DNA polymerase caught processing size-augmented nucleotide probes. *Angew Chem Int Ed Engl accepted*(2010).
12. Boosalis, M.S., Petruska, J. & Goodman, M.F. DNA polymerase insertion fidelity. Gel assay for site-specific kinetics. *J Biol Chem* **262**, 14689-96 (1987).
13. Borden, J., Crans, D.C. & Florian, J. Transition state analogues for nucleotidyl transfer reactions: Structure and stability of pentavalent vanadate and phosphate ester dianions. *J Phys Chem B* **110**, 14988-99 (2006).

14. Boudsocq, F., Ling, H., Yang, W. & Woodgate, R. Structure-based interpretation of missense mutations in Y-family DNA polymerases and their implications for polymerase function and lesion bypass. *DNA Repair (Amst)* **1**, 343-58 (2002).

15. Braman, J. *In vitro mutagenesis protocols*, xvi, 287 p. (Humana Press, Totowa, N.J., 2002).

16. Brautigam, C.A. & Steitz, T.A. Structural and functional insights provided by crystal structures of DNA polymerases and their substrate complexes. *Curr Opin Struct Biol* **8**, 54-63 (1998).

17. Castro, C. et al. Nucleic acid polymerases use a general acid for nucleotidyl transfer. *Nat Struct Mol Biol* **16**, 212-8 (2009).

18. Chargaff, E., Zamenhof, S. & Green, C. Composition of human desoxypentose nucleic acid. *Nature* **165**, 756-7 (1950).

19. Copeland, W.C., Dong, Q. & Wang, T.S. Rationale for mutagenesis of DNA polymerase active sites: DNA polymerase alpha. *Methods Enzymol* **262**, 294-303 (1995).

20. Cramer, J., Rangam, G., Marx, A. & Restle, T. Varied active-site constraints in the klenow fragment of E. coli DNA polymerase I and the lesion-bypass Dbh DNA polymerase. *Chembiochem* **9**, 1243-50 (2008).

21. Cramer, J., Strerath, M., Marx, A. & Restle, T. Exploring the effects of active site constraints on HIV-1 reverse transcriptase DNA polymerase fidelity. *Journal of Biological Chemistry* **277**, 43593-43598 (2002).

22. Creighton, S., Bloom, L.B. & Goodman, M.F. Gel fidelity assay measuring nucleotide misinsertion, exonucleolytic proofreading, and lesion bypass efficiencies. *Methods Enzymol* **262**, 232-56 (1995).

23. Dahlberg, M.E. & Benkovic, S.J. Kinetic mechanism of DNA polymerase I (Klenow fragment): identification of a second conformational change and evaluation of the internal equilibrium constant. *Biochemistry* **30**, 4835-43 (1991).

24. Deleeuw, F.A.A.M. & Altona, C. Computer-Assisted Pseudorotation Analysis of 5-Membered Rings by Means of Proton Spin Spin Coupling-Constants - Program Pseurot. *Journal of Computational Chemistry* **4**, 428-437 (1983).

25. Dess, D.B. & Martin, J.C. A Useful 12-I-5 Triacetoxyperiodinane (the Dess-Martin Periodinane) for the Selective Oxidation of Primary or Secondary Alcohols and a Variety of Related 12-I-5 Species. *Journal of the American Chemical Society* **113**, 7277-7287 (1991).

26. Detmer, I., Summerer, D. & Marx, A. DNA minor groove hydration probed with 4'-alkylated thymidines. *Chemical Communications*, 2314-5 (2002).

27. Detmer, I., Summerer, D. & Marx, A. Substrates for investigation of DNA polymerase function: Synthesis and properties of 4'-C-alkylated oligonucleotides. *European Journal of Organic Chemistry*, 1837-1846 (2003).

28. Di Pasquale, F. Mechanistische Studien der humanen DNA-Polymerase β mittels chemischer Sonden und gerichteter Evolution. *Ph.D. Thesis* (2008).

29. Di Pasquale, F. et al. Opposed steric constraints in human DNA polymerase beta and E. coli DNA polymerase I. *J Am Chem Soc* **130**, 10748-57 (2008).

30. Doublie, S., Tabor, S., Long, A.M., Richardson, C.C. & Ellenberger, T. Crystal structure of a bacteriophage T7 DNA replication complex at 2.2 A resolution. *Nature* **391**, 251-8 (1998).

31. Durniak, K.J., Bailey, S. & Steitz, T.A. The structure of a transcribing T7 RNA polymerase in transition from initiation to elongation. *Science* **322**, 553-7 (2008).

32. Echols, H. & Goodman, M.F. Fidelity mechanisms in DNA replication. *Annu Rev Biochem* **60**, 477-511 (1991).

33. Filee, J., Forterre, P., Sen-Lin, T. & Laurent, J. Evolution of DNA polymerase families: evidences for multiple gene exchange between cellular and viral proteins. *J Mol Evol* **54**, 763-73 (2002).

34. Florian, J., Goodman, M.F. & Warshel, A. Theoretical investigation of the binding free energies and key substrate-recognition components of the replication fidelity of human DNA polymerase beta. *Journal of Physical Chemistry B* **106**, 5739-5753 (2002).

35. Florian, J., Goodman, M.F. & Warshel, A. Computer simulation of the chemical catalysis of DNA polymerases: discriminating between alternative nucleotide insertion mechanisms for T7 DNA polymerase. *J Am Chem Soc* **125**, 8163-77 (2003).

36. Florian, J., Goodman, M.F. & Warshel, A. Computer simulations of protein functions: searching for the molecular origin of the replication fidelity of DNA polymerases. *Proc Natl Acad Sci U S A* **102**, 6819-24 (2005).

37. Franklin, M.C., Wang, J. & Steitz, T.A. Structure of the replicating complex of a pol alpha family DNA polymerase. *Cell* **105**, 657-67 (2001).

38. Freemont, P.S., Friedman, J.M., Beese, L.S., Sanderson, M.R. & Steitz, T.A. Cocrystal structure of an editing complex of Klenow fragment with DNA. *Proc Natl Acad Sci U S A* **85**, 8924-8 (1988).

39. Frey, M.W., Sowers, L.C., Millar, D.P. & Benkovic, S.J. The nucleotide analog 2-aminopurine as a spectroscopic probe of nucleotide incorporation by the Klenow fragment of Escherichia coli polymerase I and bacteriophage T4 DNA polymerase. *Biochemistry* **34**, 9185-92 (1995).

40. Friedberg, E.C., Wagner, R. & Radman, M. Specialized DNA polymerases, cellular survival, and the genesis of mutations. *Science* **296**, 1627-30 (2002).

41. Gaster, J. & Marx, A. Tuning single nucleotide discrimination in polymerase chain reactions (PCRs): Synthesis of primer probes bearing polar 4'-C-modifications and their application in allele-specific PCR. *Chemistry-a European Journal* **11**, 1861-1870 (2005).

42. Gaster, J., Rangam, G. & Marx, A. Increased single nucleotide discrimination in arrayed primer elongation by 4'-C-modified primer probes. *Chemical Communications*, 1692-1694 (2007).

43. Gillam, S. & Smith, M. Site-specific mutagenesis using synthetic oligodeoxyribonucleotide primers: I. Optimum conditions and minimum ologodeoxyribonucleotide length. *Gene* **8**, 81-97 (1979).

44. Glöckner, C. Gerichtete Evolution und Charakterisierung einer thermostabilen DNA-Polymerase mit erhöhter Akzeptanz für geschädigte DNA. *PhD Thesis* (2008).

45. Gloeckner, C., Sauter, K.B. & Marx, A. Evolving a thermostable DNA polymerase that amplifies from highly damaged templates. *Angew Chem Int Ed Engl* **46**, 3115-7 (2007).

46. Goodman, M.F. DNA replication fidelity: kinetics and thermodynamics. *Mutat Res* **200**, 11-20 (1988).

47. Goodman, M.F. Hydrogen bonding revisited: geometric selection as a principal determinant of DNA replication fidelity. *Proc Natl Acad Sci U S A* **94**, 10493-5 (1997).

48. Goodman, M.F. Error-prone repair DNA polymerases in prokaryotes and eukaryotes. *Annu Rev Biochem* **71**, 17-50 (2002).

49. Herschlag, D., Piccirilli, J.A. & Cech, T.R. Ribozyme-catalyzed and nonenzymatic reactions of phosphate diesters: rate effects upon substitution of sulfur for a nonbridging phosphoryl oxygen atom. *Biochemistry* **30**, 4844-54 (1991).

50. Hess, M.T., Schwitter, U., Petretta, M., Giese, B. & Naegeli, H. DNA synthesis arrest at C4'-modified deoxyribose residues. *Biochemistry* **36**, 2332-2337 (1997).

51. Huang, H., Chopra, R., Verdine, G.L. & Harrison, S.C. Structure of a covalently trapped catalytic complex of HIV-1 reverse transcriptase: implications for drug resistance. *Science* **282**, 1669-75 (1998).

52. Hubscher, U., Maga, G. & Spadari, S. Eukaryotic DNA polymerases. *Annu Rev Biochem* **71**, 133-63 (2002).

53. Hubscher, U., Nasheuer, H.P. & Syvaoja, J.E. Eukaryotic DNA polymerases, a growing family. *Trends Biochem Sci* **25**, 143-7 (2000).

54. Imanishi, T. & Obika, S. BNAs: novel nucleic acid analogs with a bridged sugar moiety. *Chemical Communications*, 1653-1659 (2002).

55. Irimia, A., Eoff, R.L., Pallan, P.S., Guengerich, F.P. & Egli, M. Structure and activity of Y-class DNA polymerase DPO4 from Sulfolobus solfataricus with templates containing the hydrophobic thymine analog 2,4-difluorotoluene. *J Biol Chem* **282**, 36421-33 (2007).

56. Jacobo-Molina, A. et al. Crystal structure of human immunodeficiency virus type 1 reverse transcriptase complexed with double-stranded DNA at 3.0 A resolution shows bent DNA. *Proc Natl Acad Sci U S A* **90**, 6320-4 (1993).

57. Johnson, A. & O'Donnell, M. Cellular DNA replicases: components and dynamics at the replication fork. *Annu Rev Biochem* **74**, 283-315 (2005).

58. Johnson, K.A. Conformational coupling in DNA polymerase fidelity. *Annu Rev Biochem* **62**, 685-713 (1993).

59. Johnson, K.A. Advances in transient-state kinetics. *Curr Opin Biotechnol* **9**, 87-9 (1998).

60. Johnson, S.J. & Beese, L.S. Structures of mismatch replication errors observed in a DNA polymerase. *Cell* **116**, 803-16 (2004).

61. Joyce, C.M. & Benkovic, S.J. DNA polymerase fidelity: kinetics, structure, and checkpoints. *Biochemistry* **43**, 14317-24 (2004).

62. Jung, G.H., Leavitt, M.C., Schultz, M. & Ito, J. Site-specific mutagenesis of PRD1 DNA polymerase: mutations in highly conserved regions of the family B DNA polymerase. *Biochem Biophys Res Commun* **170**, 1294-300 (1990).

63. Jung, K.H. & Marx, A. Nucleotide analogues as probes for DNA polymerases. *Cell Mol Life Sci* **62**, 2080-91 (2005).

64. Kim, T.W., Brieba, L.G., Ellenberger, T. & Kool, E.T. Functional evidence for a small and rigid active site in a high fidelity DNA polymerase: probing T7 DNA polymerase with variably sized base pairs. *J Biol Chem* **281**, 2289-95 (2006).

65. Kim, T.W., Delaney, J.C., Essigmann, J.M. & Kool, E.T. Probing the active site tightness of DNA polymerase in subangstrom increments. *Proc Natl Acad Sci U S A* **102**, 15803-8 (2005).

66. Kim, Y. et al. Crystal structure of Thermus aquaticus DNA polymerase. *Nature* **376**, 612-6 (1995).

67. Kim, Y. et al. Mutagenesis of the positively charged conserved residues in the 5' exonuclease domain of Taq DNA polymerase. *Mol Cells* **7**, 468-72 (1997).

68. Kintek, Corp. Model RQF-3 Chemical-Quench-Flow, *URL: http://www.kintek-corp.com/pdf/RQF-3_Brochure.pdf* **11.07.2010** (2010).

69. Kodama, E.I. et al. 4'-ethynyl nucleoside analogs: Potent inhibitors of multidrug-resistant human immunodeficiency virus variants in vitro. *Antimicrobial Agents and Chemotherapy* **45**, 1539-1546 (2001).

70. Kohgo, S. et al. Design, efficient synthesis, and anti-HIV activity of 4'-*C*-cyano- and 4 '-C-ethynyl-2 '-deoxy purine nucleosides. *Nucleosides Nucleotides & Nucleic Acids* **23**, 671-690 (2004).

71. Kool, E.T. Active site tightness and substrate fit in DNA replication. *Annu Rev Biochem* **71**, 191-219 (2002).

72. Kool, E.T., Morales, J.C. & Guckian, K.M. Mimicking the Structure and Function of DNA: Insights into DNA Stability and Replication. *Angew Chem Int Ed Engl* **39**, 990-1009 (2000).

73. Kool, E.T. & Sintim, H.O. The difluorotoluene debate - a decade later. *Chemical Communications*, 3665-3675 (2006).

74. Kornberg, A. The enzymatic replication of DNA. *CRC Crit Rev Biochem* **7**, 23-43 (1979).

75. Kornberg, A. DNA replication. *Biochim Biophys Acta* **951**, 235-9 (1988).

76. Kornberg, A., Kornberg, S.R. & Simms, E.S. Metaphosphate synthesis by an enzyme from Escherichia coli. *Biochim Biophys Acta* **20**, 215-27 (1956).

77. Korolev, S., Nayal, M., Barnes, W.M., Di Cera, E. & Waksman, G. Crystal structure of the large fragment of Thermus aquaticus DNA polymerase I at 2.5-A resolution: structural basis for thermostability. *Proc Natl Acad Sci U S A* **92**, 9264-8 (1995).

78. Kovacs, T. & Otvos, L. Simple Synthesis of 5-Vinyl- and 5-Ethynyl-2'-Deoxyuridine-5'-Triphosphates. *Tetrahedron Letters* **29**, 4525-4528 (1988).

79. Krueger, A.T. & Kool, E.T. Model systems for understanding DNA base pairing. *Curr Opin Chem Biol* **11**, 588-94 (2007).

80. Kuchta, R.D., Benkovic, P. & Benkovic, S.J. Kinetic mechanism whereby DNA polymerase I (Klenow) replicates DNA with high fidelity. *Biochemistry* **27**, 6716-25 (1988).

81. Kunkel, T.A. DNA replication fidelity. *J Biol Chem* **279**, 16895-8 (2004).

82. Kunkel, T.A. & Bebenek, K. Recent studies of the fidelity of DNA synthesis. *Biochim Biophys Acta* **951**, 1-15 (1988).

83. Kunkel, T.A. & Bebenek, K. DNA replication fidelity. *Annu Rev Biochem* **69**, 497-529 (2000).

84. Lawrence, C.W. Classical mutagenesis techniques. *Methods Enzymol* **350**, 189-99 (2002).

85. Lehmann, A.R. et al. Translesion synthesis: Y-family polymerases and the polymerase switch. *DNA Repair (Amst)* **6**, 891-9 (2007).

86. Li, Y., Korolev, S. & Waksman, G. Crystal structures of open and closed forms of binary and ternary complexes of the large fragment of Thermus aquaticus DNA polymerase I: structural basis for nucleotide incorporation. *EMBO J* **17**, 7514-25 (1998).

87. Li, Y., Mitaxov, V. & Waksman, G. Structure-based design of Taq DNA polymerases with improved properties of dideoxynucleotide incorporation. *Proc Natl Acad Sci U S A* **96**, 9491-6 (1999).

88. Li, Y. & Waksman, G. Crystal structures of a ddATP-, ddTTP-, ddCTP, and ddGTP- trapped ternary complex of Klentaq1: insights into nucleotide incorporation and selectivity. *Protein Sci* **10**, 1225-33 (2001).

89. Lindahl, T. Instability and decay of the primary structure of DNA. *Nature* **362**, 709-15 (1993).

90. Lindahl, T. & Wood, R.D. Quality control by DNA repair. *Science* **286**, 1897-905 (1999).

91. Ling, H., Boudsocq, F., Plosky, B.S., Woodgate, R. & Yang, W. Replication of a cis-syn thymine dimer at atomic resolution. *Nature* **424**, 1083-7 (2003).

92. Ling, H., Boudsocq, F., Woodgate, R. & Yang, W. Crystal structure of a Y-family DNA polymerase in action: a mechanism for error-prone and lesion-bypass replication. *Cell* **107**, 91-102 (2001).

93. Ling, H. et al. Crystal structure of a benzo[a]pyrene diol epoxide adduct in a ternary complex with a DNA polymerase. *Proc Natl Acad Sci U S A* **101**, 2265-9 (2004).

94. Liu, J. & Tsai, M.D. DNA polymerase beta: pre-steady-state kinetic analyses of dATP alpha S stereoselectivity and alteration of the stereoselectivity by various metal ions and by site-directed mutagenesis. *Biochemistry* **40**, 9014-22 (2001).

95. Loeb, L.A. & Preston, B.D. Mutagenesis by apurinic/apyrimidinic sites. *Annu Rev Genet* **20**, 201-30 (1986).

96. Maga, G. et al. 8-oxo-guanine bypass by human DNA polymerases in the presence of auxiliary proteins. *Nature* **447**, 606-8 (2007).

97. Marx, A. et al. 4'-acylated thymidine 5 '-triphosphates: a tool to increase selectivity towards HIV-1 reverse transcriptase. *Nucleic Acids Research* **26**, 4063-4067 (1998).

98. Marx, A., Detmer, I., Gaster, J. & Summerer, D. Probing DNA polymerase function with synthetic nucleotides. *Synthesis-Stuttgart*, 1-14 (2004).

99. Marx, A., MacWilliams, M.P., Bickle, T.A., Schwitter, U. & Giese, B. 4'-acylated thymidines: A new class of DNA chain terminators and photocleavable DNA building blocks. *Journal of the American Chemical Society* **119**, 1131-1132 (1997).

100. Marx, A. et al. Probing interactions between HIV-1 reverse transcriptase and its DNA substrate with backbone-modified nucleotides. *Chemistry & Biology* **6**, 111-116 (1999).

101. Marx, A. & Summerer, D. Molecular insights into error-prone DNA replication and error-free lesion bypass. *Chembiochem* **3**, 405-7 (2002).

102. Matray, T.J. & Kool, E.T. A specific partner for abasic damage in DNA. *Nature* **399**, 704-8 (1999).

103. Matsuda, S., Leconte, A.M. & Romesberg, F.E. Minor groove hydrogen bonds and the replication of unnatural base pairs. *J Am Chem Soc* **129**, 5551-7 (2007).

104. Matsuda, Y., Kohra, S., Katou, K., Uemura, T. & Yamashita, K. Synthesis of an annulenoannulenone, 3H-benzo[e]cycl [3.3.2]azin-3-one. *Heterocycles* **60**, 405-411 (2003).

105. McMinn, D.L. et al. Efforts toward expansion of the genetic alphabet: DNA polymerase recognition of a highly stable, self-fairing hydrophobic base. *Journal of the American Chemical Society* **121**, 11585-11586 (1999).

106. Minnick, D.T., Liu, L., Grindley, N.D., Kunkel, T.A. & Joyce, C.M. Discrimination against purine-pyrimidine mispairs in the polymerase active site of DNA polymerase I: a structural explanation. *Proc Natl Acad Sci U S A* **99**, 1194-9 (2002).

107. Mizukami, S., Kim, T.W., Helquist, S.A. & Kool, E.T. Varying DNA base-pair size in subangstrom increments: evidence for a loose, not large, active site in low-fidelity Dpo4 polymerase. *Biochemistry* **45**, 2772-8 (2006).

108. Morales, J.C. & Kool, E.T. Efficient replication between non-hydrogen-bonded nucleoside shape analogs. *Nat Struct Biol* **5**, 950-4 (1998).

109. Morales, J.C. & Kool, E.T. Minor groove interactions between polymerase and DNA: More essential to replication than Watson-Crick hydrogen bonds? *Journal of the American Chemical Society* **121**, 2323-2324 (1999).

110. Morales, J.C. & Kool, E.T. Varied molecular interactions at the active sites of several DNA polymerases: Nonpolar nucleoside isosteres as probes. *Journal of the American Chemical Society* **122**, 1001-1007 (2000a).

111. Morales, J.C. & Kool, E.T. Functional hydrogen-bonding map of the minor groove binding tracks of six DNA polymerases. *Biochemistry* **39**, 12979-12988 (2000b).

112. Morales, J.C. & Kool, E.T. Importance of terminal base pair hydrogen-bonding in 3'-end proofreading by the Klenow fragment of DNA polymerase I. *Biochemistry* **39**, 2626-32 (2000c).

113. Moran, S., Ren, R.X. & Kool, E.T. A thymidine triphosphate shape analog lacking Watson-Crick pairing ability is replicated with high sequence selectivity. *Proc Natl Acad Sci U S A* **94**, 10506-11 (1997a).

114. Moran, S., Ren, R.X.F., Rumney, S. & Kool, E.T. Difluorotoluene, a nonpolar isostere for thymine, codes specifically and efficiently for adenine in DNA replication. *Journal of the American Chemical Society* **119**, 2056-2057 (1997b).

115. Nomura, M., Endo, K., Shuto, S. & Matsuda, A. Nucleosides and nucleotides. 191. Ring expansion reaction of 1-[2,3,5-tri-O-TBS-4 alpha-formyl-beta-D-ribo-pentofuranosyl]uracil by treating with (methylene)triphenylphosphorane to give a new nucleoside containing dihydrooxepine ring at the sugar moiety. *Tetrahedron* **55**, 14847-14854 (1999).

116. Obika, S. et al. Synthesis and conformation of 3',4'-BNA monomers, 3 '-O,4 '-C-methyleneribonucleosides. *Tetrahedron* **58**, 3039-3049 (2002).

117. Ollis, D.L., Brick, P., Hamlin, R., Xuong, N.G. & Steitz, T.A. Structure of large fragment of Escherichia coli DNA polymerase I complexed with dTMP. *Nature* **313**, 762-6 (1985).

118. Pandey, V.N., Kaushik, N. & Modak, M.J. Role of lysine 758 of Escherichia coli DNA polymerase I as assessed by site-directed mutagenesis. *J Biol Chem* **269**, 13259-65 (1994).

119. Pandey, V.N. et al. Site directed mutagenesis of DNA polymerase I (Klenow) from Escherichia coli. The significance of Arg682 in catalysis. *Eur J Biochem* **214**, 59-65 (1993).

120. Patel, P.H., Kawate, H., Adman, E., Ashbach, M. & Loeb, L.A. A single highly mutable catalytic site amino acid is critical for DNA polymerase fidelity. *J Biol Chem* **276**, 5044-51 (2001).

121. Patel, P.H. & Loeb, L.A. DNA polymerase active site is highly mutable: evolutionary consequences. *Proc Natl Acad Sci U S A* **97**, 5095-100 (2000).

122. Pelletier, H., Sawaya, M.R., Kumar, A., Wilson, S.H. & Kraut, J. Structures of ternary complexes of rat DNA polymerase beta, a DNA template-primer, and ddCTP. *Science* **264**, 1891-903 (1994).

123. Petruska, J. et al. Comparison between DNA melting thermodynamics and DNA polymerase fidelity. *Proc Natl Acad Sci U S A* **85**, 6252-6 (1988).

124. Piccirilli, J.A., Krauch, T., Moroney, S.E. & Benner, S.A. Enzymatic Incorporation of a New Base Pair into DNA and Rna Extends the Genetic Alphabet. *Nature* **343**, 33-37 (1990).

125. Prakash, S., Johnson, R.E. & Prakash, L. Eukaryotic translesion synthesis DNA polymerases: specificity of structure and function. *Annu Rev Biochem* **74**, 317-53 (2005).

126. Radhakrishnan, R. & Schlick, T. Orchestration of cooperative events in DNA synthesis and repair mechanism unraveled by transition path sampling of DNA polymerase beta's closing. *Proc Natl Acad Sci U S A* **101**, 5970-5 (2004).

127. Radhakrishnan, R. & Schlick, T. Fidelity discrimination in DNA polymerase beta: differing closing profiles for a mismatched (G:A) versus matched (G:C) base pair. *J Am Chem Soc* **127**, 13245-52 (2005).

128. Rangam, G., Rudinger, N.Z., Muller, H.M. & Marx, A. Synthesis and application of 4 '-C-alkylated uridines as probes for uracil-DNA glycosylase. *Synthesis*, 1467-1472 (2005).

129. Rinkel, L.J. & Altona, C. Conformational analysis of the deoxyribofuranose ring in DNA by means of sums of proton-proton coupling constants: a graphical method. *J Biomol Struct Dyn* **4**, 621-49 (1987).

130. Rothwell, P.J., Mitaksov, V. & Waksman, G. Motions of the fingers subdomain of klentaq1 are fast and not rate limiting: implications for the molecular basis of fidelity in DNA polymerases. *Mol Cell* **19**, 345-55 (2005).

131. Rothwell, P.J. & Waksman, G. Structure and mechanism of DNA polymerases. *Adv Protein Chem* **71**, 401-40 (2005).

132. Rothwell, P.J. & Waksman, G. A pre-equilibrium before nucleotide binding limits fingers subdomain closure by Klentaq1. *J Biol Chem* **282**, 28884-92 (2007).

133. Sancar, A. DNA excision repair. *Annu Rev Biochem* **65**, 43-81 (1996).

134. Scharer, O.D. Chemistry and biology of DNA repair. *Angew Chem Int Ed Engl* **42**, 2946-74 (2003).

135. Schnur, A. Intrinsic properties of a KlenTaq DNA polymerase mutant with enhanced substrate specificity determined by X-ray structure analysis. *PhD Thesis* (2009).

136. Schweitzer, B.A. & Kool, E.T. Aromatic Nonpolar Nucleosides as Hydrophobic Isosteres of Pyrimidine and Purine Nucleosides. *Journal of Organic Chemistry* **59**, 7238-7242 (1994).

137. Seki, M. et al. High-efficiency bypass of DNA damage by human DNA polymerase Q. *EMBO J* **23**, 4484-94 (2004).

138. Shinkai, A., Patel, P.H. & Loeb, L.A. The conserved active site motif a of Escherichia coli DNA polymerase I is highly mutable. *Journal of Biological Chemistry* **276**, 18836-18842 (2001).

139. Showalter, A.K. & Tsai, M.D. A reexamination of the nucleotide incorporation fidelity of DNA polymerases. *Biochemistry* **41**, 10571-6 (2002).

140. Silverman, A.P., Jiang, Q., Goodman, M.F. & Kool, E.T. Steric and electrostatic effects in DNA synthesis by the SOS-induced DNA polymerases II and IV of Escherichia coli. *Biochemistry* **46**, 13874-81 (2007).

141. Sintim, H.O. & Kool, E.T. Remarkable sensitivity to DNA base shape in the DNA polymerase active site. *Angew Chem Int Ed Engl* **45**, 1974-9 (2006).

142. Skarstad, K. & Wold, S. The speed of the Escherichia coli fork in vivo depends on the DnaB:DnaC ratio. *Mol Microbiol* **17**, 825-31 (1995).

143. Smirnov, S., Matray, T.J., Kool, E.T. & de los Santos, C. Integrity of duplex structures without hydrogen bonding: DNA with pyrene paired at abasic sites. *Nucleic Acids Res* **30**, 5561-9 (2002).

144. Steitz, T.A. A mechanism for all polymerases. *Nature* **391**, 231-2 (1998).

145. Stillman, B. Origin recognition and the chromosome cycle. *FEBS Lett* **579**, 877-84 (2005).

146. Strazewski, P. & Tamm, C. Replication Experiments with Nucleotide Base Analogs. *Angewandte Chemie-International Edition in English* **29**, 36-57 (1990).

147. Streckenbach, F. Synthesis of 4'-C-alkylated DNA. *Diploma Thesis* (2006).

148. Streckenbach, F., Rangam, G., Möller, H.M. & Marx, A. Steric constraints dependent on nucleobase pair orientation vary in different DNA polymerase active sites. *Chembiochem* **10**, 1630-3 (2009).

149. Strerath, M., Cramer, J., Restle, T. & Marx, A. Implications of active site constraints on varied DNA polymerase selectivity. *Journal of the American Chemical Society* **124**, 11230-11231 (2002a).

150. Strerath, M., Detmer, I., Gaster, J. & Marx, A. Modified oligonucleotides as tools for allele-specific amplification. *Methods Mol Biol* **402**, 317-28 (2007a).

151. Strerath, M., Gaster, J., Summerer, D. & Marx, A. Increased single-nucleotide discrimination of PCR by primer probes bearing hydrophobic 4 ' C modifications. *Chembiochem* **5**, 333-339 (2004).

152. Strerath, M., Gloeckner, C., Liu, D., Schnur, A. & Marx, A. Directed DNA polymerase evolution: Effects of mutations in motif C on the mismatch-extension selectivity of Thermus aquaticus DNA polymerase. *Chembiochem* **8**, 395-401 (2007b).

153. Strerath, M. & Marx, A. Tuning PCR specificity by chemically modified primer probes. *Angewandte Chemie-International Edition* **41**, 4766-4769 (2002).

154. Strerath, M., Summerer, D. & Marx, A. Varied DNA polymerase-substrate interactions in the nucleotide binding pocket. *Chembiochem* **3**, 578-80 (2002b).

155. Sucato, C.A. et al. Modifying the beta,gamma leaving-group bridging oxygen alters nucleotide incorporation efficiency, fidelity, and the catalytic mechanism of DNA polymerase beta. *Biochemistry* **46**, 461-71 (2007).

156. Summerer, D. Die Selektivität der DNA-Replikation: Neue Einblicke durch synthetische Sonden und kombinatorisches Protein-Design. *Ph.D. Thesis* (2004).

157. Summerer, D. & Marx, A. DNA Polymerase Selectivity: Sugar Interactions Monitored with High-Fidelity Nucleotides. *Angew Chem Int Ed Engl* **40**, 3693-3695 (2001).

158. Summerer, D. & Marx, A. 4 ' C-modified nucleotides as chemical tools for investigation and modulation of DNA polymerase function. *Synlett*, 217-224 (2004).

159. Summerer, D., Rudinger, N.Z., Detmer, I. & Marx, A. Enhanced fidelity in mismatch extension by DNA polymerase through directed combinatorial enzyme design. *Angewandte Chemie-International Edition* **44**, 4712-4715 (2005).

160. Sun, G., Voigt, J.H., Filippov, I.V., Marquez, V.E. & Nicklaus, M.C. PROSIT: pseudo-rotational online service and interactive tool, applied to a conformational survey of nucleosides and nucleotides. *J Chem Inf Comput Sci* **44**, 1752-62 (2004).

161. Switzer, C., Moroney, S.E. & Benner, S.A. Enzymatic Incorporation of a New Base Pair into DNA and Rna. *Journal of the American Chemical Society* **111**, 8322-8323 (1989).

162. Tewsa, B. et al. Application of the C4 '-alkylated deoxyribose primer system (CAPS) in allele-specific real-time PCR for increased selectivity in discrimination of single nucleotide sequence variants. *Biological Chemistry* **384**, 1533-1541 (2003).

163. Upton, T.G. et al. Alpha,beta-difluoromethylene deoxynucleoside 5'-triphosphates: a convenient synthesis of useful probes for DNA polymerase beta structure and function. *Org Lett* **11**, 1883-6 (2009).

164. Verma, S. & Eckstein, F. Modified oligonucleotides: synthesis and strategy for users. *Annu Rev Biochem* **67**, 99-134 (1998).

165. Waga, T., Nishizaki, T., Miyakawa, I., Ohrui, H. & Meguro, H. Synthesis of 4'-C-Methylnucleosides. *Bioscience Biotechnology and Biochemistry* **57**, 1433-1438 (1993).

166. Watson, J.D. & Crick, F.H. Genetical implications of the structure of deoxyribonucleic acid. *Nature* **171**, 964-7 (1953a).

167. Watson, J.D. & Crick, F.H. Molecular structure of nucleic acids; a structure for deoxyribose nucleic acid. *Nature* **171**, 737-8 (1953b).

168. Wing, R. et al. Crystal-Structure Analysis of a Complete Turn of B-DNA. *Nature* **287**, 755-758 (1980).

169. Wong, I., Patel, S.S. & Johnson, K.A. An induced-fit kinetic mechanism for DNA replication fidelity: direct measurement by single-turnover kinetics. *Biochemistry* **30**, 526-37 (1991).

170. Yang, L. et al. Local deformations revealed by dynamics simulations of DNA polymerase Beta with DNA mismatches at the primer terminus. *J Mol Biol* **321**, 459-78 (2002).

171. Yang, W. & Woodgate, R. What a difference a decade makes: insights into translesion DNA synthesis. *Proc Natl Acad Sci U S A* **104**, 15591-8 (2007).

172. Yang, Z., Chen, F., Chamberlin, S.G. & Benner, S.A. Expanded genetic alphabets in the polymerase chain reaction. *Angew Chem Int Ed Engl* **49**, 177-80 (2010).

173. Yang, Z., Hutter, D., Sheng, P., Sismour, A.M. & Benner, S.A. Artificially expanded genetic information system: a new base pair with an alternative hydrogen bonding pattern. *Nucleic Acids Res* **34**, 6095-101 (2006).

174. Yang, Z., Sismour, A.M., Sheng, P., Puskar, N.L. & Benner, S.A. Enzymatic incorporation of a third nucleobase pair. *Nucleic Acids Res* **35**, 4238-49 (2007).

175. Yu, C.Z., Henry, A.A., Romesberg, F.E. & Schultz, P.G. Polymerase recognition of unnatural base pairs. *Angewandte Chemie-International Edition* **41**, 3841-3844 (2002).

9 Eidesstattliche Erklärung

Eidesstattliche Erklärung

Ich erkläre hiermit, dass ich die vorliegende Arbeit ohne unzulässige Hilfe Dritter und ohne Benutzung anderer als der angegebenen Hilfsmittel angefertigt habe. Die aus anderen Quellen direkt oder indirekt übernommenen Daten und Konzepte sind unter Angabe der Quelle gekennzeichnet. Weitere Personen, insbesondere Promotionsberater, waren an der inhaltlich materiellen Erstellung dieser Arbeit nicht beteiligt. Die Arbeit wurde bisher weder im In- noch im Ausland in gleicher oder ähnlicher Form einer anderen Prüfungsbehörde vorgelegt.

Konstanz, im Juli 2010

(Frank Streckenbach)

Danksagung

Prof. Dr. Andreas Marx möchte ich für die Vergabe des sehr ergiebigen Themas und die stete wissenschaftliche und freundschaftliche Unterstützung danken.
Prof. Dr. Jörg Hartig danke ich für die Übernahme des Zweitgutachtens sowie Prof. Dr. Ulrich Groth für die Übernahme des Prüfungsvorsitzes.

Zuerst möchte ich natürlich Maria danken, die mich seit fast 6 Jahren begleitet und unterstützt. Ich freue mich auf unsere gemeinsame Zukunft!

Vielen Dank an Gopinath Rangam! Deine Vorarbeiten haben den Grundstein für diese Arbeit gelegt und auch während der letzten Jahre standest Du mir immer mit Rat und Tat zu meiner Seite. Thank you very much!
Karin Betz gebührt Dank für die tolle Zusammenarbeit im Rahmen dieser Forschungsarbeit! Deine Kristalle haben uns den nötigen „Einblick“ geliefert!
Meinen Laborkollegen Anna-Lena, Gopinath, Meike, Claudia und Yan danke ich für das klasse Laborklima. Insbesondere Anna-Lena durfte mich die komplette Zeit mit allen meinen Macken und Kanten „ertragen“!
Anna-Lena, Karin, Stephan, Holger, Sascha, Oli, Ramon und Maria danke ich fürs fleißige Korrekturlesen meiner Arbeit!

Dem Rest der Arbeitsgruppe Marx möchte ich fürs Zuhören bei vielen Fragen und den unendlichen Diskussionen im Labor und auch außerhalb danken.

Natürlich der Pokerrunde für die Zeit abseits des Labors: Jens, Tim, Felix, Oli, Jörg, Walther, Petra und Silvia!
Jens, irgendwann schaffe auch ich die Schwägalp!

Zu guter Letzt möchte ich meiner Familie danken, ohne deren Unterstützung diese Arbeit nicht möglich gewesen wäre.